

RWT

**THE EFFECT OF BOUNDARY CONDITIONS ON
MODE SET SELECTION FOR
FLEXIBLE COMPONENTS IN MULTIBODY DYNAMICS**

by

Christopher David Sontag
B.S.M.E. Tufts University, 12 May 1991

A Thesis submitted to

The Faculty of

The School of Engineering and Applied Science of
The George Washington University in partial satisfaction
of the requirements for the degree of Master of Science

Directed by

Dr. Robert H. Tolson
Professor of Engineering and Applied Science

July 1993

This research was conducted at the NASA Langley Research Center.

ABSTRACT

A study was performed to examine the effects of boundary conditions on the selection of a reduced vibrational mode set used to represent a flexible structural component in a multibody system. To accomplish this, a finite element model was created and analyzed by employing the structural finite element code MSC/NASTRAN. The model consisted of two identical beams which were connected by a pin joint and an angular spring. The first beam was cantilevered, while the second beam was constrained only by the end joint and joint spring.

Component mode reduction was performed only on the second beam, and then component mode synthesis was performed on the entire structure in NASTRAN by coupling the generalized degrees of freedom from the second beam to the physical degrees of freedom from the unreduced first beam. The resulting system frequencies and mode shapes were then compared to the system frequencies and mode shapes of the "exact" model, i.e. the same model where no component mode reduction or synthesis was performed and all degrees of freedom were represented without approximation. Modal strain energy was also examined to aid in determining which resulting synthesized modes should be compared to exact system modes.

The parameters varied were the joint angle, the joint spring stiffness, the method of component mode reduction used on the second beam (fixed-interface, free-interface, or mixed-interface), and the number and type of normal vibrational modes of the second beam retained in the synthesis.

It was found for this study that the most accurate interface type of mode set to

use varied with configuration and system mode number and, only in some cases, with joint spring stiffness. It was concluded in general that the most accurate mode set interface type used for the reduced component could be completely predicted for a given system mode shape by examining the motion of that component within the unapproximated system mode shape. However, for the model of this study, it was found that fixed-interface component mode sets provided the most accuracy in the first and second system modes examined, independently of configuration or joint spring stiffness. It was also found that the inclusion of some types of component modes, as expected, had no effect on the accuracy of the resulting system mode examined, e.g. component torsional modes did not affect the accuracy of the system modes of bending in a plane and thus could be eliminated.

ACKNOWLEDGEMENTS

The research for this project was supported by the Assembly Dynamics and Control Team of the Controls/Structures Interaction Office at NASA Langley Research Center. The author would like express his gratitude to the fine people whose generous assistance made this project possible. Dr. R.H. Tolson is appreciated for his patient guidance and input. Dr. P.A. Cooper and Dr. C. Gerhold are thanked for their reviews and editing suggestions. Invaluable was the assistance given by Alan Stockwell who essentially became the author's mentor in structural dynamics and finite element modeling.

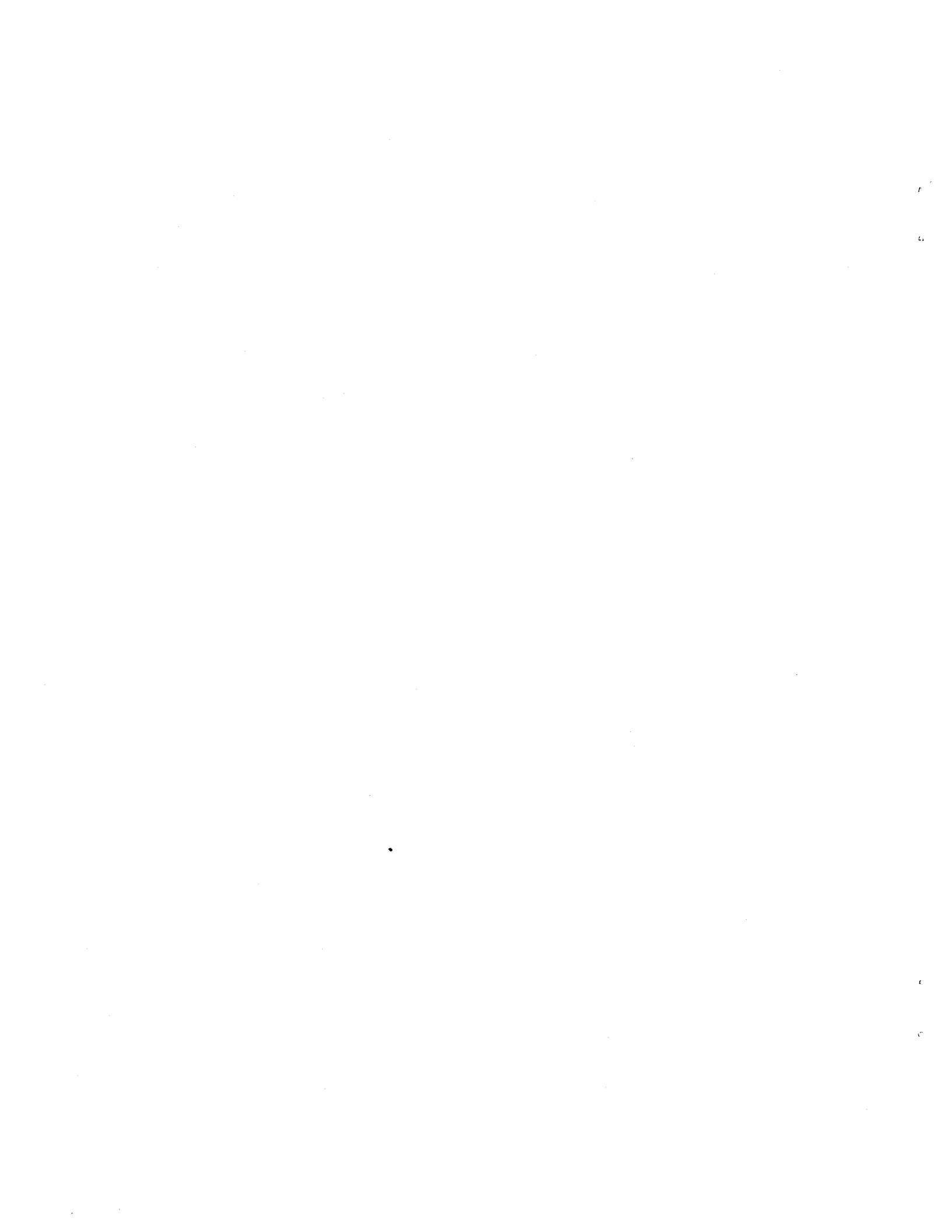


TABLE OF CONTENTS

Abstract	ii
Acknowledgements	iv
Table of Contents	v
Guide to the Text Contents	vii
List of Figures	viii
List of Tables	x
Nomenclature	xi
I. Introduction	1
II. General Description of Component Mode Synthesis (CMS)	7
2.1 Survey of Methods in Use	8
2.2 Synthesis Procedure	13
2.2.1 General Procedure	14
2.2.2 Constraint Equations and Mode Sets of Different Methods	19
2.3 Implementation of CMS in NASTRAN	22
2.3.1 Superelements	23
2.3.2 Case Control Structure	24
2.3.3 Set Description	25
III. Introduction to The Finite Element Model	29
3.1 Description	30
3.2 Material Properties	31
3.3 Derivation of Joint Angular Spring Constant	35
IV. Evaluation of the Synthesized System	39
4.1 Basic Procedure	41
4.2 Mode Sets	41
4.3 Error Criteria	44
4.4 Bending in the "Plane of Interest"	46
4.5 System Mode Limitations in General	52
V. Results for a Single Configuration	55
5.1 Realistic System Modes	55
5.2 Results	60
5.2.1 Component Mode Types	61

5.2.2	Effect of Joint Spring Stiffness	66
5.2.3	Comparison of Interface Methods	69
VI.	Extension to Multiple Configurations	73
6.1	Component Mode Types	73
6.2	Effect of Joint Spring Stiffness	75
6.3	Comparison of Interface Methods	76
6.4	A "Robust" Mode Set	83
VII.	Conclusions and Future Study	92
	References	96
	Appendices	99
A.	A NASTRAN Input File	99
B.	Exact Z-Bending System Natural Frequencies	102
C.	Error Trends, $\theta = 90^\circ$	106
D.	Guide to the Included Floppy Disk	131

GUIDE TO THE TEXT CONTENTS

The text in this report is presented in the sections given in the Table Of Contents. In **Chapter 1**, the Introduction, a discussion is given of the scientific area in which the present study is being made. The basic need is explained for research into the effect of component configuration and interface conditions on accurate mode set selection for components in multibody dynamics.

Because the study objective is obtained performing Component Mode Synthesis in MSC/NASTRAN, **Chapter 2** gives a background discussion of Component Mode Synthesis in general, as well as some information on its implementation in NASTRAN. Reasoning as to the creation of the finite element model used in this study, as well as specific information on the model physical properties is given in **Chapter 3**.

Chapter 4 explains the basic procedure followed in obtaining the data for this study. A discussion is given as to how the synthesized system mode shapes are compared to the "exact" mode shapes, as well as which shapes are "realistic" to be compared. To begin presenting results clearly, **Chapter 5** only discusses the results obtained for a single configuration, that of $\theta = 90^\circ$ (Figure 3.2). Attention is given to the importance of component mode type and error trends plotted versus joint angular spring stiffness. A summarizing comparison of the three different interface types is given. **Chapter 6** extends the discussions of Chapter 5 to the other configurations examined in the study, $\theta = 45^\circ$, 135° , and 180° , and develops the major conclusions of the study. A summary of all major conclusions is given in **Chapter 7**, as well as suggestions for future research.

LIST OF FIGURES

<u>Title</u>	<u>Page</u>
Figure 2.1: Partitioning of a Structure	15
Figure 2.2: Constraints Used in Determining Normal Modes	16
Figure 3.1: The Finite Element Model	30
Figure 3.2: Varying Model Configurations	33
Figure 3.3: Joint Spring Strain Energy, System Modes 1-5, $\theta = 90^\circ$	37
Figure 4.1: Model Z-Bending vs. XY-Bending	46
Figure 4.2: System Natural Frequencies vs. Joint Spring Stiffness, $\theta = 90^\circ$	49
Figure 4.3: Z-Bending Mode Shapes 1-4 of the Exact System, $\theta = 90^\circ$, $K/K_0 = 1$	50
Figure 4.4: Z-Bending Mode Shapes 5-8 of the Exact System, $\theta = 90^\circ$, $K/K_0 = 1$	51
Figure 5.1: Percent Frequency Error, 2nd System Z-Bending Mode, $\theta = 90^\circ$ Mixed-Interface	62
Figure 5.2: Modal Correlation Error, 2nd System Z-Bending Mode, $\theta = 90^\circ$ Mixed-Interface	62
Figure 5.3: 7th Exact System Z-Bending Mode, $\theta = 90^\circ$	65
Figure 5.4: Strain Energy Percent from Beam 2, System Modes 1-8, $\theta = 90^\circ$	68
Figure 5.5: Ranges of Percent Frequency Error, $\theta = 90^\circ$	70
Figure 5.6: Ranges of Modal Correlation Error, $\theta = 90^\circ$	71
Figure 6.1: Ranges of Percent Frequency Error, $\theta = 45^\circ$	86
Figure 6.2: Ranges of Modal Correlation Error, $\theta = 45^\circ$	87
Figure 6.3: Ranges of Percent Frequency Error, $\theta = 135^\circ$	88
Figure 6.4: Ranges of Modal Correlation Error, $\theta = 135^\circ$	89

<u>Title</u>	<u>Page</u>
Figure 6.5: Ranges of Percent Frequency Error, $\theta = 180^\circ$	90
Figure 6.6: Ranges of Modal Correlation Error, $\theta = 180^\circ$	91
Figures C.1-C.24: Error Trends, $\theta = 90^\circ$, % Freq. Error and MCE	107-130

LIST OF TABLES

<u>Title</u>	<u>Page</u>
Table 3.1: Beam Properties	33
Table 3.2: Natural Frequencies of Beam 2	34
Table 3.3: Joint Angular Spring Constants K Used	37
Table 4.1: Mode Sets Used for Beam 2	42
Table 4.2: Component Mode Numbers in the Mode Sets	43
Table 4.3: First Four Exact System Natural Frequencies, $\theta = 90^\circ$ (Hz)	48
Table 5.1: Exact Z-Bending System Natural Frequencies, $\theta = 90^\circ$ (Hz)	56
Table 5.2: Highest Frequency of the Mode Sets (Hz)	57
Table 5.3: Ability of Mode Sets to Predict Realistic System Modes for the Configuration $\theta = 90^\circ$, Via the Limiting Frequency Method	59
Table 5.4: Mode Sets That Produced System Modes Examined in the Present Study (Criteria Used For All Configurations)	60
Table 6.1: Most Accurate Interface Methods	78
Table B.1: Exact Z-Bending System Natural Frequencies, $\theta = 45^\circ$ (Hz)	102
Table B.2: Exact Z-Bending System Natural Frequencies, $\theta = 90^\circ$ (Hz)	103
Table B.3: Exact Z-Bending System Natural Frequencies, $\theta = 135^\circ$ (Hz)	104
Table B.4: Exact Z-Bending System Natural Frequencies, $\theta = 180^\circ$ (Hz)	105

NOMENCLATURE

<u>Symbol</u>	<u>Meaning</u>
α_i	Argument in mode shape equations = $\left(\frac{x}{L}\right)\lambda_i$.
β	Transformation matrix in Component Mode Synthesis.
δ	Deflection distance.
θ	Model joint angle.
μ, κ	Transformed component mass and stiffness matrices.
ϕ	System normal mode (vector).
Φ	Component normal mode set (matrix).
ω	System natural frequency
+	In plots: Mixed-interface component mode set.
a	Component identification.
A	Constraint matrix in Component Mode Synthesis.
A	In plots: Component axial mode (tension/compression).
b	Component identification.
B	In plots: Component bending mode.
e	Denotes "exact".
E	Modulus of Elasticity.
f	Component generalized forces, or denotes "interface".
\bar{f}	Transformed component generalized forces.
F	System generalized forces.

i	Simple counting variable, or denotes "interior".
I	Area moment of inertia.
K	Model joint spring constant (varied in study).
K_0	Model joint standard spring constant = 8.826 E+5 (ft-lb/rad).
K_{ee}	Element stiffness sub-matrix.
l, L	Length of beam.
m, k	Component mass and stiffness matrices.
M, K	System mass and stiffness matrices.
MCC	Modal Correlation Coefficient.
MCE	Modal Correlation Error.
o	In plots: Free-interface component mode set.
p	Component generalized modal displacement coordinates.
P	Force.
q	System generalized displacement coordinates.
s	Denotes "synthesized".
T	In plots: Component torsional mode.
u_e	Element displacement coordinate.
W_e	Element strain energy.
x	Chapter 1: Distance along beam length.
x	Chapter 2: Component generalized physical displacement coordinates.
x	Chapter 3 and on: Horizontal direction coordinate.
x	In plots: Fixed-interface component mode set.
y	Chapter 1: Mode shape displacement.

y Chapter 3 and on: Vertical direction coordinate.
z Direction coordinate.



I. INTRODUCTION

This study was performed to explore component mode set selection for flexible components in multibody dynamics. Finite element models can include articulating flexible components whose vibrational motion is based on component boundary conditions created by system configuration and interface forces and stiffnesses. Specifically, this study examines mode set selection for a two-beam linkage modelled with properties similar to those of the Space Shuttle Remote Manipulator System (SRMS).

Natural methods for the analysis of such structures involve model reduction. A model that can be reduced in some way is usually preferable due to the amount of computer time or space saved. For analysis purposes, computer time is most often minimized due to cost, but can also be minimized out of a need to conduct real-time dynamic simulations. Computer space or memory may also be restricted due to the machine being used for analysis. Obviously however, it is also important to have full, accurate finite element model representations of a design so that a preliminary analysis may be performed before a design is constructed and implemented. This is crucial in the case of large flexible space structures where there is a range of possible structural dynamics to be predicted and errors in prediction are prone to be costly. Thus, it is valuable to obtain a finite element model of a structure that is an accurate mathematical representation, but uses as few as possible degrees of freedom to perform that representation, that is, has mass and stiffness matrices that are of relatively minimal size. It is well known that instead of using a coarse finite element

model with relatively few degrees of freedom and poor accuracy, better results can be obtained by using a more accurate finite element model with many degrees of freedom and then performing some reduction method on the model that filters out some of the relatively unimportant degrees of freedom until the model has few enough to be practical.^{1,4}

Component Mode Reduction uses a Rayleigh-Ritz transformation² whereby the vibrational modes of a structural component are used to represent the motion of that component and then some of the modes that contribute the least to the motion in comparison are eliminated. This approximation by Component Mode Reduction is attractive because one can select a reduced set of modes for each component in a system and still retain a fairly accurate approximation of the motion of the system while substantially reducing the size of the system problem. Component Mode Reduction and Component Mode Synthesis, the process of coupling reduced components together into a system, are described in more detail later.

There is much literature^{3-17,20} explaining the pros and cons of the various methods of Component Mode Reduction and Component Mode Synthesis usable on structures and structural components. However, these works deal mainly with components that have constant boundary interface conditions with respect to the system to which they are attached, such as the control surfaces fixed to a missile¹⁰ or simply the partitioned section of a beam.¹⁶ Blevlock and Carney¹⁸ present three methods to reduce the order of components by selecting component modes, however as they note, all three methods are dependent upon a specific system configuration.

From large space structures to small robotic systems there are components that

are designed to move relative to their base for which some kind of modal reduction is used. For example, a remote manipulator arm on a space station would most likely be flexible because of weight restrictions, but would also be designed to experience large relative motion as well as varying control forces at its joints thus creating varying component boundary conditions. Because of the magnitude of the effort involved in implementing any space structure, there is often some type of dynamic simulation of the design where the system equations of motion are numerically integrated in order to predict structural motion and reaction to control input and external forces. In general, to incorporate a flexible component into a multibody dynamic simulation, one is to either use all the component finite element physical degrees of freedom or a modal representation consisting of a reduced set of component modes. Either set of coordinates are introduced into some simulation code that handles systems with rigid and flexible components. As stated above, however, the latter is generally favorable because a reduced set of modes will contribute less to the size of the integration problem.

Thus it is evident that there is a need to obtain mode set representations for components that may experience large relative motion with respect to the system. The difficulty here is that the total set of modes from which one can select is based on the boundary conditions of the component, which are in turn based on the configuration of the system. In a multibody system, designed such that the configuration changes with time, the boundary conditions of a specific component are time dependent. Therefore a set of component modes based on a single specific set of boundary conditions may not adequately represent the motion of that component

throughout a dynamic simulation of the system. Also, such a set of modes may not even adequately represent the component throughout several successive finite element analyses of the system if it is to be analyzed at different configurations. Varying control forces or effective stiffnesses at component-to-system interface coordinates will also obviously affect how the component acts within the system. Garcia and Inman¹⁹ demonstrated that mode shapes of a slewing flexible beam are dependent upon the servo stiffness at the axis of the beam's rotation.

Thus, the objective is to examine the effects of system configuration and component interface conditions on the selection of a mode set to represent a given component in a multibody system. In this study, a two-beam linkage with a joint angular spring is modelled with beam dimensions and material properties similar to those of the lower arm boom of the SRMS. This is done using the structural analysis finite element code MSC/NASTRAN. Boundary conditions on the second link are affected by independently varying the joint angle and the joint angular spring constant. Component Mode Reduction is performed on the second beam while also varying the mode selection method and the number of modes kept. Robustness of mode sets are evaluated by performing Component Mode Synthesis on the system including the reduced second beam and then comparing system parameters to that of an "exact" model, that is, one that has not been reduced in any way. The study can be considered "experimental", in that it is estimated that the objective is nontrivial or even impossible to attain analytically.

Conclusions derived from the analysis of a two-beam linkage are clearly most applicable to structurally similar systems such as a robotic manipulator arm, or a

space crane where long structures are connected at a joint. However, general conclusions to be found concerning the dependence of mode set interface type on the flexible interaction of connected components in a multibody system should be applicable to various types of structural systems.

Component bending, torsional, and axial (tension/compression) modes of varied interface types (fixed, free, pinned) are used to represent the second beam. Synthesized system modes and frequencies are examined only up to the eighth mode of bending in the "plane of interest" in the present study. As a related note, it is estimated that interface conditions may become less important to the selection of component modes in the regime of relatively high frequency component modes, when the component is a straight, slender, uniform beam. To illustrate this, recall that the mode shapes of such a beam in the fifth and greater (i -th) modes are approximated by: ³³

$$\begin{aligned}
 \textit{Fixed-Free:} \quad y(\alpha_i) &= \sin(\alpha_i) - \cos(\alpha_i) + e^{-\alpha_i} \\
 \textit{Free-Free:} \quad y(\alpha_i) &= \cos(\alpha_i) - \sin(\alpha_i) + e^{-\alpha_i} \\
 \textit{Free-Pinned:} \quad y(\alpha_i) &= \cos(\alpha_i) - \sin(\alpha_i) + e^{-\alpha_i}
 \end{aligned} \tag{1.1}$$

where

$$\alpha_i = \left(\frac{x}{L} \right) \lambda_i \tag{1.2}$$

Here, L is the length of the beam, x is the distance along that length, and λ is the dimensionless natural frequency parameter that is the solution to the transcendental equation resulting from the beam boundary conditions. Note that the Free-Pinned

equation is for beams pinned at $x = L$, not at $x = 0$. After the fifth mode ($i = 5$), these λ 's can be approximated by

$$\begin{aligned}
 \textit{Fixed-Free: } \lambda_i &= (4i-2)\frac{\pi}{4} \\
 \textit{Free-Free: } \lambda_i &= (4i+2)\frac{\pi}{4} \\
 \textit{Free-Pinned: } \lambda_i &= (4i+1)\frac{\pi}{4}
 \end{aligned}
 \tag{1.3}$$

When the mode number becomes relatively high, the exponential terms in Eq.s (1.1) become negligible, except near $x = 0$. Therefore, if the λ 's are equal for different boundary conditions, then the mode shapes will be equal, with the fixed-free shape differing only by a minus sign which is irrelevant to a mode shape.

Substitution of $i+1$ into the fixed-free equation for λ results in the same equation as for free-free. Thus, in the higher frequency regime, the difference between the free-free i -th shape and the fixed-free $(i+1)$ -th shape approaches zero. Also, as i increases, the difference between the i -th free-free shape and the i -th free-pinned shape approach zero. Due to the fact that these mode shapes become similar as frequency increases, it can be theorized that for very high frequency modes, accurate representation as a set of component modes becomes less dependent upon imposed interface constraints.

II. GENERAL DESCRIPTION OF COMPONENT MODE SYNTHESIS

In structural dynamics, the motion of a linear structure, whether it is freely vibrating or responding to some forced input, can be determined given information on its natural frequencies and corresponding vibrational mode shapes. For a small group of structural problems exact solutions can be calculated analytically. However, as structures and structural systems become more complex, analytical solutions become either impractical or impossible. At this point, a structure is most often analyzed by discretizing it in some way, that is, breaking it up into a finite number of small elements whose motion can be described with respect to each other and given boundary conditions. A finite element model of the structure, though an approximation, is valuable because it bounds the problem to a finite number of degrees of freedom. Often after this, a method of *reduction* is employed on the degrees of freedom of the model in order to reduce the order of the problem to a manageable size.

In general there are two main approaches to the reduction of structural dynamics problems. One is to assume that some points on the structure are dynamically more important and to *lump* mass or concentrate it at these points, thus the effected model is referred to as a lumped-mass model. This process is commonly called a "Guyan Reduction". The second method employs a Rayleigh-Ritz transformation² whereby it is assumed that the motion of the structure can be represented by linear combinations of shape functions whose amplitudes correspond to generalized coordinates, or simply the variables of the problem. Thus, it is called an

assumed-modes method. Rayleigh-Ritz reduction results when selected shape functions are truncated from the set. Generally, these shape functions are vibrational mode shapes and the truncated mode shapes are normal modes of high frequency. The type of reduction examined presently is the latter, sometimes referred to as modal reduction.

For a relatively simple structure, modal reduction can be a very effective way of producing accurate results from a reduced order problem. However, for large complex structures or structural systems, a common practice is to partition the structure into substructures or components, to which modal reduction can be performed individually. This allows the development of different components to be independent of each other with exception only to their common boundary or interface points. For example, in a large space structure this independence allows components to be developed by different contractors. When a component of a structure is analyzed and modally reduced, the process is referred to as *Component Mode Reduction*. When the generalized coordinates from these reduced components are coupled back into the full system via given transformation matrices, the process is referred to as *Component Mode Synthesis*. After the total structure has been synthesized, it is also common practice to perform a system-wide modal reduction to further reduce the order of the problem. Following is a survey of some major developments in the area of Component Mode Synthesis over the last few decades.

2.1 Survey of Methods In Use

The practice of partitioning structures has long been somewhat common in

airplane design. In retrospect however, it was not until the early 1960's that some of the most popular developments in Component Mode Synthesis were published. In 1963, Gladwell⁴ presented what he called a hybrid of the lumped-mass and assumed-modes methods, namely a method of "branch mode analysis". It involved the following procedure. Convert the structure to a lumped-mass system and then create a series of constraints such that all components are simultaneously rigid and attached to one pre-decided component that is allowed to deform. *Normal* modes and frequencies are determined and the process is repeated for each component. Normal modes are simply solutions to the eigen-problem with the given constraints. Finally, all branch modes are used in a Rayleigh-Ritz analysis of the entire system. An advantage to this method is that branch modes calculated are closely related to system modes, however there is the disadvantage that branch modes of each component cannot be found independent of the rest of the physical information of the system.

Published in 1960 and 1965, Hurty^{3,5} appears to have been the first to present a conventional component mode method. Hurty's method also divided the structure into components. The displacements of these components were represented by *rigid-body* modes, *constraint* modes and normal modes. Rigid-body modes are displacements of the component without deformation. A constraint mode is a static shape calculated by giving a boundary or interface degree of freedom a unit displacement while holding all other interface freedoms fixed. Normal modes represent the motion of the component interior degrees of freedom with respect to the interface points. Emphasis is put on the necessity of a *statically complete* mode set - a mode set with interface degrees of freedom such that the component is represented

exactly in a static analysis. In order to maintain a statically complete set, there must be one modal degree of freedom used to represent each interface degree of freedom. (A component degree of freedom is an interface degree of freedom if it is constrained in some way to the structural system). Hurty's method separated the component interface degrees of freedom into "statically determinate constraints" and "redundant constraints" or statically indeterminate constraints. The number of statically determinate constraints determined the number of rigid-body modes used, and constraint modes were then used to treat redundant interface constraints.

The method of Craig and Bampton⁶ differed from Hurty's method primarily in the treatment of interface degrees of freedom. Craig and Bampton showed that if all interface freedoms were treated similarly, it would be unnecessary to use rigid-body modes. All interface freedoms were represented by constraint modes, while all component interior freedoms were represented by "*fixed-interface*" normal modes - component normal modes computed with all interface freedoms constrained or "fixed". Thus, the Craig-Bampton method is called a fixed-interface method. The Craig-Bampton method is still very popular and is also the default Component Mode Synthesis method in MSC/NASTRAN.^{22,23,25}

Goldman⁷ appears to have been the first to present a free-interface method. He proposed the use of only rigid-body modes and free-interface normal modes. This does however make it necessary to separate interface degrees of freedom into determinate and redundant constraints as Hurty did in Ref. 5. Goldman admitted that this "in turn introduces errors that under certain ill-conditioned circumstances can be quite large." Hou⁸ presented a review of current methods and proposed a "new" free-

interface method also including rigid-body modes. It was similar to that of Goldman although the transformation matrices used to couple the components back into the system were of a different derivation. Hou also presented an "error analysis technique" as a means of selecting normal modes that produce better convergence as the number of kept modes increases.

Benfield and Hruda¹³ presented a hybrid method whereby only component normal modes were used as generalized coordinates, and these could be fixed-interface or free-interface modes. Rigid-body and constraint modes were eliminated. Fixed-interface modes were calculated as branch modes in a manner similar to that of Gladwell.⁴ One condition on this method was that if fixed-interface modes are used for one component, free-interface modes must be used for the attached component. Benfield and Hruda included the optional accuracy-improving technique of calculating the component modes while inertia and stiffness loadings are applied to the component. This modified the component modes such that they more closely approximated system modes. This method had the advantage of the elimination of interface generalized coordinates carried from component to system, which can be important for components with an excessive number of connection points. It also eliminated the need to distinguish between determinate and indeterminate interface constraints. However, the fact that the method is a branch method disallows the possibility of isolated development of a component, as information about the rest of the system is necessary to construct branch modes.

MacNeal¹⁰ presented a component mode method that used modes calculated while the interface points are free, fixed, or some free and some fixed which he

called "hybrid". This method allowed for an accuracy improvement by the addition of statically calculated "deflection influence coefficients" that are first order approximations to the mass and flexibility lost in the truncation of higher modes. Because these truncated modes are sometimes called residual modes, the approximations are called residual flexibility and residual mass. Rubin¹⁴ improved upon MacNeal's free-interface developments basically by taking his first-order static approximation of residual modes to a second order. Rubin's "residual inertia" gave a more accurate account for the effect of neglected higher modes. Hintz¹⁵ focused on the selection of the interface mode set - the modes that represent the component interface degrees of freedom. He stated that the use of either constraint modes or *attachment modes* for the interface mode set would result in a statically complete mode set. An attachment mode is a shape resulting from the imposition of a unit force on a single non-interface degree of freedom with zero force on all other freedoms, given the constraints on the component. Hintz stated that if the component was unconstrained, the resulting mode would be an inertia relief mode as defined by Rubin. A note by Craig and Chang¹⁶ involved a review of MacNeal's free-interface component mode method with residual flexibility and compared it to Hou's method with a numerical example.

This has been a brief review of some of the various approaches to the methods used in representing a structure with generalized coordinates from its components. Comprehensive surveys and comparisons of Component Mode Synthesis methods were given in 1971 by Hurty¹¹ and Hurty, Collins, and Hart⁹, as well as a concise but informative publication in 1977 by Craig¹⁷ including sixty-five references. Widrick²⁰

presented an error study across fixed, free, and hybrid methods, as well as a study of component level modeling error effects on the synthesized system.

The choice of whether to use a fixed-interface method, a free-interface method, or a hybrid method is of course ultimately up to the engineer. In general, it has been found that there are cases where some mode sets will probably represent the structure better than others.¹⁰ Fixed-interface methods are often used when a component's mass is very small relative to the system, whereas free-interface methods are often used when the component's mass is very large relative to the system, such as the fuselage of a flying launch vehicle compared to its tail stabilizer.

2.2 Synthesis Procedure

With respect to the previous discussion, the three component mode methods used in this study are: a fixed-interface method, a free-interface method, and a mixed-interface or hybrid method. All three methods use at least a set of constraint modes and a truncated set of normal modes. The way the normal modes are calculated basically determines the method. If the component normal modes are calculated with all interface coordinates constrained, then fixed-interface normal modes result, corresponding to a Craig-Bampton component mode method. For a free-interface method, the normal modes are calculated with all interface coordinates free. If this mode set is augmented by a set of inertia relief modes calculated from the rigid-body modes to account for neglected higher modes and improve accuracy, then the process corresponds to a traditional MacNeal-Rubin component mode method. A mixed-interface method uses normal modes calculated with some interface degrees of

freedom fixed and some free. This mode set can also be augmented by a set of inertia relief modes. This last method is a subset of MacNeal-Rubin component mode methods.

Specifically in this study, the three methods discussed here are used with the only exception that inertia relief modes are not used for the free and mixed-interface methods. The reason for this is that the choice of modes to be truncated consists of elastic modes and inertia relief modes. A severely truncated set of modes is used (e.g. 5 out of 60) and it is deemed that the low frequency normal modes are more important than the inertia relief shapes if one has to be chosen over the other. Also specific to this study, for the last method, the mixed-interface consists of three translational and two rotational constrained degrees of freedom and one free rotational degree of freedom - a pin joint. Thus the resulting normal modes are pinned modes.

There are many good references that describe the steps of Component Mode Synthesis as well as variations on parts of the procedure from the use of different methods,^{5-17,20} however the most generalized form of the procedure is essentially the same for any method, and it is described below.

2.2.1 General Procedure^{5,17}

In essence, the idea is to partition the structure into multiple substructures, as shown in Figure 2.1. Note that each component has interior degrees of freedom as well as interface degrees of freedom.

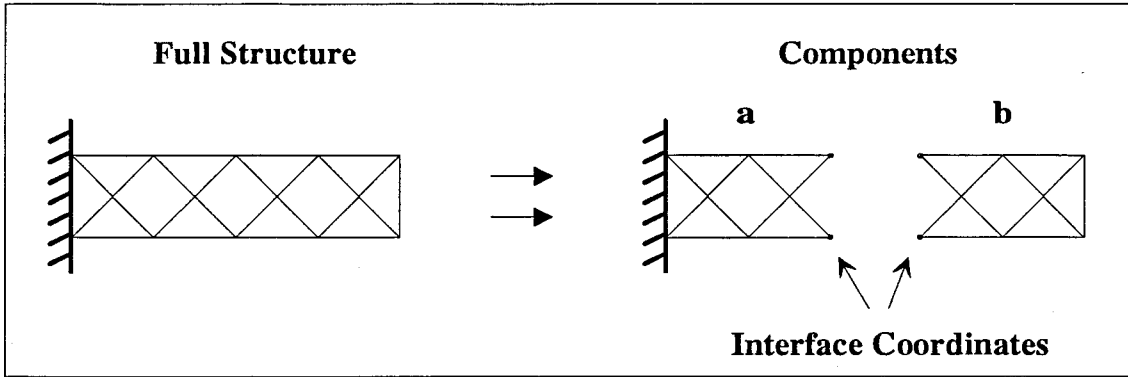


Figure 2.1: Partitioning of a Structure

The linear undamped equations of motion of components "a" and "b" are derived from the Lagrange equation and are given by

$$\begin{aligned} [m]^a \{\ddot{x}\}^a + [k]^a \{x\}^a &= \{f\}^a \\ [m]^b \{\ddot{x}\}^b + [k]^b \{x\}^b &= \{f\}^b \end{aligned} \quad (2.1)$$

Here, $[m]$ and $[k]$ represent the component mass and stiffness matrices respectively, and $\{x\}$ is the vector of component generalized *physical* displacement coordinates. For simplicity, damping will be left out of this derivation with the knowledge that it will have no net effect on the general process.⁵ The vector $\{f\}$ represents forces on the component. First, for each component, the eigen-problem is formed from Eq.s (2.1) and solved resulting in two sets of normal modes $[\Phi_N]^a$ and $[\Phi_N]^b$. These normal modes of course are specific to the constraints imposed on the components which are in turn determined by the method used. Figure 2.2 shows examples of imposed constraints for the structure in Figure 2.1 for fixed and free-interface methods.

For each component, the normal modes can be augmented by a set of rigid body modes $[\Phi_R]$, a set of constraint modes $[\Phi_C]$, and a set of attachment modes $[\Phi_A]$, depending on the method of choice for the given component. A Rayleigh-Ritz

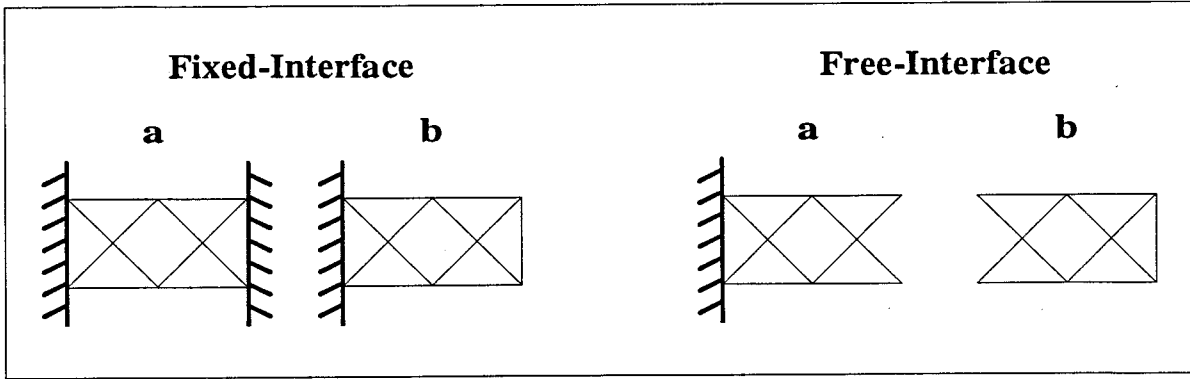


Figure 2.2: Constraints Used in Determining Normal Modes

transformation is then made for each component by

$$\{x\} = [\Phi] \{p\} = [\Phi_R \Phi_C \Phi_A \Phi_N] \begin{Bmatrix} p_R \\ p_C \\ p_A \\ p_N \end{Bmatrix} . \quad (2.2)$$

This transformation equation relates component generalized physical coordinates $\{x\}$ to component generalized *modal* coordinates $\{p\}$, which are the variables representing the amplitudes of the corresponding mode shapes. If we substitute Eq. (2.2) and its second derivative into Eq.s (2.1) and premultiply by the appropriate component transformation matrix $[\Phi]^T$, then we have the following component generalized equations of motion in the component modal spaces

$$\begin{aligned} [\mu]^a \{\ddot{p}\}^a + [\kappa]^a \{p\}^a &= [\Phi]^a T \{f\}^a \\ [\mu]^b \{\ddot{p}\}^b + [\kappa]^b \{p\}^b &= [\Phi]^b T \{f\}^b , \end{aligned} \quad (2.3)$$

where

$$[\mu]^a = [\Phi]^a T [m]^a [\Phi]^a \quad \text{and} \quad [\kappa]^a = [\Phi]^a T [k]^a [\Phi]^a , \quad (2.4)$$

with the same equations for component b . At this point the value of a truncated set of normal modes can be seen because for each component, the number of variables has decreased from the size of the vector $\{x\}$, which may be as large as 1 million, to the size of the vector $\{p\}$, which is typically on the order of 100.

We may now write the unconnected system mass and stiffness matrices as

$$[\mu] = \begin{bmatrix} \mu^a & 0 \\ 0 & \mu^b \end{bmatrix} \quad \text{and} \quad [\kappa] = \begin{bmatrix} \kappa^a & 0 \\ 0 & \kappa^b \end{bmatrix}, \quad (2.5)$$

and we can group all components to form the unconnected system equations of motion:

$$[\mu] \{\ddot{p}\} + [\kappa] \{p\} = \{\bar{f}\} \quad (2.6)$$

where

$$\{p\} = \begin{Bmatrix} p^a \\ p^b \end{Bmatrix} \quad \text{and} \quad \{\bar{f}\} = \begin{Bmatrix} [\Phi]^a T \{f\}^a \\ [\Phi]^b T \{f\}^b \end{Bmatrix}. \quad (2.7)$$

Note that if our system were composed of n components, Eq.s (2.5) would look like

$$[\mu] = \begin{bmatrix} \mu^a & & & \\ & \mu^b & & \\ & & \ddots & \\ & & & \mu^n \end{bmatrix} \quad \text{and} \quad [\kappa] = \begin{bmatrix} \kappa^a & & & \\ & \kappa^b & & \\ & & \ddots & \\ & & & \kappa^n \end{bmatrix}, \quad (2.8)$$

and Eq.s (2.7) would be altered as well. Although Eq. (2.6) may be useful as a tool of understanding the process, it is not yet directly useful to the synthesis. Of Eq. (2.6), Hurty⁵ says: "Physically interpreted, [this equation] can be considered as a set

of equations of motion for the group of components not connected together." The problem with the equation is that the vector $\{p\}$ contains coordinates that are not all independent. Duplicates will have formed at the interface points, as well as possible other independencies. However, compatibility at the interface coordinates provide us with constraint equations that can be used to put Eq.(2.6) into useful form. As shown in the next section, these constraint equations produce a transformation matrix $[\beta]$ (equivalent to Hurty's⁵ $[\beta]$ and Craig's¹⁷ $[S]$) that is a linear mapping relating system coordinates $\{p\}$ to a set of independent generalized coordinates $\{q\}$:

$$\{p\} = [\beta] \{q\} \quad . \quad (2.9)$$

If m is the size of $\{p\}$, and c is the number of constraints, then $m - c = n$ gives the size of $\{q\}$. Thus the resulting connected system will have n degrees of freedom, and the matrix $[\beta]$ will be $m \times n$ in size. Obviously then, if any normal component modes were truncated from any of the components, then the size of the system, n , will be equal to the sum of the degrees of freedom over all the components (minus external constraints) minus the number of truncated modes. Substituting Eq. (2.9) and its second derivative into Eq. (2.6) and premultiplying by $[\beta]^T$, results in a set of independent system equations of motion,

$$[M] \{\ddot{q}\} + [K] \{q\} = \{F\} \quad , \quad (2.10)$$

where

$$\begin{aligned} \{q\} &= \text{the vector of generalized system displacements} \\ \{\ddot{q}\} &= \text{the vector of generalized system accelerations} \\ [M] &= [\beta]^T [\mu] [\beta] = \text{the system generalized mass matrix} \\ [K] &= [\beta]^T [\kappa] [\beta] = \text{the system generalized stiffness matrix} \end{aligned}$$

$$[F] = [\beta]^T \{\bar{f}\} = \text{the vector of system generalized forces}$$

This equation can be solved for the system response and then Eq. (2.9) and the set of component equations of the form Eq. (2.2) can be used to back-transform and obtain the component response in the original component coordinate system.

2.2.2 Constraint Equations and Mode Sets of Different Methods

The procedure developed above is essentially the same for all traditional component mode methods with variations only on the derivation of the transformation matrix $[\beta]$ and the type and selection of mode sets used in Eq. (2.2). As has been stated previously, the calculation of component normal modes varies only with regard to the treatment of interface coordinates during the solution of the component eigenproblem. If a fixed-interface method is to be used, all interface coordinates should be constrained during the calculation as well as coordinates externally constrained, but all other coordinates in the component should remain free to vibrate. If a free-interface method is used, all interface coordinates should be free, except those externally constrained. If a mixed or hybrid method is to be used, the appropriate interface coordinates should be fixed or free in the analysis. Benfield and Hrudá¹³ calculate normal modes with mass and stiffness loaded interfaces, but they are actually calculating "branch modes" and thus do not present a traditional component mode method. The calculation of constraint and attachment modes, with inertia relief modes as a subset of attachment modes, have been described earlier and are developed in detail by Ref.s 6,12,14,15,20.

Although the derivation of the transformation matrix $[\beta]$ in Eq. (2.9) can vary (e.g. the method of Goldman⁷), the basic form is as follows^{5,6,17}. As we noted in Figure 2.1, the nodes of each component include interface coordinates $\{x_f\}$, and coordinates interior to the component $\{x_i\}$. Thus we can say

$$\{x\}^a = \begin{Bmatrix} x_i \\ x_f \end{Bmatrix}^a \quad \text{and} \quad \{x\}^b = \begin{Bmatrix} x_i \\ x_f \end{Bmatrix}^b \quad . \quad (2.11)$$

Compatibility between components however, dictates that

$$\{x_f\}^a = \{x_f\}^b \quad . \quad (2.12)$$

Equations such as these can be transformed into the system-wide p coordinate system of Eq.s (2.6) and (2.7) by using the appropriate form of transformation Eq. (2.2) for each component. Similar to Eq. (2.11), the $\{p\}$ coordinates can also be partitioned such that

$$\{p\} = \begin{Bmatrix} p_f \\ p_i \end{Bmatrix} \quad . \quad (2.13)$$

Once the equations of constraint on the set of interface coordinates have been transformed to the p system, they can be written in the form of coefficients of a constraint matrix $[A]$ by

$$[A] \{p_f\} = \{0\} \quad . \quad (2.14)$$

In general, the interior coordinates $\{p_i\}$ will be all independent, and the interface coordinates $\{p_f\}$ will contain dependent and independent coordinates, e.g. duplicate interface coordinates from adjacent components. The system generalized coordinates

$\{q\}$ can be partitioned in a manner similar to Eq. (2.13), however $\{q_f\}$, the interface subset of $\{q\}$, will be smaller than $\{p_f\}$ because $\{q_f\}$ will contain only independent coordinates. It can be immediately defined however, that

$$\{q_i\} \equiv \{p_i\} \quad , \quad (2.15)$$

because there are no compatibility constraints on the interior coordinates. This will correspond to partitions of the transformation matrix $[\beta]$ that are unity. All we seek now is a relationship between $\{q_f\}$ and $\{p_f\}$. According to the constraints, some interface coordinates $\{p_f\}$ will be dependent upon others, so $\{p_f\}$ and $[A]$ can be partitioned into dependent and independent coordinates

$$[A_1|A_2] \begin{Bmatrix} p_{f1} \\ p_{f2} \end{Bmatrix} = \{0\} \quad , \quad (2.16)$$

where $\{p_{f1}\}$ is the dependent subset, and $\{p_{f2}\}$ is the independent subset. These subsets must be chosen such that $[A_1]$ is square and nonsingular. Now, it can be said that

$$\{q_f\} \equiv \{p_{f2}\} \quad , \quad (2.17)$$

because $\{p_{f2}\}$ is an independent set. Finally, from Eq. (2.16),

$$\{p_{f1}\} = -[A_1]^{-1}[A_2] \{p_{f2}\} \quad , \quad (2.18)$$

which, combined with Eq. (2.17) produces

$$\{p_f\} = \begin{Bmatrix} p_{f1} \\ p_{f2} \end{Bmatrix} = \begin{bmatrix} -[A_1]^{-1}[A_2] \\ [I] \end{bmatrix} \{q_f\} \quad . \quad (2.19)$$

Now there is a relation between the initial system interface coordinates and the final independent system interface coordinates. This relation, combined with Eq. (2.15) through careful partitioning yields the complete transformation equation from $\{p\}$ to $\{q\}$ given by Eq. (2.9) in the previous section.

2.3 Implementation of CMS in NASTRAN

The structural analysis code MSC/NASTRAN is a finite element program that has the capability of being able to perform Component Mode Synthesis (CMS). Because NASTRAN was used in this study, the author thought it appropriate to include some remarks on the implementation of CMS in NASTRAN, because the process is not necessarily a trivial matter. There are many publications available which one can use to acquaint themselves with NASTRAN²¹⁻²⁷, as well as on-site courses²¹⁻²³ offered by the MacNeal Schwendler Corporation²⁸ to develop the finer points of structural synthesis in NASTRAN. Therefore, this section is optional reading and is in no way intended to be an encompassing source of information, but rather an illustrative discussion of how an implementation of CMS in NASTRAN varies for the methods used in this study. To begin, a discussion is necessary of some of the preliminary concepts needed to write an input file for use in NASTRAN. In the following discussion, the use of the word "card" is meant to imply a line in the NASTRAN input file. Its use still today dates the early success of the NASTRAN computer code.

2.3.1 Superelements²²

In the analysis of structures and structural systems, as has already been stated, it is beneficial to partition the structure, or break it into components. In NASTRAN, this is done with the use of the "superelement". To do so, all the engineer need do is use the "SESET" card in the "Bulk Data Deck". The Bulk Data Deck is in most cases the main part of the NASTRAN input file, and also the most intuitive. It is in the Bulk Data where the physical properties and geometry of the structure to be analyzed are input. After the structure is defined in the Bulk Data, the SESET card can be introduced to define the parts of the structure that include the interior degrees of freedom of the component or superelement. The coordinates (nodes) where the superelement interfaces with the rest of the structure are coordinates adjacent to the interior coordinates defined by the SESET card. They are automatically designated by NASTRAN as boundary coordinates of the superelement and they are called "exterior" to the superelement. It is these coordinates that will be held fixed or remain free during the eigen-analysis of the component.

Any other part or even the entire structure can be partitioned in this way. Anything not designated as interior to a superelement is left in the "residual structure" which therefore also includes exterior points of immediate superelements. Coordinates of the residual structure are left as physical coordinates during the synthesis of the system, but may be transformed to modal space later if the synthesized system is to be itself modally reduced.

2.3.2 Case Control Structure²²

The NASTRAN input file consists of only three required sections, the "Executive Control" section, the "Case Control" section, and the "Bulk Data" section. The Executive Control section, in its simplest form, basically tells NASTRAN which solution sequence to execute on the input file - statics, normal modes, transient heat transfer, etc. This section can also include user-defined alterations to the chosen solution sequence in the form of "DMAP" statements. DMAP is the Direct Matrix Abstraction Program that NASTRAN actually runs in. The Case Control is the section of the input file which tells NASTRAN more specifically what analysis to perform on the structure or its components. Here requests are made such as loading application, constraint selection, eigen-analysis method specification, displacement output, etc. It is also here where the requests to perform Component Mode Synthesis are defined.

In simple form, the Case Control can consist of a series of subcases, each performed sequentially in the order requested. When performing CMS, it is standard to use early subcases to perform individual analysis of superelements, and then a later subcase is used to synthesize these superelements, as well as any parts of the residual structure into the total system. This is accomplished by the use of the "SUPER" card, which designates which superelement or set of superelements to analyze during the subcase that the SUPER card is in. For example, if subcase 1 includes a SUPER card that designates superelements 10 and 20, then during subcase 1 superelements 10 and 20 will each individually be analyzed with no affect on the rest of the structure. In CMS, information from this subcase will be transferred to the subcase which

includes the residual structure and will be used in the synthesis. The information carried will be the generalized coordinates of the transformed component, i.e. the amplitude variables of the component mode shapes. These mode shapes can consist of normal modes, rigid-body modes, constraint modes, attachment modes, etc.

In NASTRAN, *there is no explicit command* to tell the program which CMS method to use - Craig-Bampton, MacNeal with residual flexibility, etc. It is completely up to the engineer to decide on the method and then include the correct input file statements. The default method of CMS in NASTRAN is Craig-Bampton - fixed-interface normal modes augmented with constraint modes to handle the interface coordinates. To change these settings for one's input file, one must take advantage of NASTRAN's set notation.

2.3.3 Set Description²²

In NASTRAN, structural coordinates or degrees of freedom are accounted for by their placement in a given set. When matrix partitioning is performed, it is done with respect to given set information. For example, all the physical grid points of a structure, including extra degrees of freedom called "SPOINT"s, make up the "g" set. The g set is in turn composed of the "m" set, the "s" set, and the "f" set. The m and s sets contain coordinates eliminated by applied constraints, whereas the f set contains unconstrained (*free*) coordinates making up the part of the structure free to vibrate.

Of interest in CMS are the f set, the "o" set, the "q" set, the "b" set, and the "c" set. For a given component, the f set is the sum of the o, q, b, and c sets. The o set contains coordinates omitted during structural partitioning, such as the interior

points of a superelement. The motion of these coordinates however is approximated by the generalized coordinates representing the selected normal modes of the structure. These generalized coordinates comprise the q set of a superelement. Generalized coordinates are designated to be in the q set through the use of the "SEQSET" card. If the number of generalized degrees of freedom defined on this card is less than the number of modes calculated in the superelement analysis subcase, then modal reduction will result. For example, if only ten q set freedoms are designated on the SEQSET card for a superelement whose analysis resulted in sixty normal modes, then only the first ten normal modes will be used to represent that component in the synthesis of the total structure. If more specific modes than just the high frequency modes are desired to be eliminated, then this can be accomplished by the following procedure. Use the SEQSET card to specify all the modes sequentially up to the highest mode desired to keep, then eliminate the unwanted interspersed lower modes by individually constraining their corresponding degrees of freedom previously specified. This can be accomplished with the "SPC" or Single Point Constraint card. This will give the effect that the unwanted modes were never selected to begin with.

The b and c sets consist of component boundary coordinates that are fixed or free, respectively, during the component modal analysis. It is the choice of the b and/or c set that the engineer uses to partially define the CMS method he/she will use. As a default in NASTRAN, for each structural component, boundary coordinates are put in the b set and constraint modes are generated. Thus, if no set memberships are specified otherwise, the traditional Craig-Bampton component mode

method will be used on all superelements. To specify the set membership of component boundary coordinates, the "SEBSET" and "SECSET" cards are used for the *b* and *c* sets respectively. To employ a free-interface component mode method, the user employs the SECSET card for all the boundary coordinates of the component being analyzed. Constraint modes will automatically be generated. In general normal modes analysis, the solution to the eigen-problem for a free-free component will result in free-free normal modes and rigid-body modes. However, NASTRAN checks all these modes to see if any are linear combinations of the constraint mode shapes already generated and eliminates any that are. In most cases rigid-body modes will be linear combinations of the component constraint modes and therefore will not be a part of the information sent by NASTRAN to the residual structure as generalized coordinates specified on the SEQSET card. To supplement free-free normal modes and improve accuracy, the generation of component inertia relief modes can be requested by inserting the "PARAM,INRLM,-1" card into the Bulk Data section. To perform a mixed-interface component mode method, designate boundary degrees of freedom to be in either the *b* or the *c* set, although no single degree of freedom can be allowed in both sets. In this case, the normal modes calculated will be of a mixed-interface type, and if requested, inertia relief modes will be calculated to augment the set.

As an example, a NASTRAN input file similar to those used in this study is presented in Appendix A. In NASTRAN, the dollar sign (\$) signifies a comment to follow. This input file is for the structure described in the next chapter, with Component Mode Synthesis. Modal reduction is performed on the "2nd" beam, via a

mixed-interface method. Note the SEBSET and SECSET card entries. To create pinned normal modes, three translational and two rotational degrees of freedom (1 to 5) at the base grid point were designated in the *b* set while the third rotational freedom (6) was designated in the *c* set. To represent the component in the synthesis, two bending and one torsional component modes were chosen to be kept. A priori knowledge of the pinned component modal response dictated that the necessary modes to keep would be the first two and the fourth, which correspond to degrees of freedom 1001 to 1004, while 1003 is constrained by the second SPC card. Note that these degrees of freedom occupy "scalar points" as defined on the SPOINT card. Scalar points are essentially extra one-dimensional variables added to the system for use here as generalized coordinates.

III. INTRODUCTION TO THE FINITE ELEMENT MODEL

In order to evaluate the effects of component boundary conditions and configuration on mode set selection for a component in a structural system, a finite element model was created to be analyzed in NASTRAN. This structural model was designed such that it would illustrate reasonably well the main points of the study. In this present study, it is the dynamic behavior of a structure linearized about varying given configurations that is under consideration. Therefore, it was decided that a reasonable model for this study would be one that included a component that could articulate at large angles as well as have various imposed conditions on the joint about which the component articulates. A two-component structure was selected, where one component would be the one modally reduced, and the other would be kept "exact", that is not modally reduced - fully represented by its physical degrees of freedom. This way there would be no ambiguity as to which component modal truncation would contribute the most to synthesized system frequency and mode shape error. Also, the attempt to add more than two components to the structure might have unnecessarily complicated the problem or the results achieved. The two components were selected to be of similar size so that no single component mode method would be favored over another. For example, in a given system if a reduced component is very much smaller in size and mass than the rest of the structure, then in some cases it has been proposed that a fixed-interface mode set would better suit the component¹⁰. It was decided to make both components the same size and physical properties in the event that conclusions could be drawn from their similarity.

3.1 Description

Pursuant to the above stated needs, a two-beam linkage was selected as shown in Figure 3.1. Here one of the beams, Beam 2, is the component which is modally reduced in the study. The other beam, Beam 1, was left in the finite element model as "exact", that is, it was not modally reduced but kept in a physical representation.

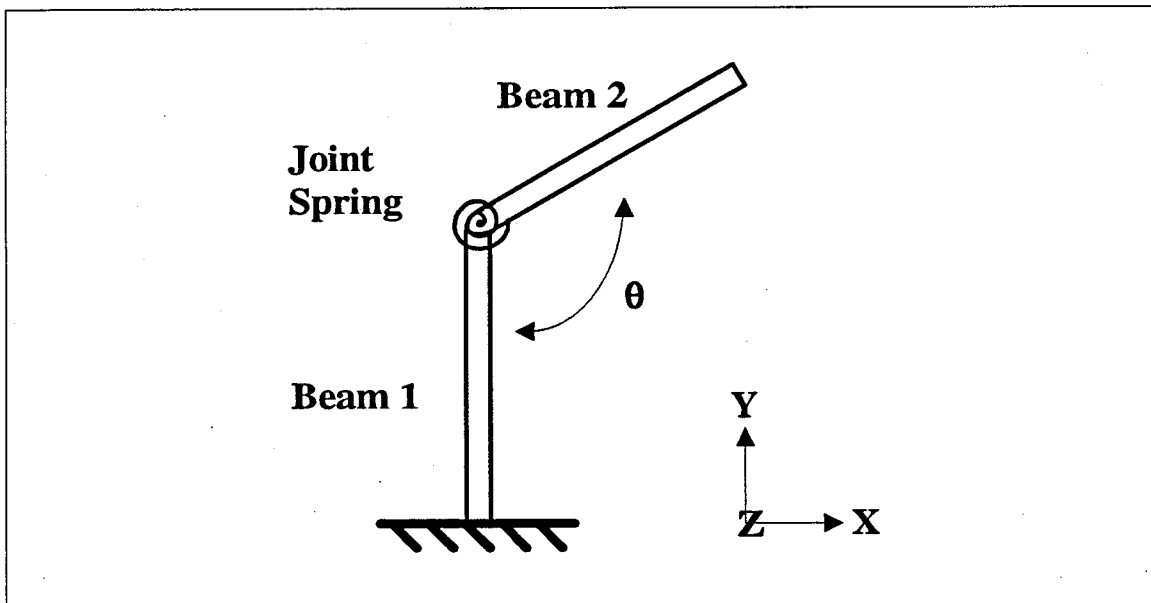


Figure 3.1: The Finite Element Model

The two beams are connected by a "pin" joint - a single degree of freedom joint allowing rotation only in the plane of the figure. Constraining motion at this joint is a linear angular spring whose spring constant values vary as a parameter in this study as described in Section 3.3. Note however, that the spring is "reset" at each new configuration, or in other words, at each configuration, there is no net force in the spring when the system is at rest. The spring is also not modally reduced. In NASTRAN, the joint angular spring and Beam 1 comprise the residual structure.

In the event that conclusions from this study might be useful to spacecraft structures and robotics applications, two more modelling decisions were made. First, Beam 1 was cantilevered to its base. The first or primary segments of many robotic systems do not slew, but are present merely to extend the overall reach area of the robotic arm. The second of these decisions was to model Beam 2 similarly to the lower arm boom of the Space Shuttle Remote Manipulator System with respect to geometry and material properties. As stated, Beam 1 was modelled using the same properties as Beam 2.

3.2 Material Properties

This section is devoted to the description of the actual physical properties chosen for use in the finite element model. As has been stated previously, the geometry and material properties of both the beams in this model are similar to those of the "lower arm boom" (Link 4) of the Space Shuttle Remote Manipulator System (SRMS). These values are not purported to be exact, as there are various sources on SRMS properties which are not in total agreement, and it is not the purpose of this study to define accurate SRMS properties. However, much of the information used here derives from the description of the lower arm boom found in the *Payload Deployment and Retrieval System Simulation Database*²⁹ (PDRS), and therefore produces a component that to some degree approximates the dynamics of the lower arm boom of the SRMS.

The two beams are both modelled as homogeneous, straight, thin-walled tubes of constant circular cross-section, which are represented in NASTRAN by a series of

ten one-dimensional "CBEAM" elements per beam with three-dimensional properties allocated to them. Coupled mass is used to increase model accuracy. Due to the one dimensional modelling, no special provisions are made for changes in geometry at the tube ends or joints. The joint is modelled in NASTRAN as an "RBE2" (a rigid body element) which is basically a set of constraint equations between the motion of two coincident grid points - one each from the connected ends of both beams. This set of constraint equations connects all but one degree of freedom from each coincident grid point - the one unconnected freedom being the rotational coordinate of the joint. The joint angular spring is modelled in NASTRAN with the "CELAS2" element. The only property of interest for the spring is the spring constant K which is a parameter of the study with the range

$$4.4129 \text{ E}+3 \leq K \leq 1.7651 \text{ E}+8 \text{ (ft-lb/rad)}.$$

Its derivation is described in Section 3.3. The properties of the beams are given in Table 3.1.

The configuration of the system (Figure 3.1) is also a parameter in this study. It is varied simply by changing the angle of Beam 2 relative to Beam 1. This is accomplished by defining Beam 2 with respect to a coordinate system, via the "CORD2R" card, which is simply redefined at each new configuration before NASTRAN is run. Dynamic issues involved with slewing a body are not examined here because this study involves only the inspection of the linearized vibrational dynamics of the system at given static configurations. The configurations chosen in this study are named by the angle θ the two beams make with each other. They are

$$\theta = 45^\circ, 90^\circ, 135^\circ, \text{ and } 180^\circ.$$

Table 3.1: Beam Properties

PROPERTY	VALUE	UNITS
Mass	5.99	slugs
Length †	23.2	feet
Tube Diameter (outside)	1.083	feet
Tube Wall Thickness	4.583 E-3	feet
Area †	0.0155	feet ²
Density †	16.66	slug/feet ³
Moment of Inertia 1 †	2.26 E-3	feet ⁴
Moment of Inertia 2 †	2.26 E-3	feet ⁴
Product of Inertia †	0.0	feet ⁴
Polar Moment of Inertia †	4.52 E-3	feet ⁴
Modulus of Elasticity †	3.02 E+9	lb/feet ²
Shear Modulus †	7.94 E+8	lb/feet ²

† Used in the NASTRAN input file.

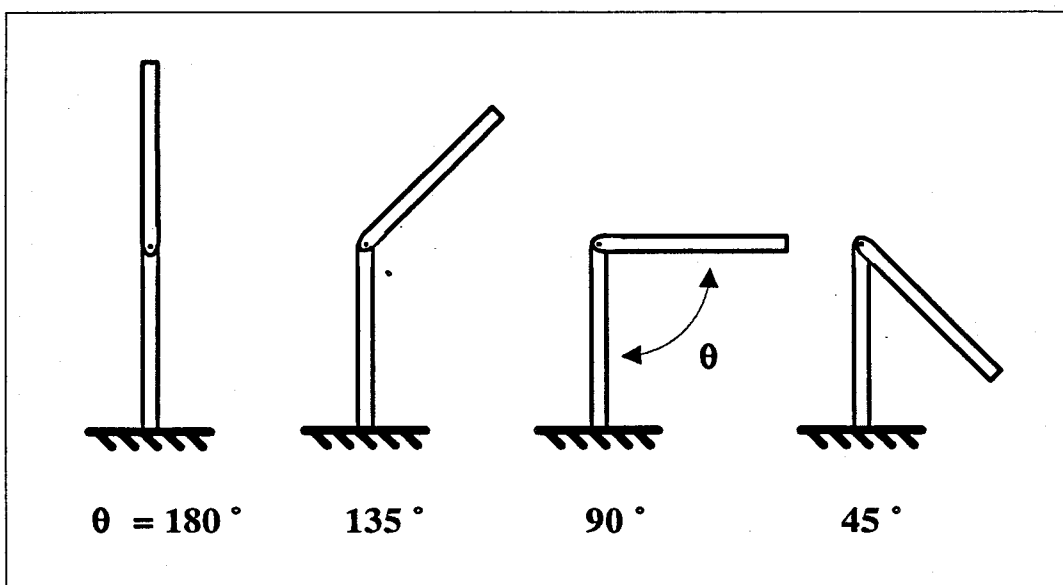


Figure 3.2: Varying Model Configurations

Figure 3.2 shows the model in the various configurations.

For reference, a listing of the natural frequencies of Beam 2 is given in Table 3.2. Combinations of these listed modes make up the normal mode sets used in this study. For example, one part of the study uses a set including the first four bending modes of the component, using each interface method. If the interface is of the fixed type, this set is given by the first four component modes. For a mixed interface, the set includes the first three and the fifth mode. Not included in the table are the one rigid body mode from mixed-interface and the six rigid-body modes from free-interface. These and all rigid-body modes are zero frequency modes.

Table 3.2: Natural Frequencies of Beam 2

Mode #	FIXED-INTERFACE		FREE-INTERFACE		MIXED-INTERFACE	
	Freq. (Hz)	Type	Freq. (Hz)	Type	Freq. (Hz)	Type
1	5.345	Bending (z) †	34.01	Bending (z)	5.345	Bending (x)
2	5.345	Bending (x)	34.01	Bending (x)	23.44	Bending (z)
3	33.50	Bending (x)	93.78	Bending (z)	33.50	Bending (x)
4	33.50	Bending (z)	93.78	Bending (x)	74.32	Torsion
5	74.32	Torsion	148.2	Torsion	75.97	Bending (z)
6	93.82	Bending (x)	184.0	Bending (z)	93.82	Bending (x)
7	93.82	Bending (z)	184.0	Bending (x)	144.9	Axial
8	144.9	Axial ‡	289.0	Axial	158.6	Bending (z)

† Coordinate in parenthesis indicate axis perpendicular to plane in which bending occurs.

‡ "Axial" refers to tension / compression.

Note that the calculation of these modes is independent of both joint stiffness and system configuration because these are the vibrational modes of the detached

component and are functions only of the imposed interface constraints. This is helpful because even though these modes are independent of system characteristics, different sets of them can affect synthesized system motion differently as the system changes joint spring stiffness and configuration. It is the point of this study to examine that affect. Note also that only the modes of Beam 2 are used in the synthesis as Beam 1 is left unreduced.

3.3 Derivation Of Joint Angular Spring Constant, K_θ

One of the parameters varied in this study is the stiffness of the joint angular spring. In order that a reasonable range of joint angular spring constants K be used in the analysis, it was decided to derive a standard spring constant K_θ for the given model, and then use multiples of it to create a range of spring constants. This would produce finite element models with relatively weak to relatively strong angular springs at the pin joint.

One appropriate standard spring constant for the joint about which the second beam rotates is as follows. If the second beam in the model were imagined to be cantilevered on the joint end and free on the other end, and a unit normal force was applied to the free end of the beam, then that end would deflect a certain amount δ , such that according to elementary theory of bending³⁰,

$$\delta = \frac{Pl^3}{3EI} \quad (3.1)$$

Now imagine a rigid beam of the same length that is pinned-free and has an angular spring on the pinned end. Then, a standard spring stiffness can be seen as

one which would allow the free end of the rigid beam to deflect the same amount δ while under the same unit normal force. For such a rigid beam and spring system, the deflection δ from statics is

$$\delta = l \sin\left(\frac{pl}{K_0}\right) \quad (3.2)$$

Combining Eq.s (3.1) and (3.2), and solving for K_0 using a small angle assumption gives

$$K_0 = 3 \frac{EI}{l} \quad (3.3)$$

For the model used in the present study, given the properties described earlier,

$$K_0 = 8.826 E+5 \left(\frac{ft-lb}{rad} \right) \quad (3.4)$$

From this K_0 , the range of angular spring constants K used in the finite element model is

$$\frac{1}{200}K_0 \leq K \leq 200K_0 \quad (3.5)$$

The actual values used for K in this range are multiples of K_0 and are listed in Table 3.3. In the table, K/K_0 is called the Model Joint Stiffness Factor, and K is the model joint stiffness used in the finite element model.

As an illustration of the worthiness of this standard spring constant, the data in general show that transitions from "weak spring" to "strong spring" models are centered around $K = K_0$, or equivalently unity Model Joint Stiffness Factor. Figure 3.3 shows joint spring strain energy in the first five exact (unreduced by CMS)

Table 3.3: Joint Angular Spring Constants K Used

Values of K in (ft-lb/rad)

$K/K_0 =$	1/200	1/100	1/50	1/20	1/10
$K =$	4.413 E+3	8.826 E+3	1.765 E+4	4.413 E+4	8.826 E+4
$K/K_0 =$	1/5	1/2	1	2	5
$K =$	1.765 E+5	4.413 E+5	8.826 E+5	1.765 E+6	4.413 E+6
$K/K_0 =$	10	20	50	100	200
$K =$	8.826 E+6	1.765 E+7	4.413 E+7	8.826 E+7	1.765 E+8

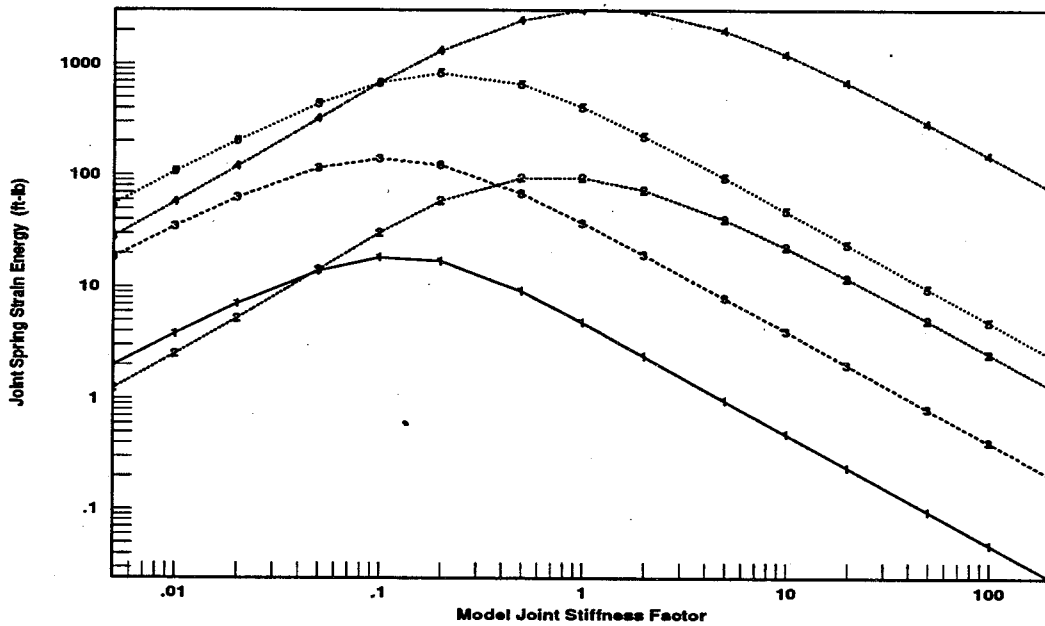


Figure 3.3: Joint Spring Strain Energy, System Modes 1-5, $\theta = 90^\circ$

system modes of deformation in the x-y plane, for the right-angle configuration ($\theta = 90^\circ$). Note that strain energy maxima occur near K_0 . This is intuitive because strain energy will be minimized when the spring constant approaches zero and the deformation is finite, or when the spring constant is finite but large enough to force the deformation to approach zero. Another approach for this criteria might be to examine the slope at the end of the beam instead of the displacement. In this case, the similar derivation gives

$$K_0 = 2 \frac{EI}{l} , \quad (3.6)$$

where the only difference in K_0 from Eq. (3.3) is the coefficient of 2 instead of 3.

As an end note, the reader is reminded that this development of K_0 is intended only so that a range of joint spring stiffnesses may be used that are *appropriate for this model*. In a sense, K_0 is found so that joint spring stiffness can be nondimensionalized as a parameter in the study.

IV. EVALUATION OF THE SYNTHESIZED SYSTEM

The objective of this study was to determine the effect of component configuration and joint spring stiffness on the selection of component mode sets. This was accomplished by modally reducing Beam 2 of the model described in Chapter 3 while individually varying given parameters. The parameters varied in this study were

- a) Number of Elastic Modes Kept for Beam 2,
- b) Type of Elastic Modes Kept for Beam 2,
- c) Joint Spring Stiffness,
- d) Configuration Angle θ .

Parameters "a" and "b" have to do with the component mode set selection process, while parameters "c" and "d" have to do with the varying of boundary conditions. In order to evaluate the robustness of the individual mode sets, they were used in a Component Mode Synthesis of the entire structural system. It is only logical for a study on mode set selection, that component mode sets find their evaluation in their performance within Component Mode Synthesis. To evaluate something that is inherently an approximation, it is also logical to compare it to an unapproximated counterpart. Therefore, the mode sets in this study were evaluated simply by using them in a Component Mode Synthesis of the system and then comparing the characteristics of the synthesized system to the predetermined characteristics of the "exact" system (system meaning of course the model). Exact is used here in the sense that the exact system is the full finite element model of the

system including all the degrees of freedom in the model in the physical, unreduced form. Exact is not used in the sense of a real life laboratory-type setup of two physical beams, because it is not the accuracy of the finite element method that is in question here.

Because Beam 2 is the only modally reduced component, obviously if Beam 2 from the synthesized system were unapproximated then the exact and synthesized systems would be equivalent. Note also that if *all* the normal modes were included in any of the mode sets used for Beam 2 in the synthesis, then the characteristics of the synthesized and exact systems would be equivalent. This is a consequence of the Rayleigh-Ritz transformation². If component eigenvectors $[\Phi]$ are used as the Ritz shapes then the transformation from physical to modal space, given by

$$\{x\} = [\Phi] \{p\} \quad , \quad (4.1)$$

is exact until component modes are truncated. Therefore, the truncation of modes is the only parameter to cause inconsistencies between the characteristics of the synthesized and physical systems, for a given joint angle and joint spring stiffness. These inconsistencies, or errors, will vary with each synthesis method. Therefore, varying the type of modes kept will give an interesting view of the robustness of different types of mode sets.

The characteristics of the synthesized system used for this evaluation were system natural frequencies and mode shapes. Strain energy from static mode shape deformation was used as an aid in deciding which synthesized system modes should be compared to which exact system modes.

4.1 Basic Procedure

In general, the procedure used for this study was as follows. Examining a single configuration at a time, first the exact model was analyzed with the fifteen different joint spring stiffnesses given in Table 3.3. Next, the synthesized reduced models were analyzed, each with the fifteen different stiffnesses. These models were simply systems where Beam 2 was represented in the synthesized system by a set of six constraint modes and a truncated set of elastic normal modes. The type of reduced model was determined completely by the mode set used as generalized coordinates for the reduced component, Beam 2. Table 4.1 lists the types of mode sets used according to the interface constraint employed and the number of kept modes. As stated, for each entry in this table as well as the exact system, there were actually fifteen NASTRAN input files, each corresponding to a stiffness from Table 3.3. Finally, the entire process was repeated for each different configuration. Four configurations were examined: $\theta = 45^\circ$, 90° , 135° , and 180° .

4.2 Mode Sets

In this study, the reduced models were chosen to be of three main types: fixed-interface, free-interface, and mixed-interface. Under each interface type, there were six sub-types defined by the number of kept modes, as shown in Table 4.1. Given the natural frequencies and mode types (i.e. bending, torsion, tension, etc.) of the component to be reduced listed in Table 3.2, the component mode numbers used in each set are given in Table 4.2.

Table 4.1: Mode Sets Used for Beam 2

Interface Constraints	Elastic Modes Kept	Total Kept
Fixed-Interface	2 Bending	2
	2 Bending, 1 Torsion	3
	4 Bending	4
	4 Bending, 1 Torsion	5
	6 Bending, 1 Torsion	7
	6 Bending, 1 Torsion, 1 Axial	8
	Free-Interface	2 Bending
2 Bending, 1 Torsion		3
4 Bending		4
4 Bending, 1 Torsion		5
6 Bending, 1 Torsion		7
6 Bending, 1 Torsion, 1 Axial		8
Mixed-Interface		2 Bending
	2 Bending, 1 Torsion	3
	4 Bending	4
	4 Bending, 1 Torsion	5
	6 Bending, 1 Torsion	7
	6 Bending, 1 Torsion, 1 Axial	8

The last column of Table 4.2, headed Total Z-Modes, lists the number of component bending modes about the z-axis that are found in the mode set. For example, the set of 2 bending modes is composed of one z-bending component mode and one x-bending component mode. Here, x and z are given in the sense of the

Table 4.2: Component Mode Numbers in the Mode Sets

Elastic Mode Sets	Total	Component Mode Numbers			Total Z - Modes
	Kept	Fixed	Free	Mixed	
2 Bending	2	1,2	1,2	1,2	1
2 Bending, 1 Torsion	3	1,2,5	1,2,5	1,2,4	1
4 Bending	4	1 to 4	1 to 4	1,2,3,5	2
4 Bending, 1 Torsion	5	1 to 5	1 to 5	1 to 5	2
6 Bending, 1 Torsion	7	1 to 7	1 to 7	1 to 6,8	3
6 Bending, 1 Torsion, 1 Axial	8	1 to 8	1 to 8	1 to 8	3

coordinate system of the model (Figure 3.1), and the component is imagined standing up along the y-axis while its component modes are being calculated. The number of z-bending component modes used in the set are of interest because it is z-bending modes that affect system z-bending motion. Results not shown here indicated that as expected, the x-bending component modes had no affect on z-bending system modes. X-bending component modes are included in the mode sets here for the following simple reason. For the fixed- and free-interface cases, component x- and z-bending modes come in pairs with the same natural frequency for a bending-symmetric model, and there is no way to predict which will come first or that it will be the same during each analysis. Therefore, to avoid possible errors, component bending modes were taken in these pairs when kept in a mode set. Pinned modes from the mixed-interface cases of course do not occur in equal-frequency bending mode pairs, however for easier comparison to the other types of interface cases, the mixed-interface x-bending

component modes were also kept.

Note that some mode sets use "non-sequential" component modes. For example, the second fixed-interface mode set uses component modes 1, 2, and 5. This is to create a set that has only 2 bending and one torsion mode. The severe truncation (e.g. 3 out of 60 modes) of the mode sets used in this study makes this sort of specialized selection necessary. To include the 3rd and 4th component mode for completeness significantly reduces the error - such a mode set is its own case for comparison. The severity of the mode set truncation is a tribute to the accuracy of the Rayleigh-Ritz reduction. In other words, to get any kind of recognizable error in the low frequency synthesized system modes, it was necessary to truncate most of the component mode set of about 60 total modes (60 - fixed; 66 - free; 61 - pinned).

Note also that the mode sets themselves in comparison will produce information on the effect of adding certain types of component modes to the set. For example, comparing the results of the mode set with 2 modes to the results of a mode set with three modes will show the effects of adding only a torsion mode. Similarly, the next set will show the effects of adding only bending modes to the set. The last two sets will show the difference between including a tension mode and not including it, which in some cases will be seen to be a relatively large difference.

4.3 Error Criteria

In general, synthesized system modes were compared to exact system modes by computing the error in natural frequency and mode shape. In this study, natural frequency error was calculated as a standard percent error according to

$$\% \text{ ERR} = 100 * \frac{|(\omega_e - \omega_s)|}{\omega_e} , \quad (4.2)$$

where ω_e and ω_s are the exact and synthesized system frequencies respectively.

Although frequency error can be a reliable test of comparison, a more complete test can be made by using mode shape error as well. This way, both the temporal and spatial qualities of the systems can be compared. In structural dynamics, a good geometrical parameter often used is the Modal Correlation Coefficient (MCC) given by

$$MCC = \frac{|\phi_e^T \phi_s|}{\|\phi_e\| \cdot \|\phi_s\|} . \quad (4.3)$$

where ϕ_e and ϕ_s are the exact and synthesized system mode shapes respectively, with the single and double lines representing the absolute value and norm respectively. An MCC value of one indicates that the two mode shapes are equal whereas a value of zero indicates that the two shapes are orthogonal. Wei and Allemang³¹ give a background of some modal comparison parameters such as the Modal Assurance Criteria (MAC) as well as a new one. The MAC is commonly used to compare analytical shape vectors to experimental shape vectors. The MCC given above is the square root of the MAC, and suffices for the purposes of this study. For comparison to frequency error however, what was actually used in this study will be referred to as the "Modal Correlation Error" (MCE). MCE is related to the MCC simply by

$$MCE = 1 - MCC . \quad (4.4)$$

This way, low frequency error can correspond to low mode shape error.

4.4 Bending in the "Plane of Interest"

Although it may not be obvious from Figure 3.1, the model used in this study is three-dimensional. The configuration is changed by varying the angle θ . This only occurs within the "x-y" plane, however the two beams deform out of the x-y plane as well as encounter torsion. In general, when the synthesized system modes are computed, all *bending* mode shapes fall into two categories. These are: 1) bending about an axis parallel to the "z" axis such that all translational deformation occurs in the x-y plane, and 2) bending about axes such that translational deformation occurs in the z direction and little or no deformation occurs in the x-y plane, and more importantly, no deformation occurs that effects the angle θ between the two beams. These types of bending will be called 1) "z-bending" and 2) "xy-bending", respectively. An illustration of these two types of bending is given in Figure 4.1.

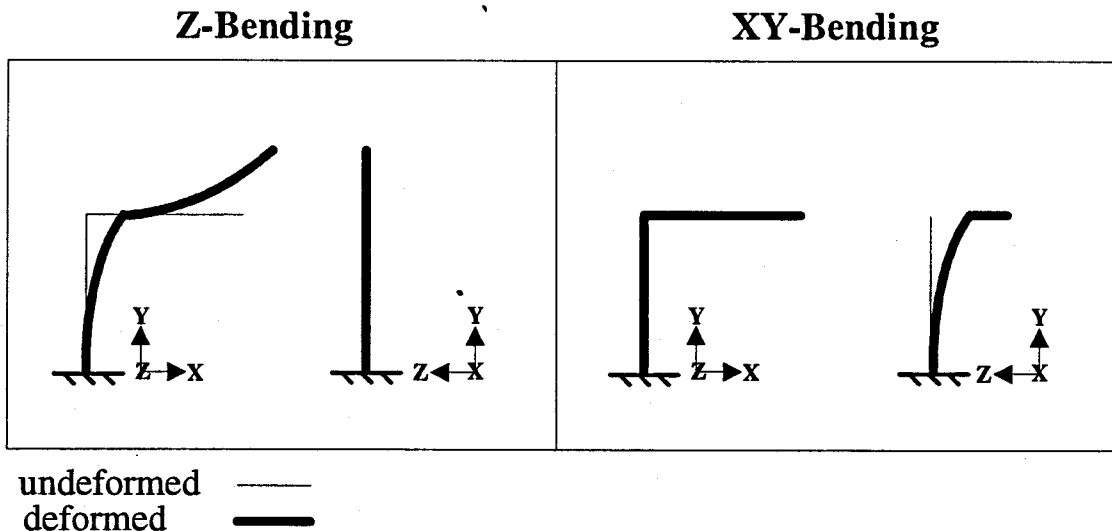


Figure 4.1: Model Z-Bending vs. XY-Bending

Note however, that the model is defined such that configuration only changes in the x-y plane about an axis parallel to the z-axis, and the joint angular spring only affects motion in the x-y plane. Due to these facts, the only bending mode shapes of interest to this study are the "z-bending" shapes because they are mode shapes of deformation within the "plane of interest".

In general, when system modes shapes were calculated for this model, the low frequency shapes consisted mostly of z-bending and xy-bending modes, with one after the other. To vary the effects of the joint angular spring, the system frequencies and modes were calculated in sets of fifteen different joint angular spring constants in logarithmic increments as given by Eq. (3.5) and Table 3.3. Because the joint angular spring affects z-bending motion, the z-bending modes in general were a function of the spring stiffness. Thus, for example, the fundamental frequency of a system that included a "stiff" spring would in general be higher than the fundamental frequency of a system including a "weak" spring. The xy-bending modes however, were not a function of spring stiffness, because they did not involve motion in the x-y plane. Thus the fundamental system frequencies of xy-bending modes would be equal for varying stiffnesses. With this in mind, when the natural frequencies were calculated for fifteen models differing only in joint spring stiffness, a matrix of frequencies was generated with fifteen columns and as many rows as there were system natural frequencies. Table 4.3 gives an example of the first four rows of the frequency matrix generated from the exact model of $\theta = 90$ degrees.

Table 4.3: First Four Exact System Natural Frequencies, $\theta = 90^\circ$ (Hz)

K/K_0	1/200	1/100	1/50	1/20	1/10	1/5	1/2	1
1	0.320	0.448	0.621	0.929	1.199	1.442	1.515	1.515
2	1.515	1.515	1.515	1.515	1.515	1.515	1.641	1.712
3	2.380	2.393	2.420	2.505	2.651	2.927	3.495	3.950
4	4.382	4.382	4.382	4.382	4.382	4.382	4.382	4.382

K/K_0	2	5	10	20	50	100	200
1	1.515	1.515	1.515	1.515	1.515	1.515	1.515
2	1.747	1.768	1.774	1.778	1.780	1.780	1.781
3	4.311	4.382	4.382	4.382	4.382	4.382	4.382
4	4.382	4.605	4.721	4.783	4.822	4.835	4.841

As stated above, the z-bending modes are the modes that deform in the plane of interest and thus were the modes examined in this study. Because each natural frequency corresponds to only one mode shape, the frequency matrix such as that in the table can be used to identify the modes of interest. As an example, for the data given in Table 4.3, the first z-bending mode of each model can be identified as the first system mode for models $K/K_0 = 1/200$ to $K/K_0 = 1/5$ and the second system mode for models $K/K_0 = 1/2$ to $K/K_0 = 200$. The z-bending modes in the table are the ones that are not shaded. The first z-bending mode "switches" after column 6 from the first system mode to the second system mode. The first system modes from columns 7 to 15 are xy-bending modes, and are not of interest. This switching is illustrated in Figure 4.2 which essentially shows the data in Table 4.3.

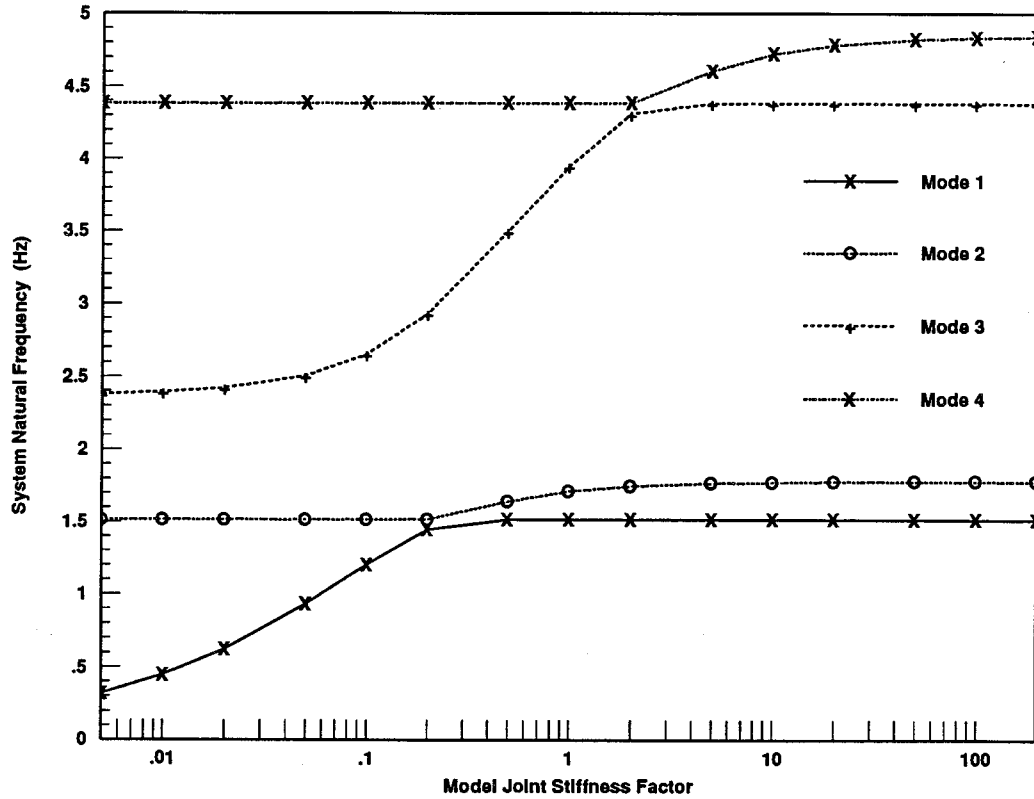
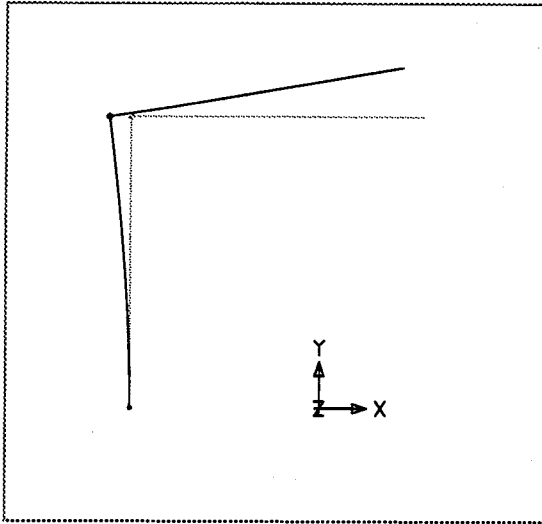


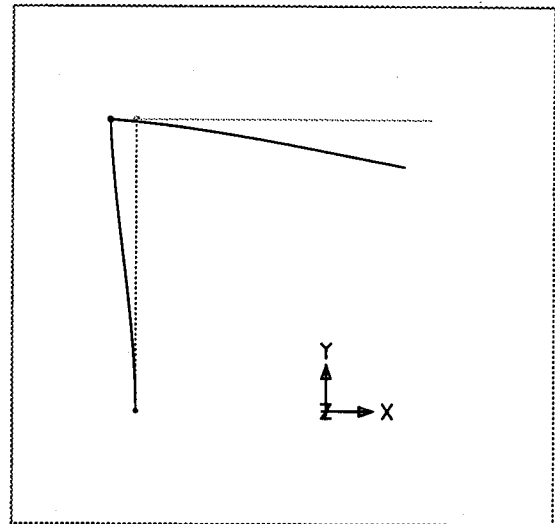
Figure 4.2: System Natural Frequencies vs. Joint Spring Stiffness, $\theta = 90^\circ$

The modes of interest of course can also be determined by examining the shape vectors themselves to see which type of motion they produce, however inspecting the frequency matrix is generally a much quicker way to make this determination. In this study, both the vectors themselves and the frequency matrix were inspected to make this determination. This process is necessary because one cannot arbitrarily state before examining the system modes which will be z-bending, and which will be xy-bending. Also, if the switching points are determined for a set of fifteen exact models with given stiffnesses, they may not be the same switching points for a set of fifteen reduced models with the same stiffnesses.

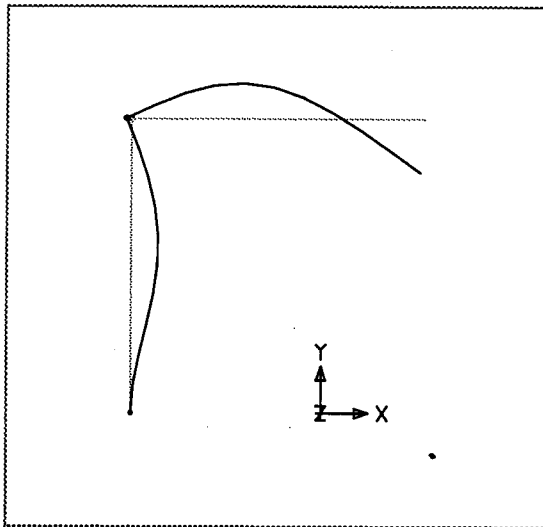
For reference, Figures 4.3 and 4.4 illustrate the first eight z-bending mode



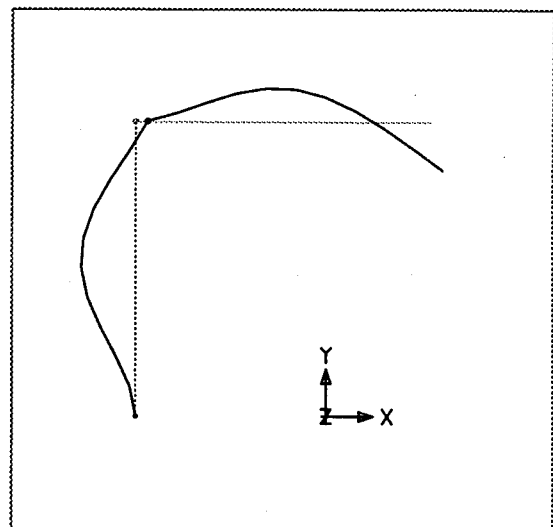
1st Z-Bending Mode (Mode 2)



2nd Z-Bending Mode (Mode 3)



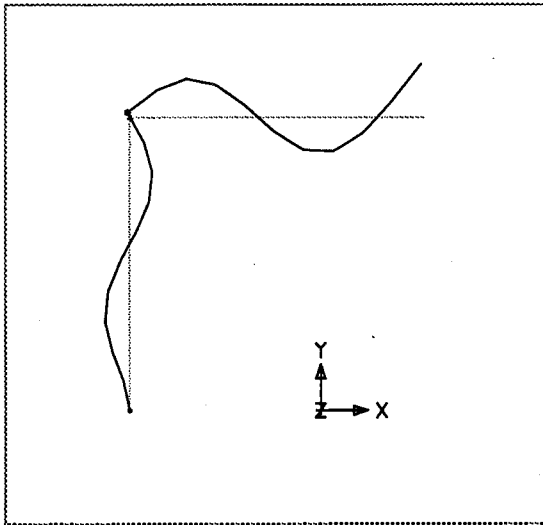
3rd Z-Bending Mode (Mode 6)



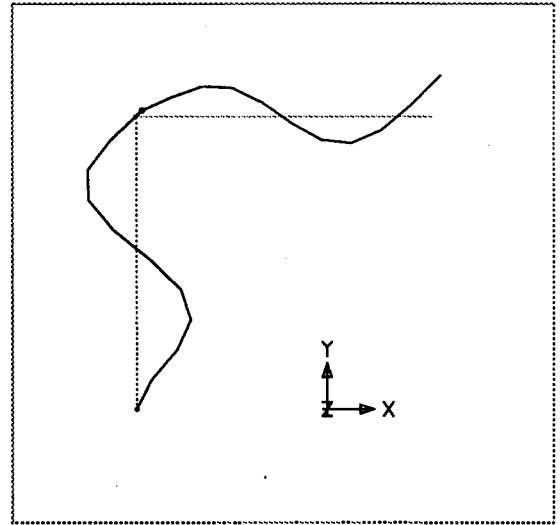
4th Z-Bending Mode (Mode 7)

Figure 4.3: Z-Bending Mode Shapes 1 - 4 of the Exact System, $\theta = 90^\circ$, $K/K_0 = 1$

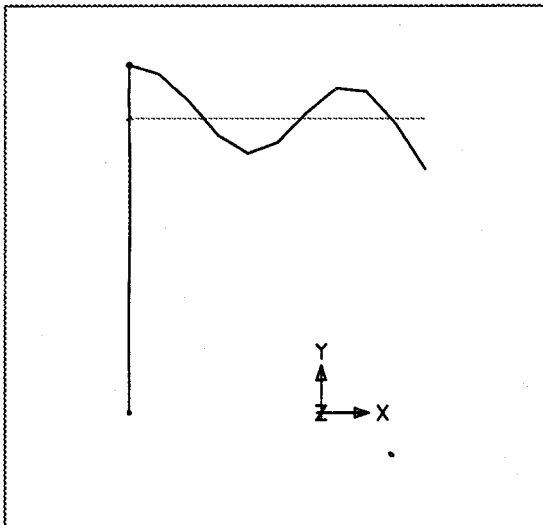
shapes for the exact model where $\theta = 90^\circ$, and Model Joint Stiffness Factor is unity.



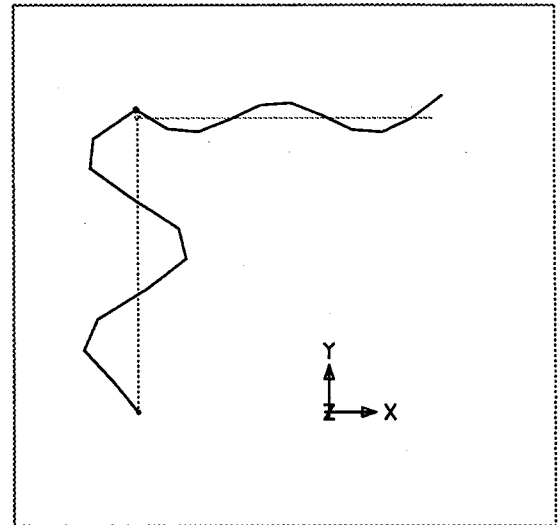
5th Z-Bending Mode (Mode 10)



6th Z-Bending Mode (Mode 12)



7th Z-Bending Mode (Mode 14)



8th Z-Bending Mode (Mode 16)

Figure 4.4: Z-Bending Mode Shapes 5 - 8 of the Exact System, $\theta = 90^\circ$, $K/K_0 = 1$

4.5 System Mode Limitations in General

Generally in Component Mode Synthesis, the extent to which the component normal mode set is truncated is dictated by one of two possibilities. Often there is either a given number of degrees of freedom allowable for a component, or a frequency above which value the vibration of the component is negligible compared to its lower frequency vibratory motion. In general, higher frequency motion can be neglected because the product of its high nodal velocities and structural damping causes it to damp out relatively quickly. However, when the component mode set is truncated, part of the system information is lost. Therefore, when the system of components is recoupled in the synthesis, the system will not be able to completely represent the dynamics of the exact system due to the truncated information from the high frequency component modes. Statically, the synthesized system will completely represent the exact system if constraint modes are used, because only the component stiffness is involved, and constraint modes are the result of a static reduction of the interior coordinates to the interface coordinates. Dynamically though, in the case of the truncation of high frequency component modes, the loss of information will manifest itself in the inability of the synthesized system to mimic the high frequency vibratory motion of the exact system. Component Mode Synthesis in general can be a very accurate tool, however, its accuracy can be limited to low system frequencies if high frequency component modes are the ones truncated.

With the above discussion in mind, an obvious question is: what is the limit on the number of system modes or the frequency of the highest frequency system mode, that will be approximated well in the modal synthesis? Hurty³² discusses the idea of

"realistic" system modes and presents a criterion for their selection based on the number of degrees of freedom of the system and components. Rubin¹⁴ suggests that for conservative results, system modes should not be examined whose frequencies are above two thirds the limiting component frequency. The limiting component frequency is defined as the frequency value of the highest frequency mode retained in a component mode set. If more than one component exists, the limiting frequency for each component mode set is found and the lowest of these is used. For example, if a structure has two components which are represented by mode sets whose highest frequencies are 150 Hz and 200 Hz, then the limiting frequency is 150 Hz and Rubin's method suggests not examining system modes over 100 Hz. In spite of this, it is otherwise generally accepted that system modes should not be examined whose frequencies are above a frequency *equal to* the limiting frequency. In Ref. 11, Hurty admits that this intuitive criterion can be used for any given number of degrees of freedom in an example he presents. This is generally the procedure adopted by this study. However, there are cases where the system modes can be represented relatively well by sets of component modes whose highest frequency is below the frequency of the system mode. These cases are noted where they occur in the later description of results.

In all cases for this study, the modal strain energy trends of the synthesized structure across varying joint spring stiffnesses were compared to the modal strain energy trends of the exact structure for the given system mode. These trends were used to ensure that the system modes are comparable, i.e. the same general motion is occurring in both mode shapes. For example, the major motion in the *i*-th *exact*

system mode for a given configuration may be occurring in the spring and Beam 2 when Beam 1 remains undeformed. This shape will vary with spring constant according to a given trend. The i -th *reduced* mode may not deform the same components or may not have a trend that varies similarly to that of the exact mode. Inspecting the mode shape vectors will produce this information, however strain energy is an excellent indicator of modal deformation as well as the fact that it is a scalar quantity and can be summed over an entire component making it readily plotted. Strain energy plots are not included here, but their use is discussed more in the next chapter.

V. RESULTS FOR A SINGLE CONFIGURATION

As a starting point, this chapter will discuss the results obtained for a single configuration. This discussion will include the determination of the effects of the joint spring stiffness on the accuracy of mode sets employed. The next chapter will discuss the expansion of the study to different configurations. An intuitive configuration to start with in this chapter is that of $\theta = 90^\circ$, because it is one where some of the more complex issues of the dynamics of the model appear. The process of determining mode set accuracy used in this chapter can be assumed similar for all other configurations.

5.1 Realistic System Modes

For each configuration, the first eight system z-bending modes were compared to the first eight z-bending modes of the reduced systems. Note that these modes do not correspond to the first eight system modes, but because of xy-bending modes they may correspond to system modes interspersed from the first up through the sixteenth or higher. Obviously therefore, the z-bending modes were selected from the system modes for examination. Also, note that this selection process would not be necessary for a planar problem, however a planar problem would not allow for component torsional modes. The natural frequencies of the first eight exact system z-bending modes for the configuration $\theta = 90^\circ$ are given in Table 5.1. Shown here are only the minimum and maximum values which correspond to minimum and maximum spring stiffnesses respectively. A full listing for each configuration is given in

Table 5.1: Exact Z-Bending System Natural Frequencies, $\theta = 90^\circ$ (Hz)

$K/K_0 =$	System Mode Number							
	1	2	3	4	5	6	7	8
1/200	0.320	2.380	23.35	24.71	74.62	77.08	132.2	158.2
200	1.781	4.841	23.87	34.80	75.60	92.21	132.2	161.4

Appendix B.

As has been stated, each of these eight exact frequencies and mode shapes were compared to reduced model frequencies and mode shapes. However, not all of the reduced models produced frequencies and mode shapes that realistically compared to exact. For example, a fixed-interface mode set including only two modes can not be used in a synthesized system to accurately predict system motion out to the eighth system z-bending mode. As discussed in the previous chapter, there is a point at which it is no longer "realistic" to compare these synthesized modes to exact system modes, because they will not be similar. System modes which are realistic can compare to exact because they have enough information from each component to represent component motion in the system mode. An example of an unrealistic system mode might be a high frequency system mode where the bending motion of a component in the synthesized system mode does not have as many nodes and anti-nodes ("humps") as the same component would exhibit in the exact system mode. According to what can be referred to as a "limiting frequency method", the point at which the comparison is no longer realistic can be determined by comparing the highest frequency in the mode set - the limiting frequency - to the frequency of the

exact system mode in question. In general, if the limiting frequency is higher than the exact system mode frequency, then the synthesized frequency and mode shape will be realistic, and thus comparable. It should be noted that the determination of which system modes will be realistic, given a used mode set, has one sole purpose. That is to decide which comparisons of synthesized modes to exact modes should be examined and which comparisons will be moot. This in turn determines the error results on which conclusions can be based and presented.

However, towards this end, Table 5.2 lists the limiting frequency for each mode set used to represent Beam 2. Some of the mode sets used in the present study (Table 4.2) complicate matters because they do not include a "sequential" set. For example, the second fixed-interface mode set includes component modes 1, 2, and 5 and skips modes 3 and 4. In these types of cases, Table 5.2 notes that the set skips modes so that the reader will be aware that the high limiting frequency may be misleading in prediction of realistic system modes via the limiting frequency method.

Table 5.2: Highest Frequency of the Mode Sets (Hz)

Mode Set	Fixed Freq.	Free Freq.	Mixed Freq.
2 Bending	5.345	34.01	23.44
2 Bending, 1 Torsion	74.32 †	148.2 †	74.32 †
4 Bending	33.50	93.78	75.97 †
4 Bending, 1 Torsion	74.32	148.2	75.97
6 Bending, 1 Torsion	93.82	184.0	158.6 †
6 Bending, 1 Torsion, 1 Axial	144.9	289.0	158.6

† Mode set is not sequential.

Given Tables 5.1 and 5.2, according to a limiting frequency method, mode sets that produce "realistic" system modes are those whose highest frequency is greater than or equal to the system frequency to be calculated. Due to the fact that this study involves a range of system frequencies arising from the varying joint stiffness, the system frequency used in the comparison will be the maximum. Using a limiting frequency method, the component mode sets predicted to produce realistic system modes for the configuration $\theta = 90^\circ$ are given in Table 5.3 and indicated by check marks. As a reminder to the reader, the system modes in the table are z-bending modes, whereas the component mode sets include bending modes that bend about *both* the x and z axes.

As will be shown, for a given mode set, this limiting frequency method does not always predict the system mode number at which the synthesized frequency and mode shape errors will tend to experience a large relative increase. The method does however give a "ballpark" estimate of where the error transition will occur. It should be noted that for the mode sets that are non-sequential, if the limiting frequency is redefined as that of the highest mode before any are skipped, the resulting predictions still do not all correspond to actual results.

Given the information in Table 5.3 and the obvious fact that unrealistic frequencies and modes will show up when they produce large error, the following decision was made. As has been stated, the sole impact on the present study of determining realistic system modes was to decide which error results should be presented, and which were meaningless. In actuality, all types of mode sets were

Table 5.3: Ability of Mode Sets to Predict Realistic System Modes for the Configuration $\theta = 90^\circ$, Via the Limiting Frequency Method

Fixed-Interface	System Z-Bending Mode							
	1	2	3	4	5	6	7	8
2 Bending	✓	✓						
2 Bending, 1 Torsion †	✓	✓	✓	✓				
4 Bending	✓	✓	✓					
4 Bending, 1 Torsion	✓	✓	✓	✓				
6 Bending, 1 Torsion	✓	✓	✓	✓	✓	✓		
6 Bending, 1 Torsion, 1 Axial	✓	✓	✓	✓	✓	✓	✓	
Free-Interface								
2 Bending	✓	✓	✓					
2 Bending, 1 Torsion †	✓	✓	✓	✓	✓	✓	✓	
4 Bending	✓	✓	✓	✓	✓	✓		
4 Bending, 1 Torsion	✓	✓	✓	✓	✓	✓	✓	
6 Bending, 1 Torsion	✓	✓	✓	✓	✓	✓	✓	✓
6 Bending, 1 Torsion, 1 Axial	✓	✓	✓	✓	✓	✓	✓	✓
Mixed-Interface								
2 Bending	✓	✓						
2 Bending, 1 Torsion †	✓	✓	✓	✓				
4 Bending †	✓	✓	✓	✓	✓			
4 Bending, 1 Torsion	✓	✓	✓	✓	✓			
6 Bending, 1 Torsion †	✓	✓	✓	✓	✓	✓	✓	
6 Bending, 1 Torsion, 1 Axial	✓	✓	✓	✓	✓	✓	✓	✓

† Mode set is not sequential.

used to produce system modes and error results, though not all are presented.

Because in this study it is important to be able to compare the three interface types, it was decided that the same criteria be used for each interface type (regardless of differing system frequency values) in determining which mode sets would produce system modes that should be compared to exact. This in turn determines the error results on which conclusions should be based. Table 5.4 illustrates the system modes corresponding to each mode set for which error results were presented, for all configurations in this study. The only error results on which conclusions were based were those dictated by Table 5.4.

Table 5.4: Mode Sets That Produced System Modes Examined in the Present Study (Criteria Used For All Configurations)

All Interface Types	System Z-Bending Mode							
	1	2	3	4	5	6	7	8
2 Bending	✓	✓	✓					
2 Bending, 1 Torsion	✓	✓	✓					
4 Bending	✓	✓	✓	✓	✓			
4 Bending, 1 Torsion	✓	✓	✓	✓	✓			
6 Bending, 1 Torsion	✓	✓	✓	✓	✓	✓	✓	✓
6 Bending, 1 Torsion, 1 Axial	✓	✓	✓	✓	✓	✓	✓	✓

5.2 Results

For the configuration $\theta = 90^\circ$, Figures 5.1 and 5.2 illustrate the percent frequency error and modal correlation error from the second system z-bending mode using *mixed-interface* mode sets, as an example. These are plotted with respect to the

Model Joint Stiffness Factor referred to in Chapter 3. Each point on the plots represents a synthesized system of a certain joint spring stiffness. In these plots, the legend uses "B", "T" and "A" which stand for bending, torsion, and axial respectively and identify the mode set used in the modal synthesis. The plots for the remaining system modes for this configuration are given in Appendix C. Due to space considerations, the corresponding plots for the other three configurations are not included, but some plots that condense the information are given in the next chapter.

As will be seen, many of the curves in the error plots overlap. Identification of the curves can be accomplished with the legend as well as with the information in the following discussion. With regards to Appendix C, one point that should be made immediately is that the extremely low error exhibited by the first system z-bending mode plots in Appendix C is not necessarily representative of the results in general. Fixed-interface methods over any stiffness resulted in representing the first system frequency and mode shape much more accurately than the free- or mixed-interface methods. As the system mode number increases however, errors do become substantial.

5.2.1 Component Mode Types

In Figure 5.1, it can be seen that the percent frequency error of the first two mode sets (2 bending and 2 bending, 1 torsion) are equal for all model joint stiffness factors. This is for the mixed-interface method representation of the frequency of the second system z-bending mode in the $\theta = 90^\circ$ configuration. Figure 5.2 shows that this is also true of the modal correlation error of the two mode sets. The figures in

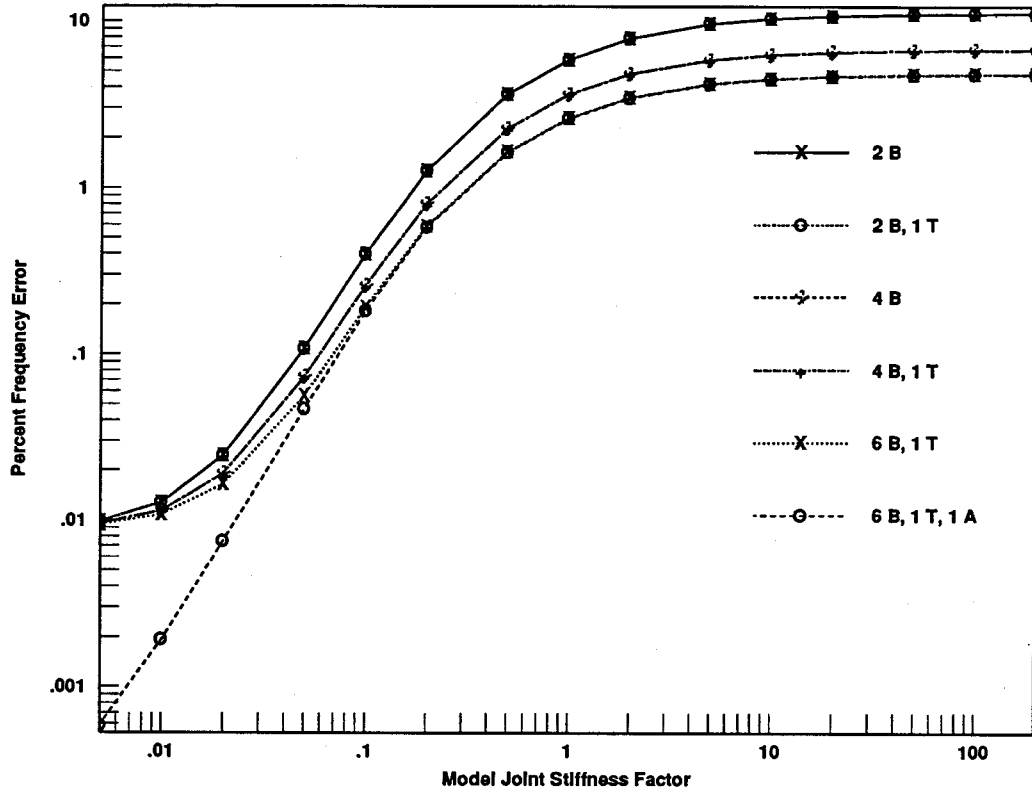


Figure 5.1: % Freq. Error, 2nd System Z-Bending Mode, $\theta = 90^\circ$, Mixed-Interface

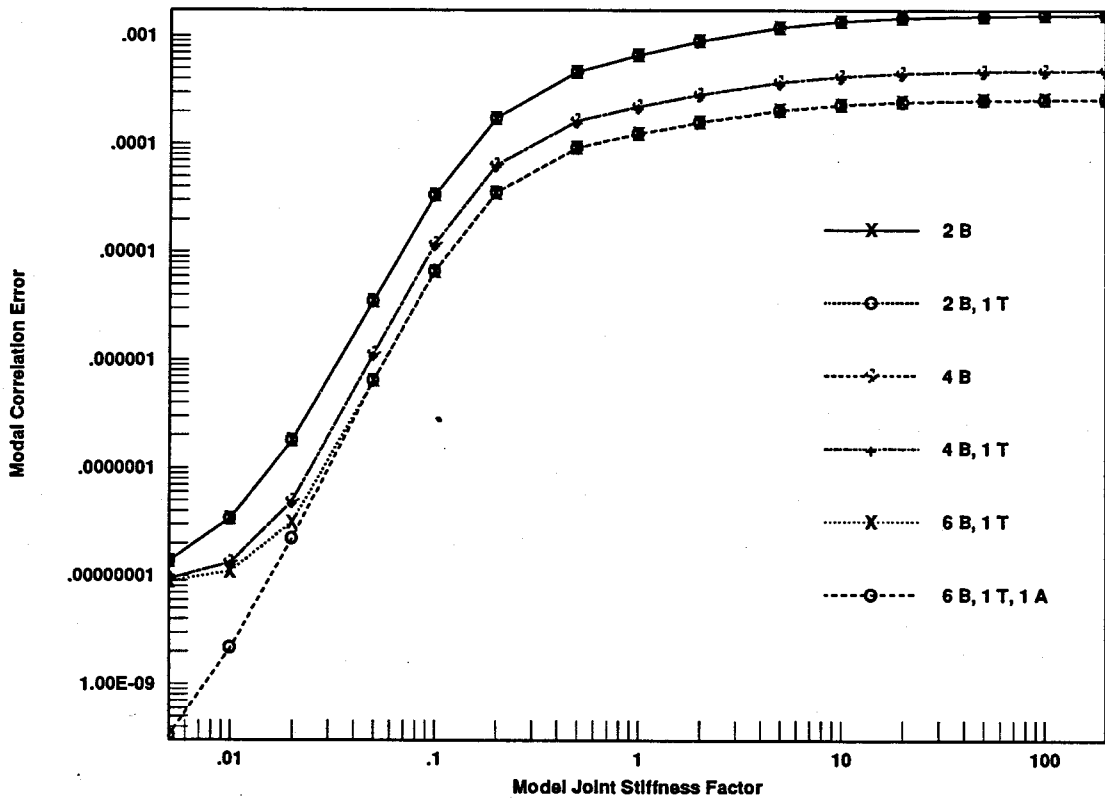


Figure 5.2: MCE, 2nd System Z-Bending Mode, $\theta = 90^\circ$, Mixed-Interface

Appendix C show that this is also true of the second two mode sets (4 bending and 4 bending, 1 torsion). In fact, the data in general show that these two statements are also true for the two other interface methods, for all system frequencies, and all configurations. This obviously points to the fact that the addition of a torsional mode to the set does not increase accuracy in system z-bending modes in this study. It is intuitive that a torsional component mode will not affect a system bending mode if bending and torsion are not coupled, as they are not for the system z-bending motion. They can be coupled for system *xy-bending* motion for configurations other than $\theta = 0$ or 180° , but including the examination of system xy-bending modes was beyond the scope of this study. Although the data is not shown here, early in the study a similar observation was made about component x-bending modes not affecting system z-bending motion, which is also intuitive. Component x-bending modes are included in the mode sets as described earlier, however their elimination from the sets in this study had no adverse affect on synthesized system mode accuracy.

Two conclusions can be drawn from this information about the torsional and x-bending component modes. First, the inclusion of another degree of freedom to the set representing the component may not always increase the accuracy of the synthesized mode or frequency. Special attention must be paid to the *type* of modes being used to represent a component as well as the number of modes being used. Because there was one component x-bending mode for every component z-bending mode, the elimination of the unnecessary x-bending modes would have reduced the number of component generalized degrees of freedom substantially. Also, although the torsional mode significantly increased the highest frequency of the mode set when

included, the set was no more able to represent system motion of that frequency than if the torsional mode had not been included. This points to the conclusion that the previously discussed limiting frequency of a mode set should not be based simply on the highest frequency mode in the set. Rather, it should depend on whether the set is composed of a sequential array of component modes, or whether some interspersed modes deemed unnecessary were eliminated from the set. In any case, more development should be done in the area of determining a criteria for realistic system frequencies in systems synthesized from non-sequential component mode sets.

Finally, note that the inclusion of the axial mode (tension/compression) in the last mode set in many cases reduced the synthesized system errors as compared to the results of the mode set composed of only 6 bending and 1 torsional component mode. A likely explanation for this is that in this configuration ($\theta = 90^\circ$), the motion of Beam 2 in the system z-bending modes is composed of bending as well as a small amount of tension and compression. To support this, consider that in this configuration, the horizontal (x-direction) swaying motion of Beam 1 during deformation in the system z-bending vibrational mode (Figure 4.1) causes tension and compression in Beam 2, while Beam 2 is experiencing bending. If this were so, this effect would be greatest at $\theta = 90^\circ$ because at this configuration the horizontal motion of the joint directly affects the horizontal motion of Beam 2, whereas at other configurations, this motion also affects the rotation of Beam 2. Careful inspection of the exact system modes of the 90° configuration reveals that the joint itself does move horizontally in most modes during deformation. One exception is the seventh system z-bending mode, illustrated in Figure 5.3, where the joint only moves

vertically (y-direction) during deformation, independent of spring stiffness. Because the joint has no motion in the direction of the axis of Beam 2 for this system mode, there should be no tension/compression in the motion of Beam 2. In support of this, it is found that of all mode sets and interface types used in the synthesis of the seventh system z-bending mode in the configuration $\theta = 90^\circ$, none gain any accuracy with the addition of the axial component mode (Appendix C). Also in support of this it is found that for the configurations $\theta = 45^\circ$ and 135° , where such a system mode is less likely to occur (one that creates no joint motion along the axis of Beam 2), in general higher system modes examined (i.e. z-bending modes 3 through 8) *do* benefit from the inclusion of the axial component mode.

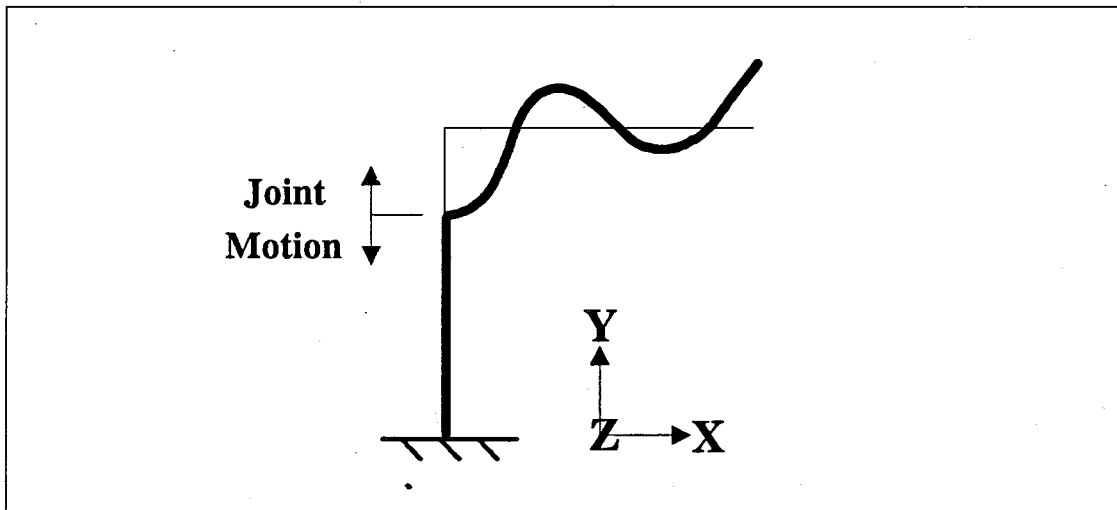


Figure 5.3: 7th Exact System Z-bending Mode, $\theta = 90^\circ$

For all configurations, it is found that in some cases the low frequency system modes (i.e. z-bending modes 1 and 2) also do not benefit from the addition of the axial mode. This may either be because the motion of the low system modes do not induce much horizontal joint motion, or because in these modes Beam 2 acts as a

rigid body and thus motion of the joint translates simply to rigid body motion of Beam 2 without tension or compression.

To summarize, it is found that *for a given component the inclusion of a component axial mode in the component mode set increases the system mode accuracy only for a system mode where the interface point to that component deforms in the direction of the axis of that component.*

5.2.2 Effect of Joint Spring Stiffness

To determine the effect of varying the angular joint spring stiffness, the trends of percent frequency error and modal correlation error versus model joint stiffness factor were inspected. As can be seen from these error trends in Appendix C, for a given system mode and mode set case, the percent frequency error and the modal correlation error curves in general have similar shapes. That is, they generally both either increase or decrease along joint stiffness. This shows that the spatial and temporal results are in agreement, which is expected.

An intuitive guess at what causes the curves to increase or decrease along the plot might be that error is strongly a function of interface method. For example, error from fixed-interface methods might decrease as joint stiffness increases and a fixed interface better approximates actual conditions. Conversely, error from free-interface methods might increase as joint stiffness increases and a free interface strays further from actual conditions.

Although this sort of effect may have been an influence on error trends, it seems that a different effect had the stronger influence, at least for the fixed- and

free-interface methods. This is an equally intuitive effect and arises from the role that the reduced component - Beam 2 - plays in the system mode. This role can be easily quantified in modal strain energy - the strain energy arising from the deformation of the structure into the form of a given mode. In NASTRAN, strain energy (W_e) is computed for each element by

$$W_e = \frac{1}{2} \{u_e\}^T [K_{ee}] \{u_e\} \quad , \quad (5.1)$$

where $[K_{ee}]$ is the element stiffness sub-matrix and $\{u_e\}$ is the displacement of the corresponding nodes - in this case referring to modal deformation. Element strain energy can be summed over all the elements in a component for component strain energy. In this study, element strain energy was summed over the entire structure as well as the reduced component, and component strain energy percent of total was employed for Beam 2 to gain an insight into its motion within the system modes. The argument here is that because Beam 2 is the only part of the structure that is reduced, it will of course be the source of system mode error.

As can be seen from the data in Appendix C, with interfaces fixed and free, the error trends mostly increase as joint stiffness increases for system z-bending modes 1, 2, 4, 6, 7, and 8, whereas the error trends for system z-bending modes 3 and 5 include some decreasing curves. These increasing and decreasing trends correspond to the system z-bending modes where the component strain energy percent from Beam 2 increases and decreases respectively plotted along joint spring stiffness. Thus, for the interface types fixed and free, and for the configuration $\theta = 90^\circ$, error generally increases with Beam 2 strain energy percent.

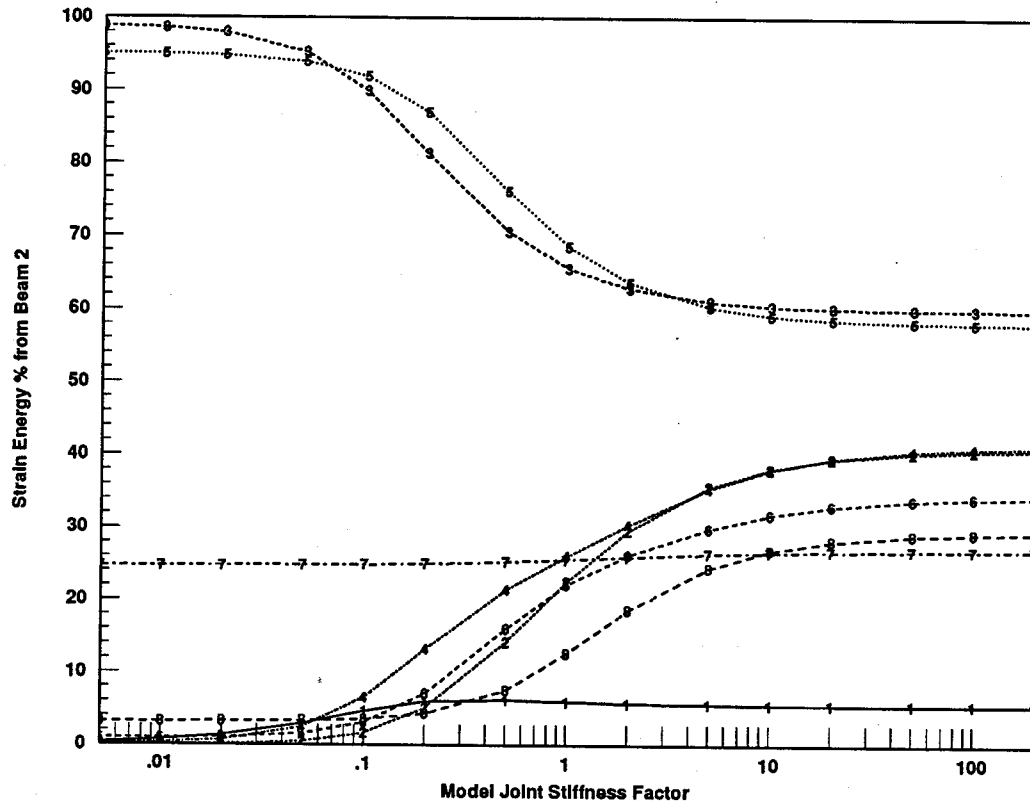


Figure 5.4: Strain Energy Percent from Beam 2, System Modes 1-8, $\theta = 90^\circ$

The strain energy percent trends are shown for the first eight system z-bending modes in Figure 5.4. The system z-bending modes are indicated by the number symbols on the plot curves. Although the strain energy during the seventh mode appears to be constant, it is slightly increasing.

Of the data for the mixed-interface mode sets, it can be seen from the plots in Appendix C that frequency and mode shape error consistently increase for all cases (except one in the eighth system mode). This may point out that the stronger effect on mixed-interface error was the idea described earlier, that mixed-interface error decreases as the physical conditions on the interface coordinates more closely

approximate an actual pin joint, i.e. joint spring stiffness decreases. *The error from mixed-interface methods seemed to be less strongly a function of the strain energy percent trends of Beam 2 than error from fixed- and free-interface methods.* As was seen, this was basically true for all configurations examined.

5.2.3 Comparison of Interface Methods

In order to easily compare the three interface methods (fixed, free, and mixed) it is necessary to compress the data in Appendix C. Therefore, instead of examining the error trends, we will examine the range of error produced by the error trends. Figures 5.5 and 5.6 illustrate the ranges of error for the eight system z-bending modes of the configuration $\theta = 90^\circ$. In the plots, the symbols denote the interface method while the number of modes across the abscissa denotes the mode set for each interface method. The symbols "x", "o", and "+" represent fixed, free, and mixed, respectively. The number of kept modes are able to represent the mode set (given an interface method) because there is a unique total number of kept modes in each type of set (Table 4.2). The totals 2, 3, 4, 5, 7, and 8, represent the mode sets from 2 bending respectively through 6 bending, 1 torsion, 1 axial. The placing of the symbol itself represents the error value corresponding to the *maximum* joint spring stiffness.

One conclusion that can be immediately drawn from the figures is that for each system z-bending mode, each interface method seems to fare consistently for all mode sets of that method. For example, for the first system frequency observed, a fixed-interface method produces by far the least error compared to the other two methods, consistently for any size mode set used. In comparing the three methods, it is seen

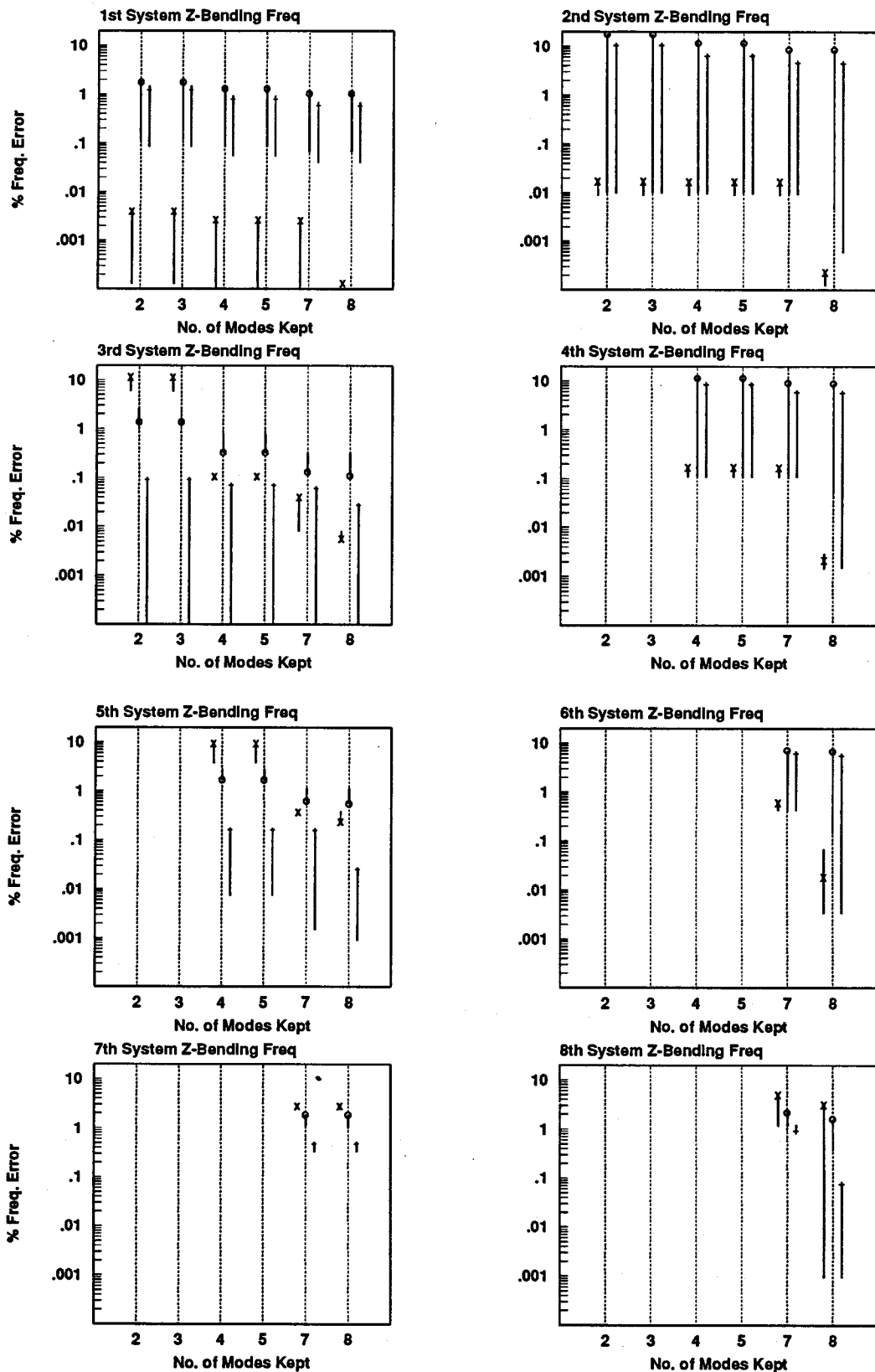


Figure 5.5: Ranges of Percent Frequency Error, $\theta = 90^\circ$
 Symbols: x = Fixed-Interface, o = Free-Interface, + = Mixed-Interface
 Symbols Plotted at Maximum Joint Spring Stiffness

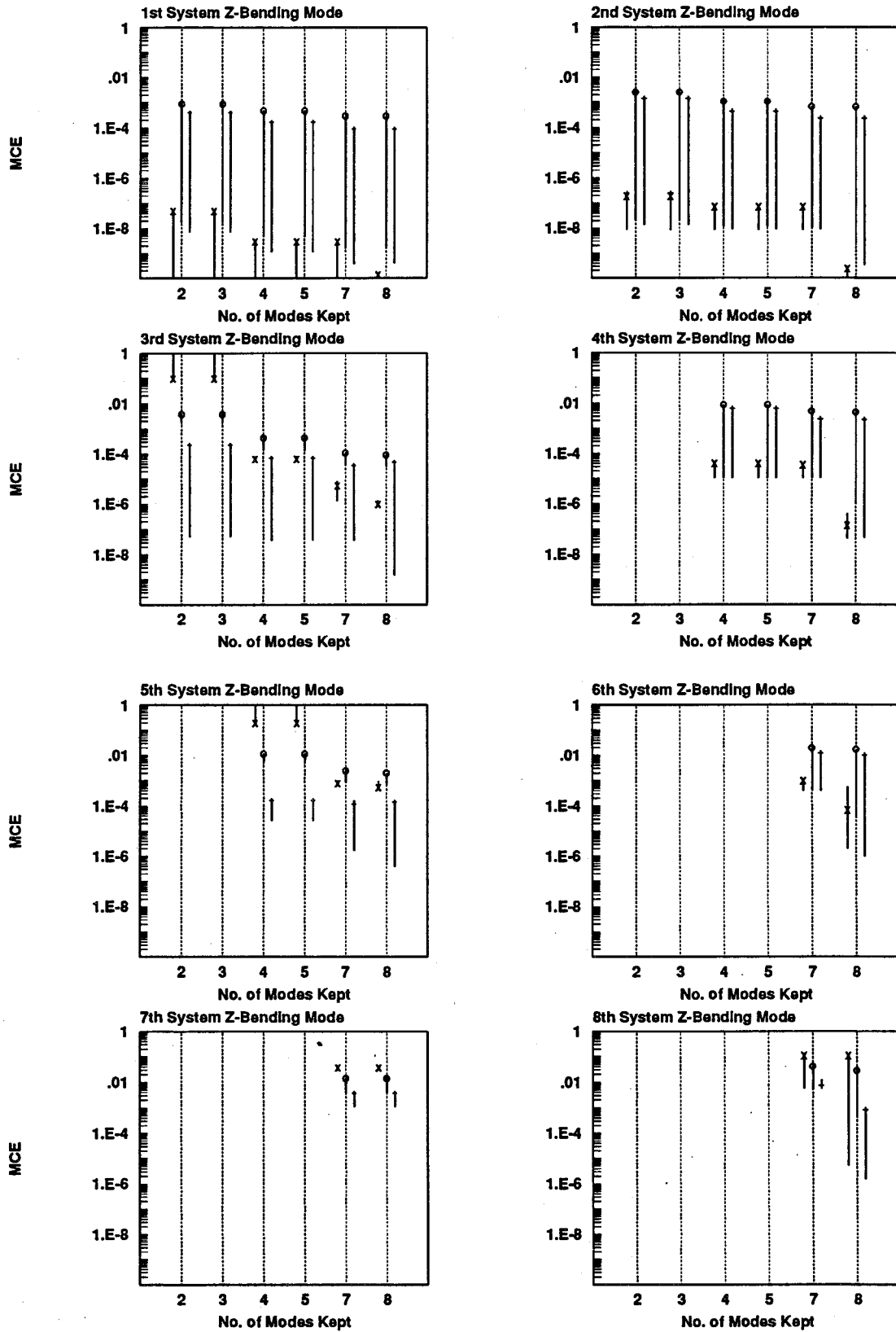


Figure 5.6: Ranges of Modal Correlation Error, $\theta = 90^\circ$
 Symbols: x = Fixed-Interface, o = Free-Interface, + = Mixed-Interface
 Symbols Plotted at Maximum Joint Spring Stiffness

for this configuration that mode sets with fixed and mixed interfaces perform generally better than the mode sets with free interfaces. The fixed-interface mode sets perform the best for system z-bending modes 1, 2, 4, and 6, while the mixed-interface sets perform best for modes 3, 5, 7, and 8. Inspection of the exact system mode shapes may point to a reason for this. The deformation of Beam 2 in exact system z-bending modes 3, 5, and 7 exhibit classical pinned-free mode shapes with the first occurring in system mode 3. The deformation of Beam 2 in exact system z-bending modes 1, 2, and 4 exhibit classical rigid body forms for the low spring stiffness modes and classical cantilever-free forms for the high spring stiffnesses. The problem here is that as the system mode number increases, it becomes increasingly difficult to distinguish between cantilever-type motion and pinned-type motion for Beam 2 in the system modes. This discussion is extended to other configurations and continued in the next chapter.

VI. EXTENSION TO MULTIPLE CONFIGURATIONS

This chapter will discuss the results obtained in extending the study to the configurations $\theta = 45^\circ$, 135° , and 180° . Comparisons between the results of all configurations will be given. However, the plots of percent frequency error and modal correlation error versus model joint stiffness factor are not included for the configurations other than $\theta = 90^\circ$.

6.1 Component Mode Types

The last chapter discussed some of the observations on the contributions of joint spring stiffness and varying mode types to the accuracy of the mode set. In general however, some of the observations of the first configuration examined hold for all configurations examined. They are that, while component z-bending modes are important, component x-bending modes and torsional modes need not be retained in a set to be used only for system z-bending motion. For all the configurations examined except $\theta = 180^\circ$, the exact and synthesized system modes (up to at least the 25th mode) were composed entirely of z-bending and xy-bending mode shapes (Figure 4.1). For the system where $\theta = 180^\circ$, when the model is configured in a straight line, the system modes also included torsional and axial mode shapes and combinations thereof in addition to the z-bending and xy-bending mode shapes. Although the results are not included here, it was found that for the configuration of $\theta = 180^\circ$, the addition of component torsional and axial modes to the mode set increased the accuracy of the system torsional and axial modes respectively, as expected.

The conclusion here is that if a given system is likely to be in a configuration where torsional motion of a component will result in the system mode, then for more accurate results, it is important to include component torsional shapes in the mode set used to represent that component. For example, in this study the z-bending system modes were the only system modes compared to exact. In these modes, it was found that there was no torsional motion of Beam 2 (this observation may be intuitive, but was decided not to be assumed at the start of this study). Because z-bending modes were the only system modes examined and thus considered to be "of importance", it was concluded that component torsional modes had no positive effect on the mode sets used for the important system modes. As another example, in the xy-bending system modes for the configuration $\theta = 90^\circ$ (Figure 4.1), the motion of Beam 1 was often composed of bending and torsion as Beam 2 swings from side to side. Thus, if Beam 1 were modally approximated in the synthesis, it is intuitive that the addition of component torsional modes to the set representing Beam 1 would increase the accuracy of the synthesized system xy-bending modes.

The role axial modes played in the mode sets of configurations other than $\theta = 90^\circ$ was generally similar to that of $\theta = 90^\circ$. That is that the addition of the component axial mode to the mode set generally increased system mode accuracy with the exception of the first and second system z-bending mode from free- and mixed-interface mode sets where the addition had little or no effect as described earlier. Also, the inclusion of the axial component mode in mode sets used for the $\theta = 180^\circ$ configuration had no beneficial effect for *any* system z-bending mode. Inspection of the system mode shapes provides an explanation of this which is consistent with

earlier conclusions on the subject. In the first eight system z-bending modes of the configuration $\theta = 180^\circ$, across all stiffnesses, the joint either moves horizontally (x-direction) or does not move at all. Because in this configuration, Beam 2 is aligned along the y-direction and there is no joint motion in that direction, there is no tension or compression included in the deformation of Beam 2. Therefore, an axial mode will not improve the representation of that motion. In higher frequency system modes of the same configuration ($\theta = 180^\circ$), there is axial motion in Beam 1 with bending motion in Beam 2 which would cause also axial motion in Beam 2, but because these types of system modes did not occur within the first eight z-bending system modes so they were not considered.

In summary, over all configurations examined, *torsional component modes were generally unnecessary because the only system motion of interest was z-bending motion. Axial component modes added to the mode sets did improve z-bending system modes 3 through 8 in most cases for the configurations $\theta = 45^\circ$, 90° and 135° with the greatest improvement at $\theta = 90^\circ$, but not for any system z-bending modes examined at $\theta = 180^\circ$, as described. Axial component modes generally only improved system z-bending modes 1 and 2 when added to the fixed-interface mode set, except again, at $\theta = 180^\circ$.*

6.2 Effect of Joint Spring Stiffness

For the configuration $\theta = 90^\circ$, it was found that in general two effects determined the shapes of the plots of error versus joint spring stiffness. One effect is the variation of the modal strain energy percent of Beam 2 in the system mode. The

second effect is the proximity of the interface constraints used, to the physical conditions of the exact model. *It was found that for the 90 ° configuration the former effect dominated the results given by the fixed- and free-interface methods, while the latter effect dominated the results of the mixed-interface method.*

In extending the study to other configurations, it was found that the same effects basically determined the percent frequency and modal correlation error trends along joint spring stiffness. As stated however, those trend error plots are not included. The mixed-interface method through the four configurations examined, consistently exhibited the trend (with very few exceptions) that both percent frequency error and modal correlation error increased with joint spring stiffness. Given that mixed-interface follows the "proximity" effect described above, this is expected because as stiffness increases, the interface conditions become less and less like a pin joint, and instead approach a cantilevered interface. Of the fixed- and free-interface methods, error trends corresponded well with the Beam 2 strain energy percent trends. In general, free-interface errors made this correspondence more consistently than fixed-interface errors. Both interface methods however, produced error trends in the 135 ° configuration that corresponded almost exactly with strain energy percent trends. In this sense, and in the sense that percent frequency error agreed very well with modal correlation error, the configuration of $\theta = 135^\circ$ produced the most "well behaved" results for this study.

6.3 Comparison of Interface Methods

As for the configuration $\theta = 90^\circ$, the ranges of error results were plotted so

that the results of the three interface methods could be easily compared to each other. Figures 6.1 through 6.6, included at the end of the chapter, illustrate the ranges of percent frequency error and modal correlation error in all examined synthesized system z-bending modes for the configurations $\theta = 45^\circ$, 135° , and 180° , respectively. In examination of the figures, a few observations can be made immediately. For the first system z-bending mode of all configurations examined, given any number of modes in the set, comparison of the interface methods reveals that fixed-interface provided the greatest accuracy. In fact, fixed-interface mode sets were often most accurate in the second system z-bending mode also. For the rest of the system z-bending modes it was found that either fixed- or mixed-interface was most accurate. Free-interface mode sets provided generally poor results in comparison with the exception of the $\theta = 180^\circ$ configuration.

Because for each given configuration and system mode there is generally one interface method that provides better results than the other two, for each size mode set, it is possible to create a general table of the most accurate interface methods given each situation. Table 6.1 lists the "best" interface types for each eight system z-bending modes of each configuration, in both the high and low joint spring stiffness regimes, as well as from the frequency error and the modal error data. The first symbol in a cell represents the most accurate interface method of the data from minimum spring stiffness, while the second symbol in a cell corresponds to the maximum spring stiffness data. The data from modal correlation error is presented only where it differs from frequency data. As in the error range plots, the symbols "x", "o", and "+" denote fixed-interface, free-interface, and mixed-interface,

respectively. The general determinations of the most accurate interface types were made simply by visual inspection of the error plots such as Figures 6.1 through 6.6. In cases where more than one interface method excelled for different size mode sets in the same plot, then the interface method that was most accurate for the most mode set sizes was the one listed in the table.

Table 6.1: Most Accurate Interface Methods

Symbols: x = Fixed-Interface, o = Free-Interface, + = Mixed-Interface

1st symbol: Minimum spring stiffness 2nd symbol: Maximum spring stiffness

θ	Source Data	System Z-Bending Mode Number							
		1	2	3	4	5	6	7	8
45 °	PFE †	x x	x x	+ x	x x	+ +	x x	+ +	+ +
	MCE ‡				+ x		+ x		
90 °	PFE	x x	x x	+ +	x x	+ +	x x	+ +	+ +
	MCE			+ x					
135 °	PFE	x x	x x	+ +	x x	+ +	+ x	+ +	+ +
	MCE				+ x				
180 °	PFE	x x	+ x	+ +	o x	+ +	o x	+ +	o o
	MCE								

† Percent Frequency Error

‡ Modal Correlation Error

From the table it is more easily seen where different interface methods produce the best results. The first system z-bending mode is represented most accurately in all configurations with the use of the fixed-interface method. This is also mostly true for the second z-bending mode, and also for the fourth and sixth modes although less strongly. Of all configurations examined, at the third, fifth,

seventh and eighth z-bending modes a transition occurs at which point the mixed-interface method instead generally provides the best results. The free-interface mode sets however, did produce the most accurate results for some cases in the configuration $\theta = 180^\circ$.

At this point, the most obvious question is: why are certain mode set interface types performing better than the others in each situation? Inspection of the system z-bending mode shapes provides a simple answer. *The component mode type whose motion most closely approximates the motion of Beam 2 in the system mode, produces the best results.* For example, in the third and fifth system z-bending modes of all configurations, the motion of Beam 2 is basically in the form of classical pinned-free beam motion. Correspondingly, these system modes are the cases where mixed-interface mode sets perform better than the other two interface methods. In the configuration $\theta = 180^\circ$, during the third, fifth, and seventh z-bending system modes, Beam 2 exhibits pinned motion, which matches results. In the fourth, sixth, and eighth system z-bending modes of the same configuration ($\theta = 180^\circ$), Beam 2 exhibits free-free motion due to the large motion of the joint. This is especially pronounced in models with low spring stiffness, which also match results. In all configurations examined, during the first two system z-bending modes, Beam 2 exhibits either rigid body motion or strict cantilever (fixed-free) motion. In these cases, it is found that fixed-interface mode sets provide the best results. In the fourth and sixth system z-bending modes for $\theta = 45^\circ$, 90° , and 180° , the motion of Beam 2 becomes more difficult to distinguish between cantilever and pinned motion. At $\theta = 180^\circ$, the motion is either cantilever or free for these two system modes. In

each configuration the motion of Beam 2 in the fourth and sixth system z-bending mode is likely a combination of two types of motion. In these cases, Beam 2 is generally represented best by a fixed-interface mode set for the high spring stiffness model, and either a mixed- or free-interface mode set for the low spring stiffness model, which is expected.

It is now known that the situation in which each interface type will perform best is simply a function of the type of motion of the represented component in the system mode. Thus, to utilize this information, the next obvious question is: why does Beam 2 exhibit the different types of motion in the different system modes and configurations? *If the motion of a component in the system mode is able to be predicted, then, according to the above statements, the best mode set interface type to represent that component will be known.* This would be extremely useful information. For the model in this study, the motion of Beam 2 in the system mode is somewhat predictable. The following discussion describes this, and should be extendable to other models with slender beam components that articulate.

The only parameter to distinguish the three interface types of mode sets is the treatment of the boundary coordinates during the calculation of the component eigenvectors. For a fixed-interface, all degrees of freedom of the one interface point are constrained. For a free-interface, all are unconstrained. For a mixed-interface in this study, all but the rotational freedom about the z-axis are constrained. In system z-bending modes, the motion is planar and thus the important degrees of freedom at the interface point are two translations (x and y), and one rotation (about z).

In the third, fifth, and seventh z-bending modes of the four configurations, the

motion of Beam 2 is generally of a pinned type. This occurs because the high resistance of Beam 1 to tension and compression "constrains" y-direction motion of the joint, which eliminates the possibility of free-free beam shapes that need large motion at the base of the beam. Also, in system modes higher than the second, Beam 1 is vibrating in ways that cause angular motion of the section of Beam 1 near the joint. This has the effect of slightly freeing the rotational coordinates at the joint, no matter what the spring stiffness. This effect favors motion of the pinned-type for Beam 2, and disfavors cantilever motion of Beam 2 which needs zero rotation at the beam sections near the joint. Thus, pinned motion of Beam 2 results. If Beam 1 were stiffer near the joint - less susceptible to rotational motion of the beam sections near the joint, this effect would be less obvious and cantilever motion would probably be favored. For these listed reasons, it is expected that system z-bending mode shapes higher than the eighth would also exhibit pinned motion in Beam 2 and thus be better represented with mixed-interface mode sets for that component.

In contrast, some of the system modes in the configuration $\theta = 180^\circ$ produce large joint motion perpendicular to the axis of Beam 2. This difference from other configurations is due to the greater ease with which Beam 1 is able to bend than stretch/compress. In the $\theta = 180^\circ$ configuration, bending of Beam 1 causes the joint to move perpendicularly to Beam 2. This allowance of the translation of the base of Beam 2, combined with low spring stiffness which relaxes the rotational freedom, provides enough of the necessary conditions for the free-free motion of Beam 2. Thus, for low spring stiffnesses at this configuration ($\theta = 180^\circ$), free-interface mode sets perform well in the system modes where the joint moves (modes 4, 6, and 8). In

system modes of this configuration ($\theta = 180^\circ$) where the joint does not move (modes 3, 5, and 7), the motion of Beam 2 is generally of the pinned-type because the sections of Beam 1 near the joint cause rotation of the joint. Although for the other configurations, it is predictable that the higher system modes will exhibit pinned-type motion in Beam 2, such a prediction for the configuration $\theta = 180^\circ$ is not possible. It may be likely that for this configuration, system z-bending modes will continually alternate between those with large joint translation in the x-direction and those with zero joint translation in the x-direction, thus alternately favoring free-interface mode sets and mixed-interface mode sets respectively (for the low spring stiffness models; substitute fixed-interface for free-interface for the high spring stiffness models).

For all configurations, however the first two z-bending modes were composed of the deformation of either Beam 1 or Beam 2, but generally not both, where the beam not deforming stays essentially rigid. The author theorizes that because the sections of Beam 1 near the joint do not flex very much rotationally in the first two system z-bending modes, any joint stiffness causes cantilever motion to be favored and pinned-type motion to be disfavored for Beam 2. Also, because the joint does not translate perpendicularly to Beam 2 much in these system modes, free-free motion is not likely for Beam 2 either. Thus, the fixed-interface mode sets provide the most accurate representation of the first two system z-bending modes.

As stated above, if the motion of the component in the system mode is predictable given the model physical information and information of the configuration of the model, then, using these conclusions, a reasonably good prediction can be made as to the most accurate interface type to be selected for a mode set to represent the component.

6.4 A "Robust" Mode Set

Obviously it is important for a component mode set to be one that represents the component well in the synthesized system. If the component is going to be subject to varying configurations or varying conditions at the interface, a "robust" mode set would be one that continually represents the component accurately through these changes. The present study has given some observations on mode set selection for a model whose linearized dynamics have been examined about static configuration changes. These results therefore do not necessarily extend to mode set selection for components whose motion includes rapid slewing, however the results may give a solid basis for mode set selection for components whose configuration changes slowly enough that the dynamics can be considered linearized about several static configurations. Given such linearized configurations for this model, the higher frequency system modes examined are generally better represented by a mixed-interface mode set - especially in configurations other than $\theta = 180^\circ$. It is estimated that even higher frequency system modes will follow the same pattern. This is however, due to the attributes of the model selected. If, for example, the first beam was modelled shorter, thicker, and with more mass, it is likely that fixed-interface mode sets would excel in representation of Beam 2 in the "lower" *and* "higher" system modes simply due to the different effects Beam 1 would have on Beam 2 during system mode deformation. The quantification of "low" and "high" is dependent on the model and the total number of degrees of freedom, and may not be trivial. The results of this study are not enough to speculate on that quantification. In any case, it is seen that if component mode sets are selected carefully, there can be

a substantial reduction in the number of degrees of freedom in the set needed to accurately represent the component. For example, if a given number of component modes of a poorly chosen interface type are needed to obtain a certain accuracy, the same or greater accuracy may be obtained with less modes from a mode set of a more wisely chosen interface type, which may be reduced further with the elimination of unnecessary mode types, e.g. x-bending component modes to represent system z-bending.

In general, the mode set selection process suggested as a result of this study is two steps. First, examine the entire system and the physical properties of the components at the interfaces of the component in question. Select the interface type for the mode set based on what directions if any, the connected components will deform easiest, and the degree to which they are expected to deform. As an example, observations made in this study, which are intuitive, included that a connected beam will flex more in bending to produce interface coordinate motion than it will flex in tension in a different configuration to produce interface coordinate motion in the same direction. After the interface type is decided and the component modes are calculated, the second step is to eliminate unnecessary mode types from the set. For example, if the motion of a sensor in a certain direction is important in an analysis, then component modes which produce system motion in an orthogonal direction may be unnecessary and may substantially reduce the size of the mode set when eliminated. If the component is symmetric such that a fixed- or free-interface method would produce pairs of bending modes of equal frequency in two perpendicular directions, an advantage to using a mixed-interface component mode method is that

modes of bending in different directions will be easier to distinguish from each other during the component mode synthesis process in a finite element code. This will make it easier to eliminate the unnecessary modes.

In this study, it was found that system modes of "low" frequency and the system modes of "high" frequency were best approximated by different interface type mode sets given a number of kept modes. If a *mode set of the system* is sought for some analysis where system motion is a combination of all system modes, one option presents itself from the results of this study. A set of system modes could be created that is composed of low frequency system modes calculated via fixed-interface mode sets from its components, and a set of higher frequency system modes calculated via mixed-interface mode sets (or whatever appropriate) from its components. Care would need to be given to the determination of the orthogonality of a set of system modes composed as such, however the results may prove worth the extra complexity.

As a final note, one disadvantage to mixed-interface component modes is that they may be more difficult or more costly to obtain experimentally for model verification than free-interface modes where no attachment is necessary. However, if a mixed-interface mode set proves to be the more accurate choice for a component, the resulting errors in prediction of the system motion due to a poorly chosen mode set may translate to much higher costs. Obviously then, before the interface method is chosen a preliminary assessment of the potential danger of synthesized system error should be made in order to determine if more background research into mode set selection is necessary.

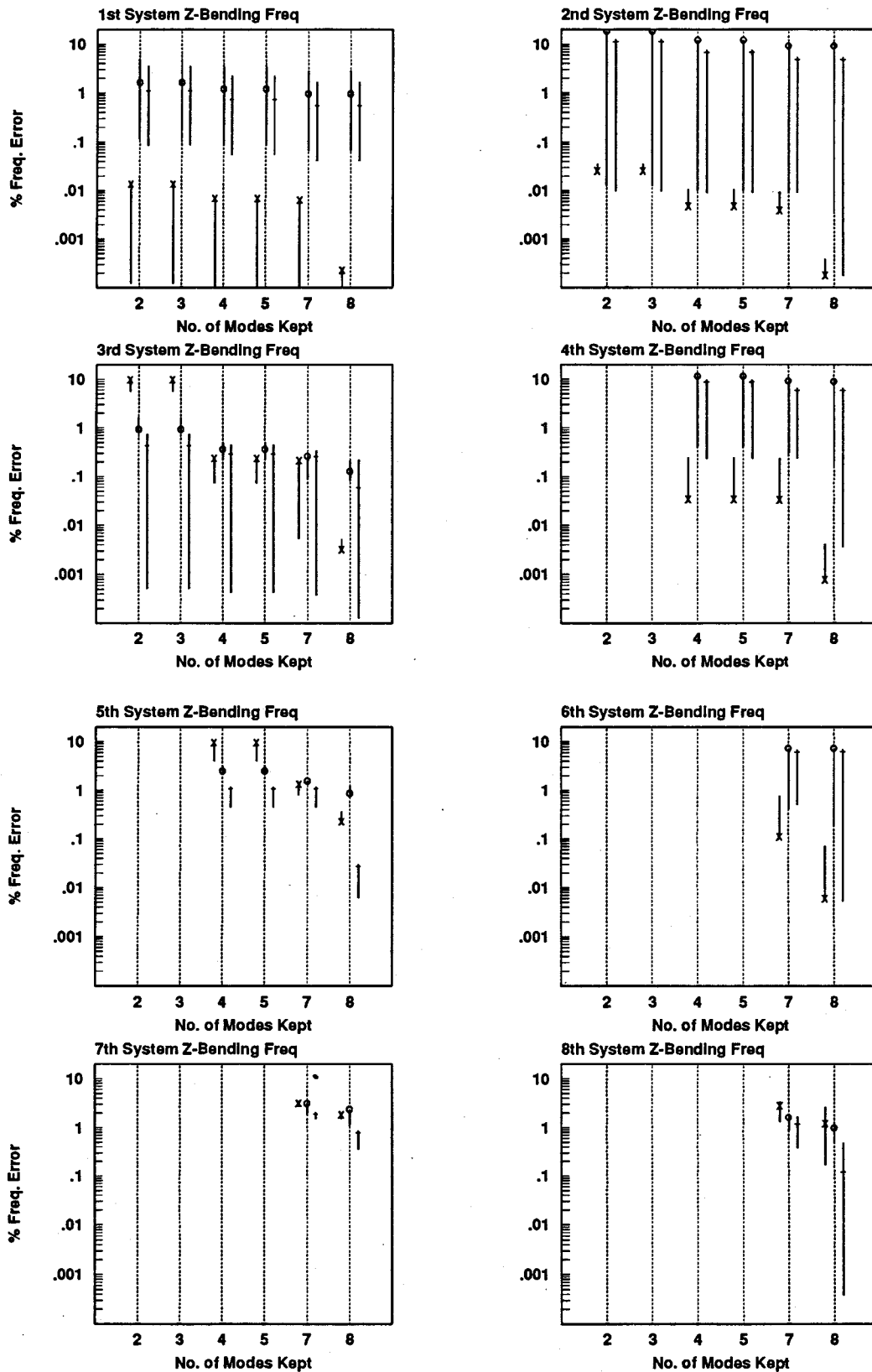


Figure 6.1: Ranges of Percent Frequency Error, $\theta = 45^\circ$
 Symbols: x = Fixed-Interface, o = Free-Interface, + = Mixed-Interface
 Symbols Plotted at Maximum Joint Spring Stiffness

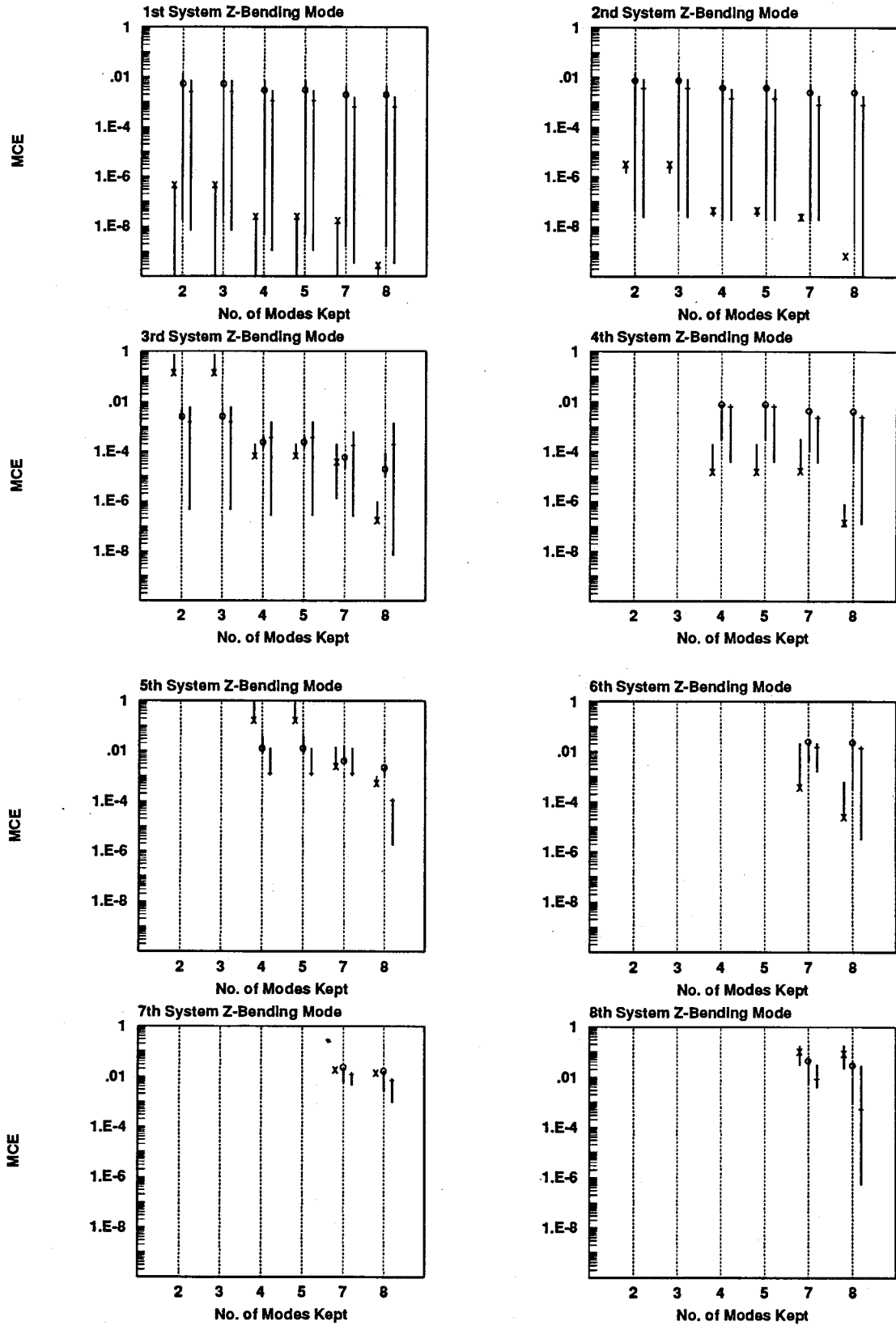


Figure 6.2: Ranges of Modal Correlation Error, $\theta = 45^\circ$
 Symbols: x = Fixed-Interface, o = Free-Interface, + = Mixed-Interface
 Symbols Plotted at Maximum Joint Spring Stiffness

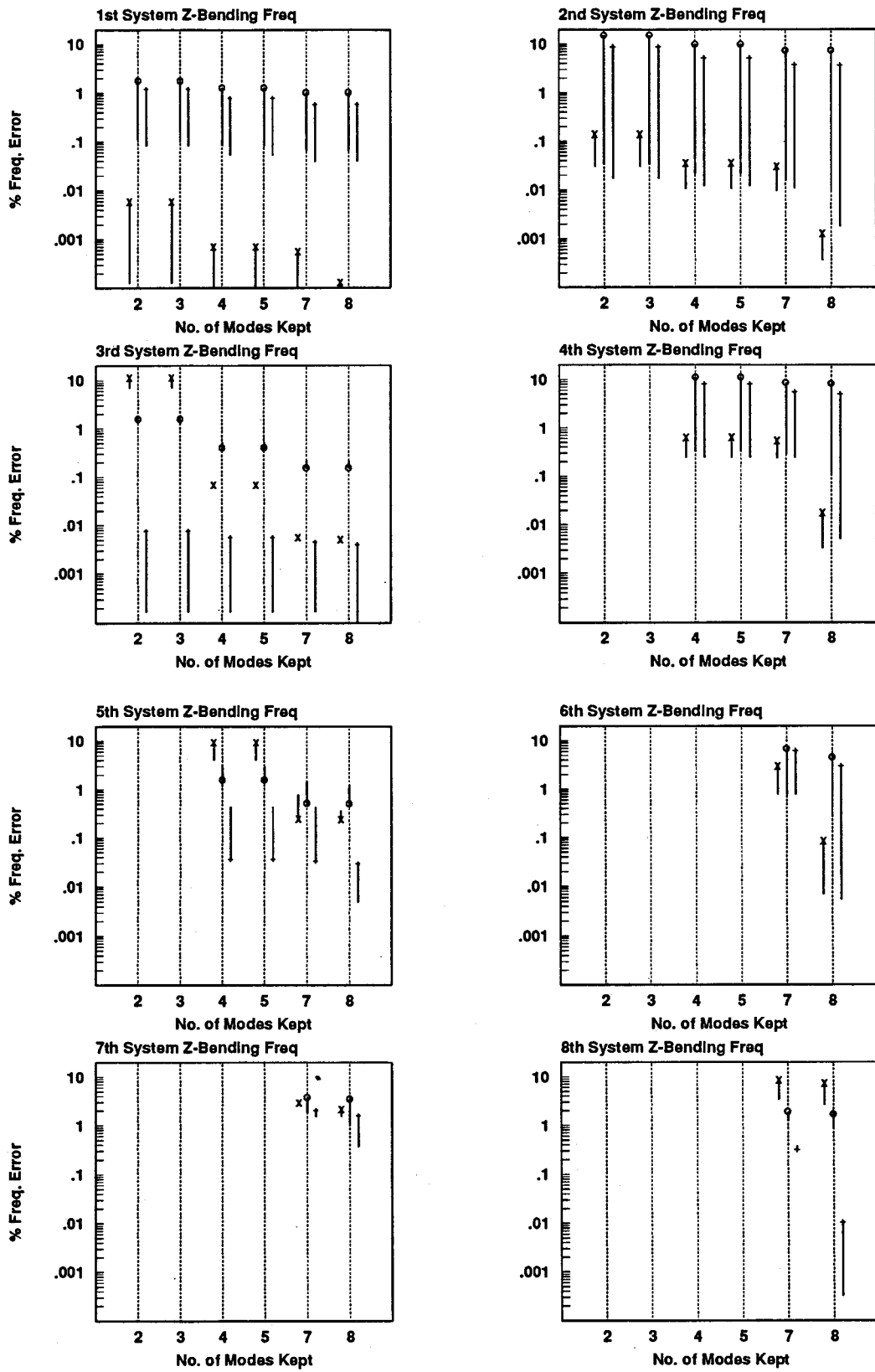


Figure 6.3: Ranges of Percent Frequency Error, $\theta = 135^\circ$
 Symbols: x = Fixed-Interface, o = Free-Interface, + = Mixed-Interface
 Symbols Plotted at Maximum Joint Spring Stiffness

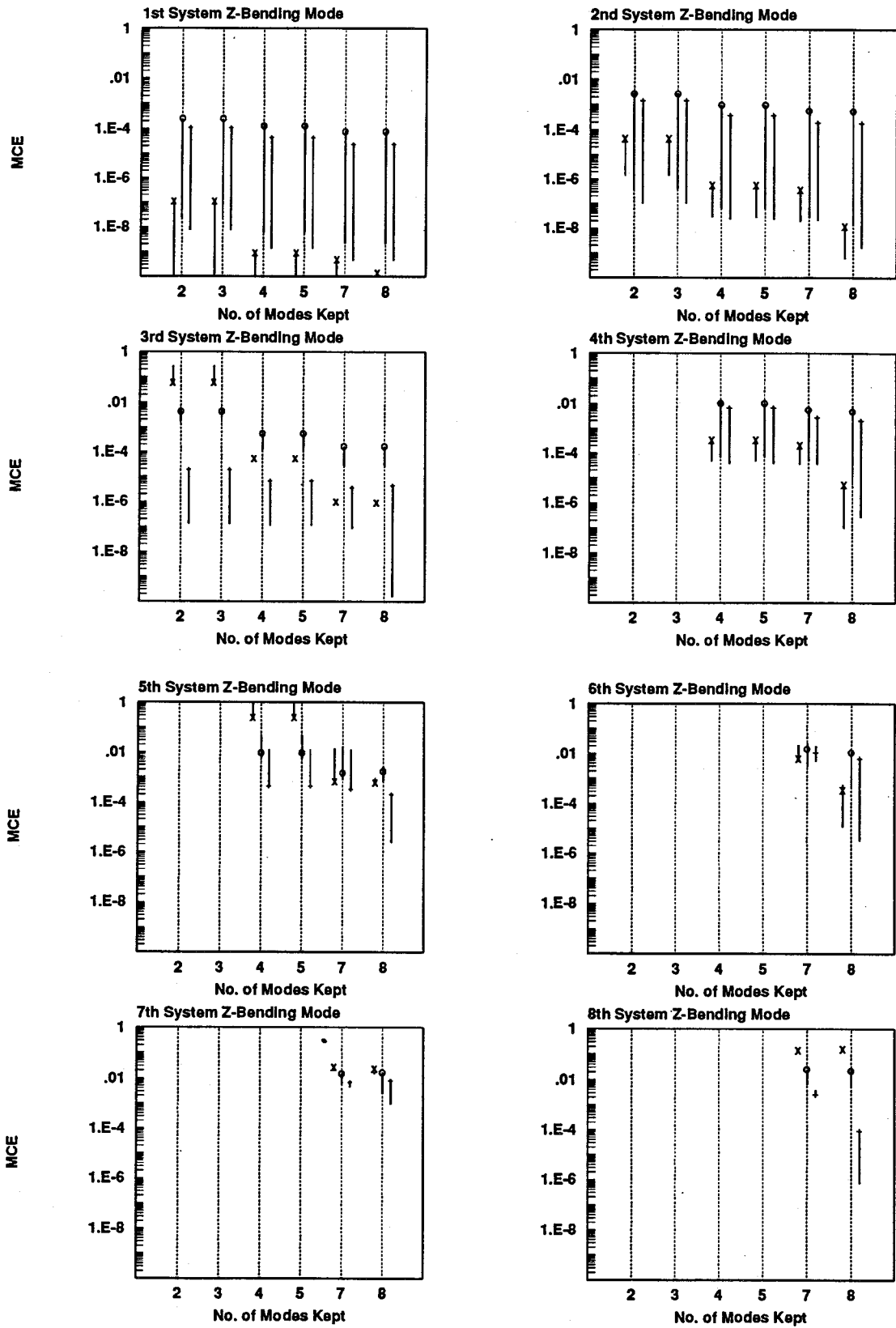


Figure 6.4: Ranges of Modal Correlation Error, $\theta = 135^\circ$
 Symbols: x = Fixed-Interface, o = Free-Interface, + = Mixed-Interface
 Symbols Plotted at Maximum Joint Spring Stiffness

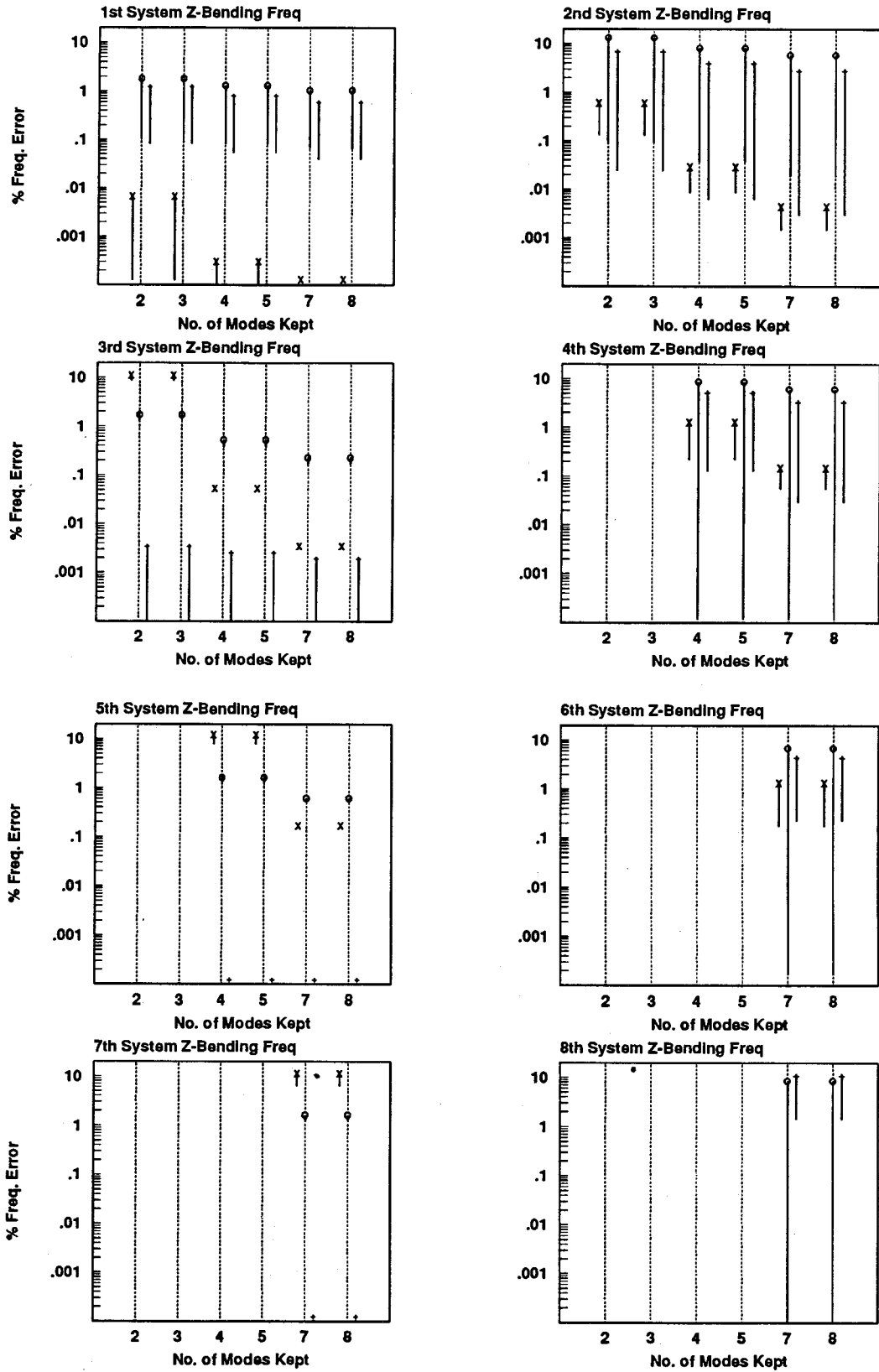


Figure 6.5: Ranges of Percent Frequency Error, $\theta = 180^\circ$
 Symbols: x = Fixed-Interface, o = Free-Interface, + = Mixed-Interface
 Symbols Plotted at Maximum Joint Spring Stiffness

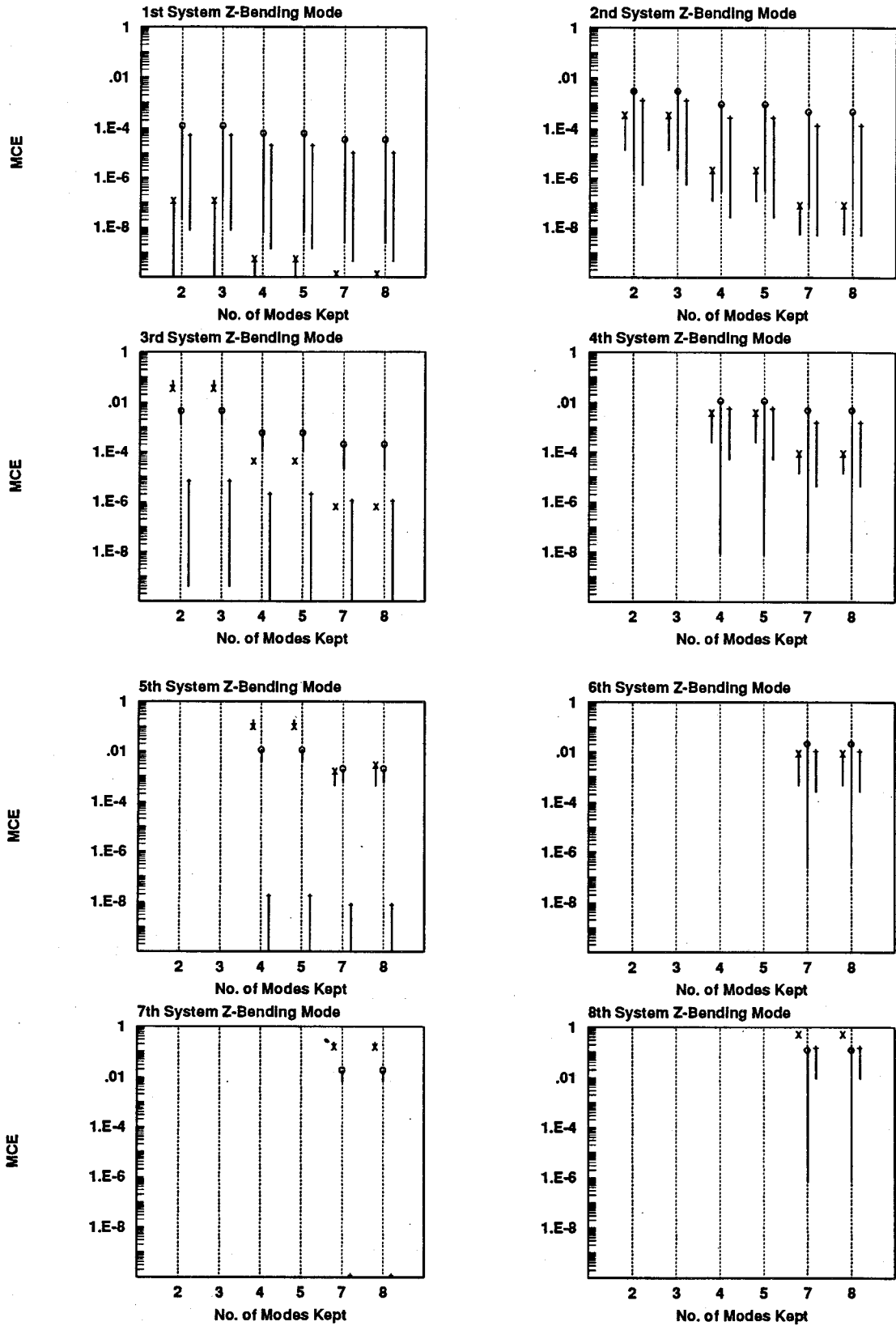


Figure 6.6: Ranges of Modal Correlation Error, $\theta = 180^\circ$
 Symbols: x = Fixed-Interface, o = Free-Interface, + = Mixed-Interface
 Symbols Plotted at Maximum Joint Spring Stiffness

VII. CONCLUSIONS AND FUTURE STUDY

A study was performed in order to determine the effects of component configuration and varying boundary conditions on selection of a reduced mode set used to represent a component in multibody dynamic analyses. A finite element model of a two beam linkage and a joint angular spring (Figure 3.1) was designed and Component Mode Synthesis was performed on it in MSC/NASTRAN while one beam (Beam 2) was modally reduced and the other was left unreduced. Three mode set interface types were used in mode sets of varying sizes including varied combinations of component mode types (bending, torsion, tension/compression). The same analyses were performed at varied joint angular spring stiffnesses and then all analyses were performed at varied configurations.

Examination of the error trends along increasing joint spring stiffness showed that there were two main influences on error. **These influences were: the proximity of the interface conditions on the component mode set to the actual model conditions on the component, and the variance in modal strain energy percent of the reduced beam in the system mode (percent is of system total strain energy).** The data showed that the former was the strongest influence on error for all mixed-interface mode set cases examined, while the latter was the strongest influence on error in general for the fixed- and free-interface cases.

In comparing interface types, it was found that **the component mode set interface types that produced the most accurate system modes were those which most closely approximated the motion of the reduced component in the system**

mode. For example if, within the system deformation for a given system mode, the reduced beam was found to exhibit motion similar to that of a pinned-free beam vibrational shape, then for that system mode and configuration, the most accurate synthesized representation of the system was one that employed a mixed-interface (pinned) mode set to represent the reduced component. As a result of this, it was found that for the model of this study, **if the motion of the reduced component in the system mode could be predicted, then the most accurate mode set to use for that component could also be predicted (for that system mode only).** It was also found that **despite the additional degrees of freedom and increased maximum frequency of a mode set, the addition of some types of component modes had no positive effect on the synthesized system accuracy of a given kind of system mode.** For example, the inclusion of component torsional modes in the mode set of the reduced component produced no increase in accuracy in the synthesized system modes of bending in the x-y plane.

Due to the physical attributes of the model used in this study, it was found that for most configurations, **fixed-interface component mode sets performed most accurately for the "low" frequency system modes examined (the first two modes of bending in the x-y plane); but mixed-interface component mode sets performed most accurately in the "higher" frequency system modes examined (third, fifth, seventh, and eighth modes of bending in the x-y plane).** This conclusion was independent of mode set size, so long as compared mode sets of varying interface types were of the same size, e.g. a mode set of four fixed-interface bending component modes was compared to a mode set of four mixed-interface bending

component modes. Based on the conclusions about predicting component motion in a system mode shape, it was estimated that for the model of this study, the mixed-interface mode set would continue to contribute more accurately than mode sets of other interface types to system modes of higher frequency than those examined.

Because only the first eight system modes of bending in the plane of interest were examined in the present study, future developments might involve extending the research to higher frequency system modes or to the system modes of bending not in the plane examined in this study. The examination of higher system modes could confirm the estimations made presently about the performance of mixed-interface mode sets. Also in the future, further examination of the first two system modes of bending for other types of models might help illustrate whether fixed-interface mode sets are generally more accurate for these low system modes, or whether the results obtained here in that regard were strictly due the model used in this study. The examination of system "xy-bending" modes could determine the value of component torsional modes in the set. Other research might include varying the mass of the unreduced beam (Beam 1) to determine such an effect on mode set selection. Popular theory on this subject is that when the mass of the attached structure becomes much larger than the mass of the reduced component, then the dynamics of the component become negligible and fixed-interface mode sets are more appropriate for the component, which is intuitive. A study where the physical attributes of Beam 1 is varied might also pronounce the effects of varying configuration on mode set selection found in this study.

On the topic of mixed-interface and free-interface mode sets, two other

contributions might be made in the future. A study could be performed similar to the present study where inertia relief modes are included in the component mode sets. Recall that in this study such severely truncated mode sets were used, it was decided that inertia relief modes would not contribute as much to the system accuracy as would the important low frequency component normal modes that the inertia relief modes would replace in order to keep the mode set size small. In this study, it was also decided not to use inertia and stiffness interface loaded component modes because joint angular spring was varied and the addition of interface loaded component modes to the study might unnecessarily complicate the results obtained by varying the joint angular spring stiffness. The results of the use of such component modes though, might prove informative if presented carefully.

One final suggestion for future study has to do with the use of "non-sequential" component mode sets, e.g. component mode sets composed of all the component modes up to a certain number or frequency with the exception of certain modes before that number or frequency which have been eliminated from the set. Using component mode sets that are fully sequential up to the cut-off number or frequency has the advantage that there are popular and commonly used criteria (section 5.1) somewhat effective in determining a number or frequency up to which the resulting synthesized system modes can be seen as "realistic". The synthesized system modes below this number or frequency generally have much lower error than those above. Future study might include the determination of some type of criteria to determine such a transition point for systems whose components use non-sequential mode sets.

REFERENCES

- 1) Meirovitch, L. and Kwak, M.K., "Convergence of the Classical Rayleigh-Ritz Method and the Finite Element Method," *AIAA Journal*, Vol. 28, No. 8, August 1990, pp. 1509-1516.
- 2) Clough, R.W. and Penzien, J., *Dynamics of Structures*, McGraw Hill, Inc., New York, 1975, p. 239.
- 3) Hurty, W.C., "Vibrations of Structural Systems by Component Mode Synthesis," *Proc. of the Am. Soc. of Civil Engrs., J. Eng. Mech. Div.* 86, 1960, pp. 51-69.
- 4) Gladwell, G.M.L., "Branch Modes Analysis of Vibrating Systems," *Journal of Sound and Vibration*, Vol. 1, 1964, pp. 41-59.
- 5) Hurty, W.C., "Dynamic Analysis of Structural Systems Using Component Modes," *AIAA Journal*, Vol. 3, No. 4, April 1965, pp. 678-685 (Based on JPL Tech. Memo 32-530, January 1964).
- 6) Craig, R.R. and Bampton, M.C.C., "Coupling of Substructures for Dynamic Analyses," *AIAA Journal*, Vol. 6, No. 7, July 1968, pp. 1313-1319.
- 7) Goldman, R.L., "Vibration Analysis by Dynamic Partitioning," *AIAA Journal*, Vol. 7, No. 6, 1969, pp. 1152-1154.
- 8) Hou, S.N., "Review of Modal Synthesis Techniques and a New Approach," *Shock and Vibration Bulletin*, Bulletin 40, Part 4, 1969, pp. 25-30.
- 9) Hurty, W.C., Collins, J.D., and Hart, G.C., "Dynamic Analysis of Large Structures by Modal Synthesis Techniques," *Computers & Structures*, Vol. 1, 1971, pp. 535-563.
- 10) MacNeal, R.H., "A Hybrid Method of Component Mode Synthesis," *Computers & Structures*, Vol. 1, 1971, pp. 581-601.
- 11) Hurty, W.C., "Introduction to Modal Synthesis Techniques," *Synthesis of Vibrating Systems*, ASME, 1971, pp. 1-13.
- 12) Bamford, R., Wada, B.K., Garba, J.A. and Chisholm, J., "Dynamic Analysis of Large Structural Systems," *Synthesis of Vibrating Systems*, ASME, 1971, pp. 57-71.
- 13) Benfield, W.A. and Hruda, R.F., "Vibration Analysis of Structures by Component Mode Substitution," *AIAA Journal*, Vol. 9, No. 7, July 1971, pp. 1255-1261.

- 14) Rubin, S., "Improved Component-Mode Representation for Structural Dynamic Analysis," *AIAA Journal*, Vol. 13, No. 8, August 1975, pp. 995-1006.
- 15) Hintz, R.M., "Analytical Methods in Component Modal Synthesis," *AIAA Journal*, Vol. 13, No. 8, August 1975, pp. 1007-1016.
- 16) Craig, R.R. and Chang, C.J., "Free-Interface Methods of Substructure Coupling for Dynamic Analysis," *AIAA Journal*, Vol. 14, No. 11, 1976, pp. 1633-1635.
- 17) Craig, R.R. "Methods of Component Mode Synthesis," *Shock and Vibration Digest*, Naval Research Lab., Washington D.C., Vol. 9, 1977, pp. 3-10.
- 18) Blueloch, P.A. and Carney, K.S., "Selection of Component Modes," AIAA Dynamic Specialist Conference, Long Beach, CA, April 5-6, 1990.
- 19) Garcia, E. and Inman, D.J., "Modeling of the Slewing Control of a Flexible Structure," *Journal of Guidance*, Vol. 14, No. 4, 1990, pp. 736-742.
- 20) Widrick, T., "Determining the Effects of Modal Truncation and Modal Errors In Component Mode Synthesis Methods," Master Thesis, The George Washington University, NASA Langley Research Center, July 1992.
- 21) MSC/NASTRAN *Linear Static and Normal Modes Analysis Seminar Notes*, seminar by Glenn Grassi, The MacNeal-Schwendler Corporation, May 1992.
- 22) MSC/NASTRAN *Superelement Analysis Seminar Notes*, seminar by J.C. Muskivitch, The MacNeal-Schwendler Corporation, June 1991.
- 23) MSC/NASTRAN *Dynamics Seminar Notes*, The MacNeal-Schwendler Corporation, December 1990.
- 24) MSC/NASTRAN *Users Manual*, The MacNeal-Schwendler Corporation, Version 67, August 1991.
- 25) MSC/NASTRAN *Applications Manual*, The MacNeal-Schwendler Corporation, April 1981, pp. 2.4-16, 2.4-17.
- 26) MSC/NASTRAN *Handbook for Linear Analysis*, The MacNeal-Schwendler Corporation, August 1985.
- 27) MSC/NASTRAN *Handbook for Dynamic Analysis*, The MacNeal-Schwendler Corporation, June 1983.
- 28) Corporate Headquarters, The MacNeal-Schwendler Corporation, 815 Colorado Blvd., Los Angeles, CA 90041-1777, Tel: (213) 258-9111 or (800) 336-4858.

- 29) *Payload Deployment and Retrieval System Simulation Database*, Version 1.0, 1 July 1991, RMS Operations, Lyndon B. Johnson Space Center, Houston, Texas.
- 30) Ugural, A.C. and Fenster, S.K., *Advanced Strength and Applied Elasticity*, Elsevier Science Publishing Co., New York, 1975, pp. 138-141.
- 31) Wei, J.J.C. and Allemang, R.J., "Model Correlation and Orthogonality Criteria Based on Reciprocal Modal Vectors," *Proc. 9th Intrnl. Modal Analysis Conference*, Part 1, 1991, pp. 486-491.
- 32) Hurty, W.C., "A Criterion for Selecting Realistic Natural Modes of a Structure," Jet Propulsion Laboratory Technical Memorandum 33-364, Pasadena, November, 1967.
- 33) Blevins, R.D., *Formulas for Natural Frequency and Mode Shape*, Robert E. Krieger Publishing Co., Malabar, Florida, 1984, chapter 8.

APPENDICES

A. A NASTRAN Input File

```
ID SONTAG, THESIS MODEL
$
$ ---- THIS IS THE EXECUTIVE CONTROL SECTION ----
$
$ MODEL AT 90 DEG
$ CMS METHOD: MIXED-INTERFACE
$ MODES KEPT: 2 BENDING, 1 TORSION
$ UNITS ARE FT, LB, SEC
$
SOL 103
TIME 10
$
$ -----
$ -----
$
$ ---- THIS IS THE CASE CONTROL SECTION -----
$
CEND
$
DISP = ALL
SET 333 = 0 $ RESIDUAL STRUCTURE
SET 444 = 20 $ SE 20
$
SUBCASE 1 $ SUPERELEMENT 20
  SUPER = 444
  METHOD = 40
SUBCASE 2 $ RESIDUAL STRUCTURE
  SUPER = 333
  METHOD = 40
  SPC=50
$
$ -----
$ -----
$
$ ---- THIS IS THE BULK DATA SECTION -----
$
BEGIN BULK
$
```

```

$ SUPERELEMENT and COMPONENT MODE SYNTHESIS
$ INFORMATION HERE
$
SESET,20,202,THRU,211
SEBSET1,20,12345,201
SECSET1,20,6,201
$
$ MODAL VARIABLES
SPOINT,1001,THRU,1004
SEQSET1,20,0,1001,THRU,1004$ 4 MODES FROM SE 20
$
PARAM,POST,0                $ Makes an XL database
PARAM,USETPRT,0             $ Outputs set membership of each point
PARAM,COUPMASS,1           $ Forces the use of Coupled Mass
PARAM,GRDPNT,0              $ Enacts the Grdpnt Wgt Gen about grid 0
$
$ Beam 1
$
GRID,101,0,0.0,0.0,0.0,0
=,*1,=,=,*(2.32),==
=9
CBEAM,1,20,101,102,1.0,0.0,0.0
=,*1,=,*1,*1,==
=8
$
$ Beam 2
$
GRID,201,10,0.0,0.0,0.0,10
=,*1,=,=,*(2.32),==
=9
CBEAM,11,20,201,202,1.0,0.0,0.0
=,*1,=,*1,*1,==
=8
$
$ The Pin Joint and Joint Spring (about DOF-6)
$
RBE2,60,111,12345,201 $ DOF-6
CELAS2,90,8.8257+5,111,6,201,6
$   K/K0 = 1 at K=8.8257+5
$
$ The 2nd Coordinate System
CORD2R,10,0,0.,23.2,0.,0.,23.2,1.,C123
$+123,-1.0,23.2,0.          $ theta = 0 deg
$+123,-0.5,22.7,0.         $ theta = 45 deg
+123,0.0,22.2,0.0          $ theta = 90 deg

```

```
$+123,0.5,22.7,0.          $ theta = 135 deg
$+123,1.0,23.2,0.          $ theta = 180 deg
$
SPC1,50,123456,101          $ To cantilever the lower beam
SPC1,50,0,1003             $ To remove these modes from SEQSET
$
PBEAM,20,30,.0155,.00226,.00226,0.,.00452,,P12
+12,,,,,,,,,P23
+23,NO,1.0,,,,,,,,,P34
+34,0.,0.
MAT1,30,3.02E+9,7.94E+8,,16.66
$
EIGR,40,AGIV,,,,,100
$
ENDDATA
```

B. Exact Z-Bending System Natural Frequencies (Hz)

Table B.1: Exact Z-Bending System Natural Frequencies, $\theta = 45^\circ$ (Hz)

$K/K_0 =$	Mode 1	Mode 2	Mode 3	Mode 4
1/200	0.3212	2.8341	23.446	26.346
1/100	0.4523	2.8355	23.489	26.349
1/50	0.6345	2.8381	23.573	26.354
1/20	0.9795	2.8466	23.817	26.372
1/10	1.3330	2.8618	24.188	26.407
1/5	1.7528	2.8973	24.810	26.507
1/2	2.2808	3.0379	25.750	27.205
1	2.5038	3.2763	26.005	28.653
2	2.5902	3.5413	26.078	30.344
5	2.6296	3.7829	26.111	32.128
10	2.6407	3.8823	26.120	32.958
20	2.6460	3.9362	26.124	33.436
50	2.6490	3.9700	26.127	33.747
100	2.6500	3.9815	26.128	33.855
200	2.6505	3.9873	26.128	33.909
	Mode 5	Mode 6	Mode 7	Mode 8
1/200	74.493	76.914	120.97	158.50
1/100	74.508	76.944	120.97	158.55
1/50	74.536	77.004	120.97	158.63
1/20	74.613	77.191	120.98	158.89
1/10	74.714	77.512	120.98	159.30
1/5	74.850	78.165	120.98	160.08
1/2	75.029	79.986	121.00	162.12
1	75.124	82.337	121.01	164.69
2	75.180	85.294	121.03	167.62
5	75.218	88.986	121.06	169.78
10	75.231	90.944	121.07	170.25
20	75.237	92.146	121.09	170.44
50	75.241	92.957	121.10	170.53
100	75.243	93.244	121.10	170.56
200	75.243	93.391	121.10	170.58

Table B.2: Exact Z-Bending System Natural Frequencies, $\theta = 90^\circ$ (Hz)

$K/K_0 =$	Mode 1	Mode 2	Mode 3	Mode 4
1/200	0.3195	2.3802	23.354	24.706
1/100	0.4477	2.3934	23.373	24.735
1/50	0.6214	2.4203	23.409	24.795
1/20	0.9289	2.5046	23.497	24.986
1/10	1.1192	2.6506	23.594	25.322
1/5	1.4423	2.9272	23.694	25.990
1/2	1.6407	3.4948	23.788	27.627
1	1.7116	3.9495	23.826	29.368
2	1.7467	4.3111	23.864	31.168
5	1.7675	4.6408	23.859	33.006
10	1.7744	4.7207	23.863	33.847
20	1.7778	4.7828	23.865	34.329
50	1.7798	4.8215	23.866	34.641
100	1.7805	4.8346	23.867	34.749
200	1.7808	4.8413	23.867	34.803
	Mode 5	Mode 6	Mode 7	Mode 8
1/200	74.619	77.084	132.18	158.23
1/100	74.637	77.109	132.18	158.25
1/50	74.673	77.160	132.18	158.29
1/20	74.769	77.318	132.18	158.41
1/10	74.900	77.595	132.18	158.60
1/5	75.081	78.176	132.18	158.92
1/2	75.321	79.851	132.19	159.60
1	75.445	82.044	132.19	160.19
2	75.517	84.793	132.20	160.68
5	75.563	88.193	132.21	161.07
10	75.579	89.981	132.21	161.22
20	75.587	91.077	132.22	161.29
50	75.592	91.815	132.22	161.34
100	75.594	92.076	132.22	161.36
200	75.595	92.210	132.22	161.37

Table B.3: Exact Z-Bending System Natural Frequencies, $\theta = 135^\circ$ (Hz)

$K/K_0 =$	Mode 1	Mode 2	Mode 3	Mode 4
1/200	0.3161	2.8768	23.404	26.405
1/100	0.4385	2.9205	23.405	26.465
1/50	0.5973	3.0062	23.406	26.585
1/20	0.8522	3.2485	23.410	26.929
1/10	1.0462	3.5976	23.414	27.463
1/5	1.2023	4.1243	23.420	28.397
1/2	1.3288	4.9872	23.427	30.442
1	1.3780	5.5925	23.431	32.455
2	1.4040	6.0431	23.433	34.419
5	1.4201	6.3925	23.435	36.318
10	1.4256	6.5268	23.436	37.155
20	1.4283	6.5798	23.436	37.626
50	1.4299	6.6418	23.436	37.927
100	1.4305	6.6567	23.436	38.030
200	1.4308	6.6642	23.436	38.083
	Mode 5	Mode 6	Mode 7	Mode 8
1/200	74.497	76.912	120.98	158.46
1/100	74.516	76.919	120.99	158.46
1/50	74.553	76.955	121.00	158.46
1/20	74.656	77.067	121.05	158.47
1/10	74.800	77.264	121.12	158.48
1/5	75.009	77.682	121.24	158.50
1/2	75.302	78.909	121.55	158.54
1	75.457	80.494	121.91	158.58
2	75.546	82.387	122.34	158.61
5	75.603	84.569	122.83	158.64
10	75.622	85.653	123.08	158.65
20	75.631	86.297	123.24	158.66
50	75.637	86.723	123.34	158.67
100	75.639	86.872	123.37	158.67
200	75.640	86.948	123.39	158.67

Table B.4: Exact Z-Bending System Natural Frequencies, $\theta = 180^\circ$ (Hz)

$K/K_0 =$	Mode 1	Mode 2	Mode 3	Mode 4
1/200	0.3143	3.8266	23.439	33.850
1/100	0.4337	3.9000	23.439	33.939
1/50	0.5855	4.0405	23.440	34.114
1/20	0.8208	4.4150	23.440	34.611
1/10	0.9934	4.9126	23.441	35.357
1/5	1.1304	5.6209	23.443	36.597
1/2	1.2427	6.6320	23.445	39.053
1	1.2873	7.2951	23.446	41.172
2	1.3112	7.7609	23.447	43.000
5	1.3261	8.1069	23.448	44.581
10	1.3311	8.2364	23.448	45.228
20	1.3337	8.3042	23.448	45.579
50	1.3352	8.3459	23.448	45.800
100	1.3357	8.3600	23.448	45.875
200	1.3360	8.3671	23.448	45.913
	Mode 5	Mode 6	Mode 7	Mode 8
1/200	75.969	93.888	158.59	184.06
1/100	75.969	93.978	158.59	184.15
1/50	75.969	94.156	158.59	184.33
1/20	75.969	94.674	158.59	184.86
1/10	75.969	95.483	158.59	185.70
1/5	75.969	96.927	158.59	187.24
1/2	75.969	100.20	158.59	191.01
1	75.969	103.56	158.59	195.32
2	75.969	106.94	158.59	200.16
5	75.969	110.30	158.59	205.51
10	75.969	111.76	158.59	208.08
20	75.969	112.60	158.59	209.58
50	75.969	113.14	158.59	210.57
100	75.969	113.32	158.59	210.91
200	75.969	113.41	158.59	211.08

C. Error Trends, $\theta = 90^\circ$

This appendix includes the percent frequency error and the modal correlation error plots for each interface method and each synthesized system z-bending mode examined. This data is only from the $\theta = 90^\circ$ configuration. Data from the other configurations is not included for space considerations. The plot legends are as described in Chapter 5. Here is the list of figures in this section.

- Figure C.1: 1st System Z-Bending Mode, Fixed-Interface, $\theta = 90^\circ$
- Figure C.2: 1st System Z-Bending Mode, Free-Interface, $\theta = 90^\circ$
- Figure C.3: 1st System Z-Bending Mode, Mixed-Interface, $\theta = 90^\circ$

- Figure C.4: 2nd System Z-Bending Mode, Fixed-Interface, $\theta = 90^\circ$
- Figure C.5: 2nd System Z-Bending Mode, Free-Interface, $\theta = 90^\circ$
- Figure C.6: 2nd System Z-Bending Mode, Mixed-Interface, $\theta = 90^\circ$

- Figure C.7: 3rd System Z-Bending Mode, Fixed-Interface, $\theta = 90^\circ$
- Figure C.8: 3rd System Z-Bending Mode, Free-Interface, $\theta = 90^\circ$
- Figure C.9: 3rd System Z-Bending Mode, Mixed-Interface, $\theta = 90^\circ$

- Figure C.10: 4th System Z-Bending Mode, Fixed-Interface, $\theta = 90^\circ$
- Figure C.11: 4th System Z-Bending Mode, Free-Interface, $\theta = 90^\circ$
- Figure C.12: 4th System Z-Bending Mode, Mixed-Interface, $\theta = 90^\circ$

- Figure C.13: 5th System Z-Bending Mode, Fixed-Interface, $\theta = 90^\circ$
- Figure C.14: 5th System Z-Bending Mode, Free-Interface, $\theta = 90^\circ$
- Figure C.15: 5th System Z-Bending Mode, Mixed-Interface, $\theta = 90^\circ$

- Figure C.16: 6th System Z-Bending Mode, Fixed-Interface, $\theta = 90^\circ$
- Figure C.17: 6th System Z-Bending Mode, Free-Interface, $\theta = 90^\circ$
- Figure C.18: 6th System Z-Bending Mode, Mixed-Interface, $\theta = 90^\circ$

- Figure C.19: 7th System Z-Bending Mode, Fixed-Interface, $\theta = 90^\circ$
- Figure C.20: 7th System Z-Bending Mode, Free-Interface, $\theta = 90^\circ$
- Figure C.21: 7th System Z-Bending Mode, Mixed-Interface, $\theta = 90^\circ$

- Figure C.22: 8th System Z-Bending Mode, Fixed-Interface, $\theta = 90^\circ$
- Figure C.23: 8th System Z-Bending Mode, Free-Interface, $\theta = 90^\circ$
- Figure C.24: 8th System Z-Bending Mode, Mixed-Interface, $\theta = 90^\circ$

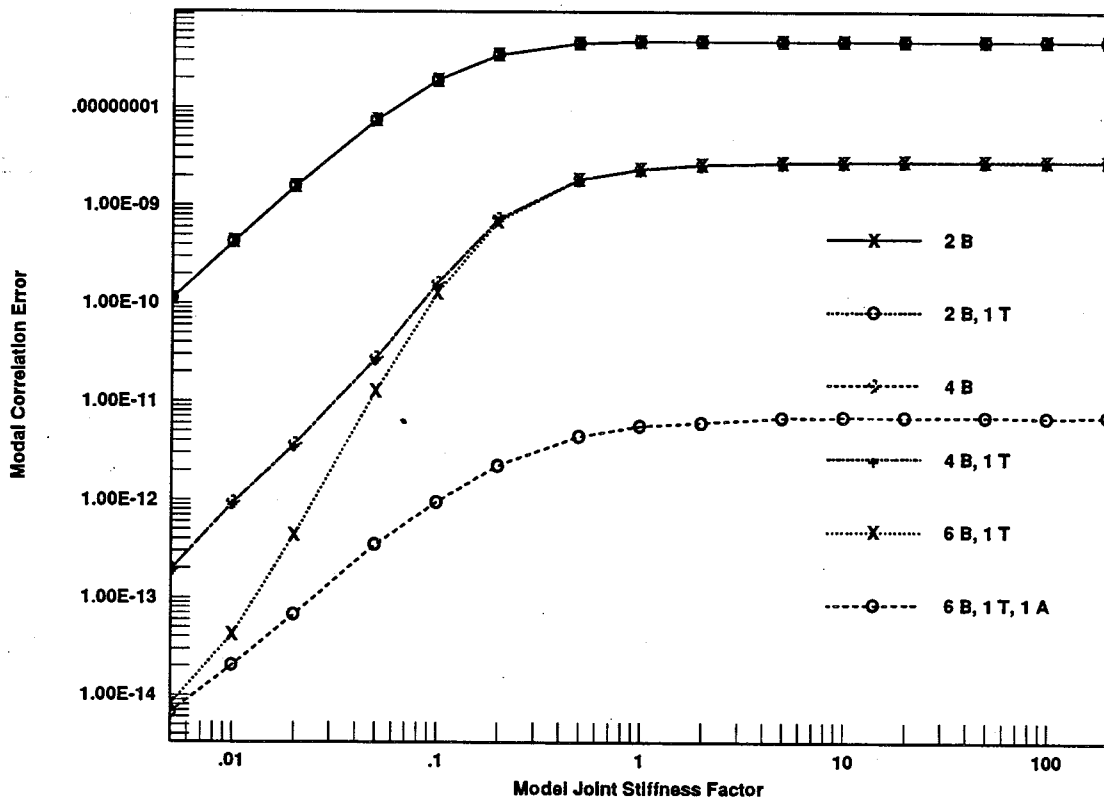
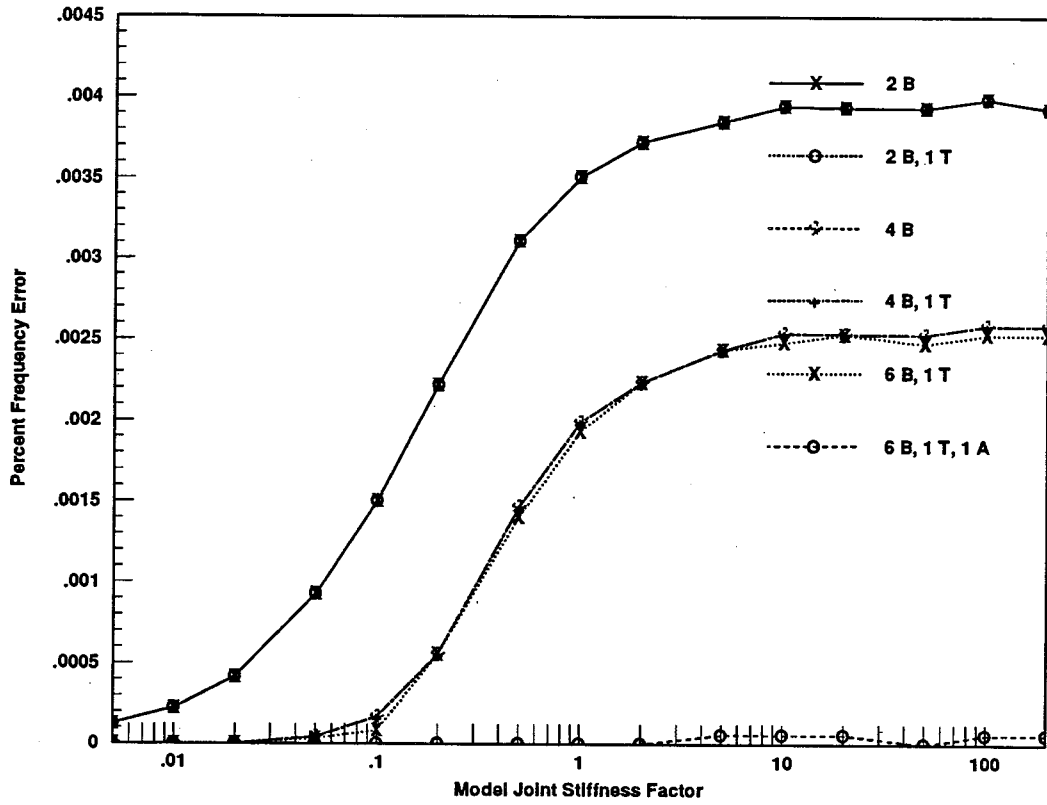


Figure C.1: 1st System Z-Bending Mode, Fixed-Interface, $\theta = 90^\circ$

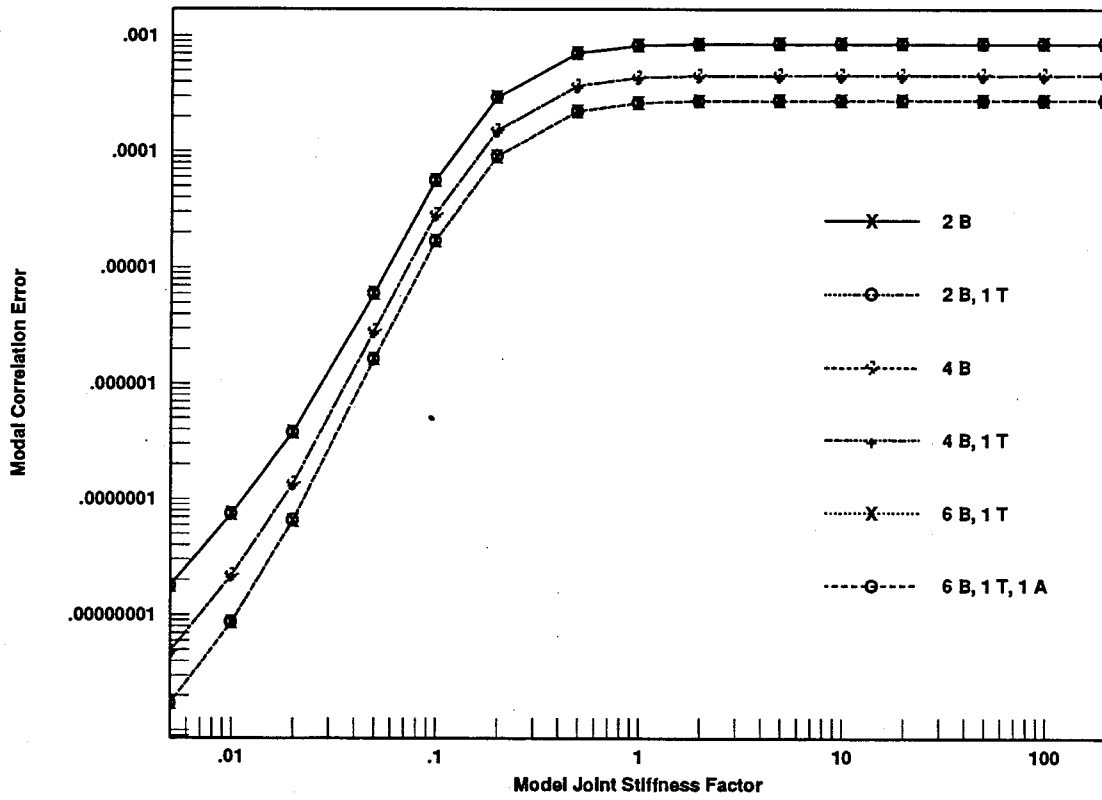
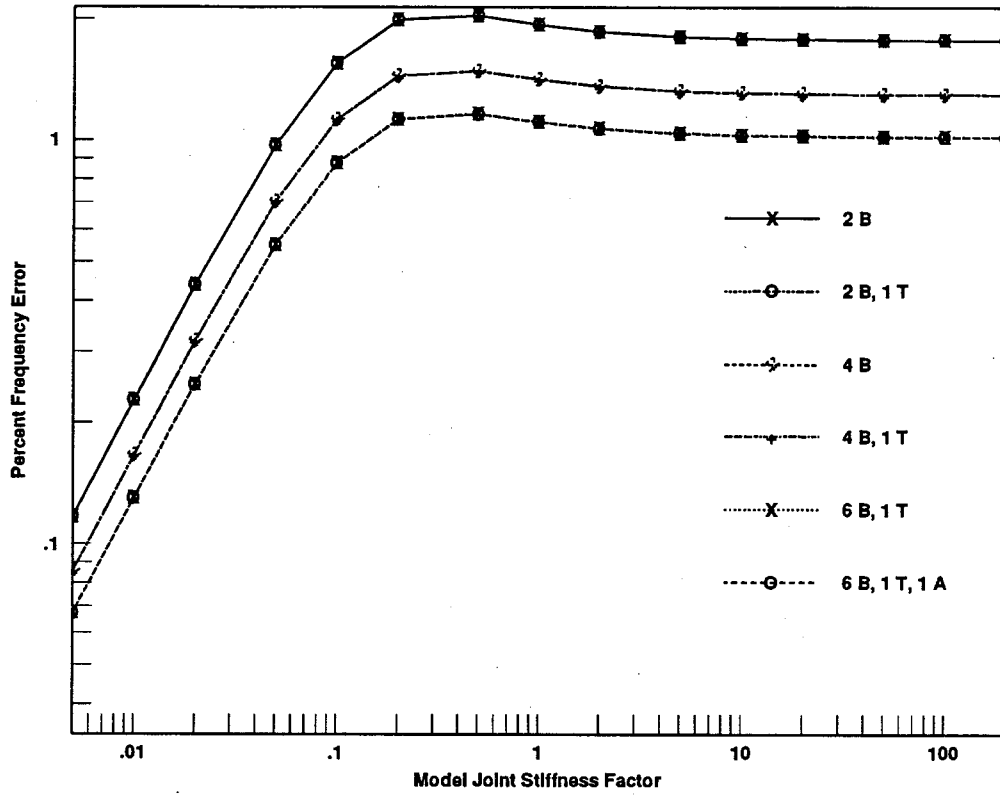


Figure C.2: 1st System Z-Bending Mode, Free-Interface, $\theta = 90^\circ$

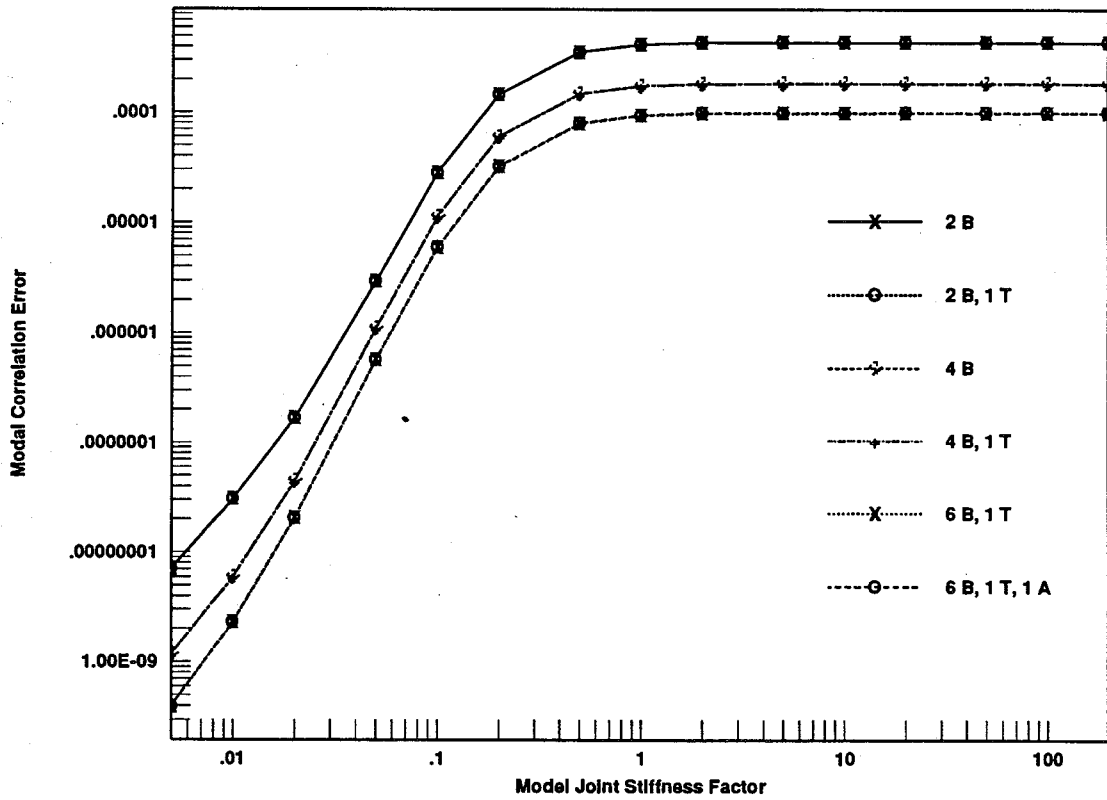
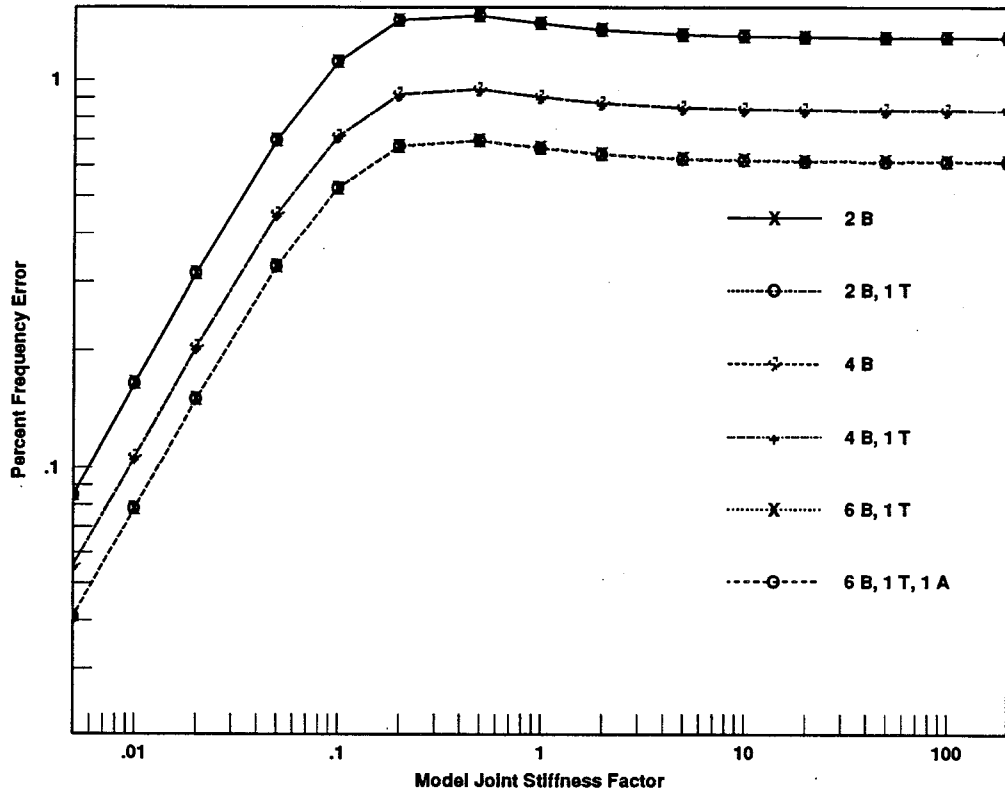


Figure C.3: 1st System Z-Bending Mode, Mixed-Interface, $\theta = 90^\circ$

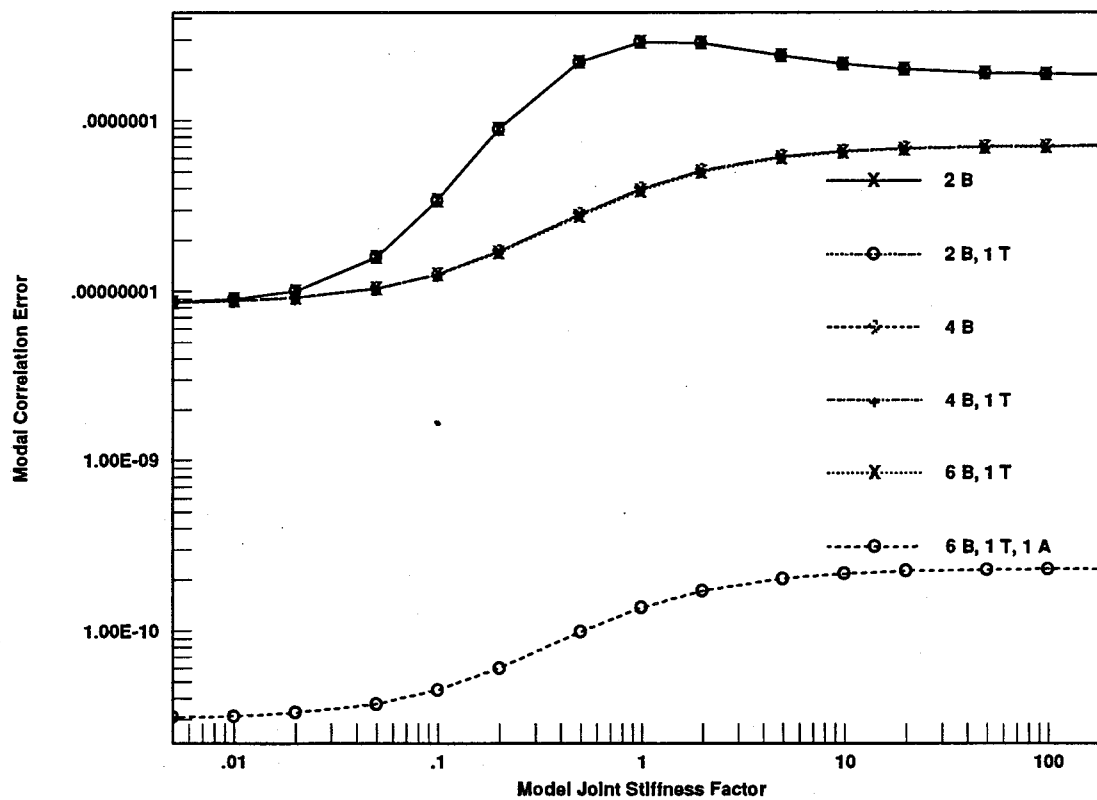
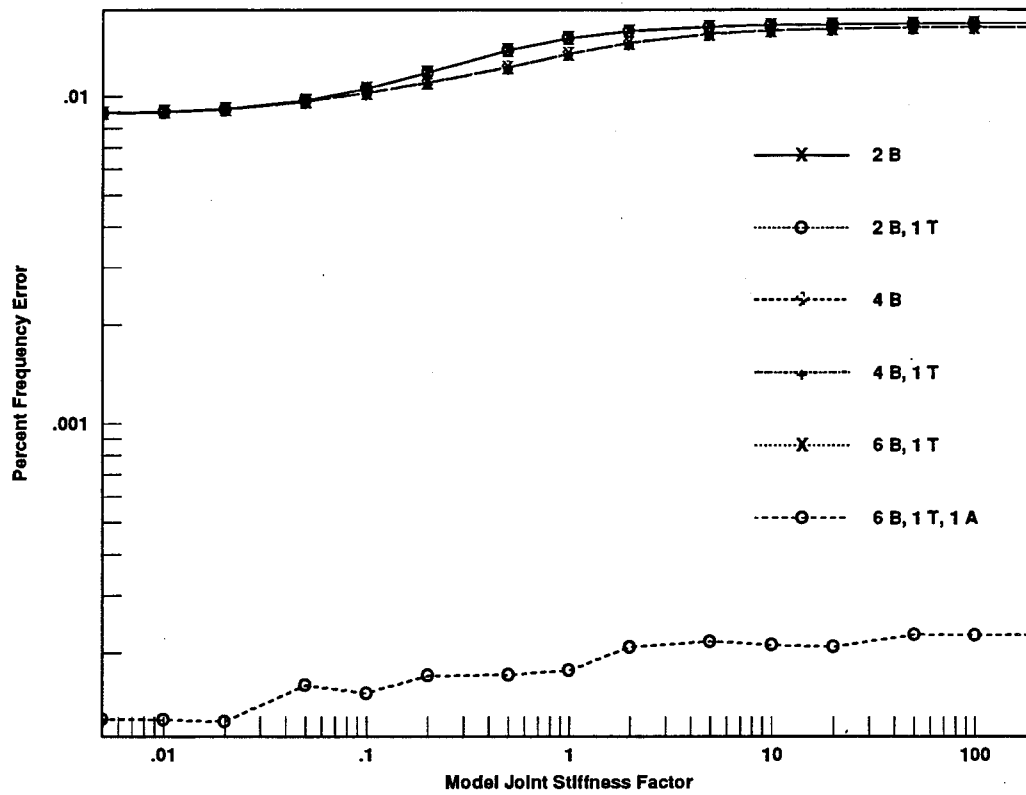


Figure C.4: 2nd System Z-Bending Mode, Fixed-Interface, $\theta = 90^\circ$

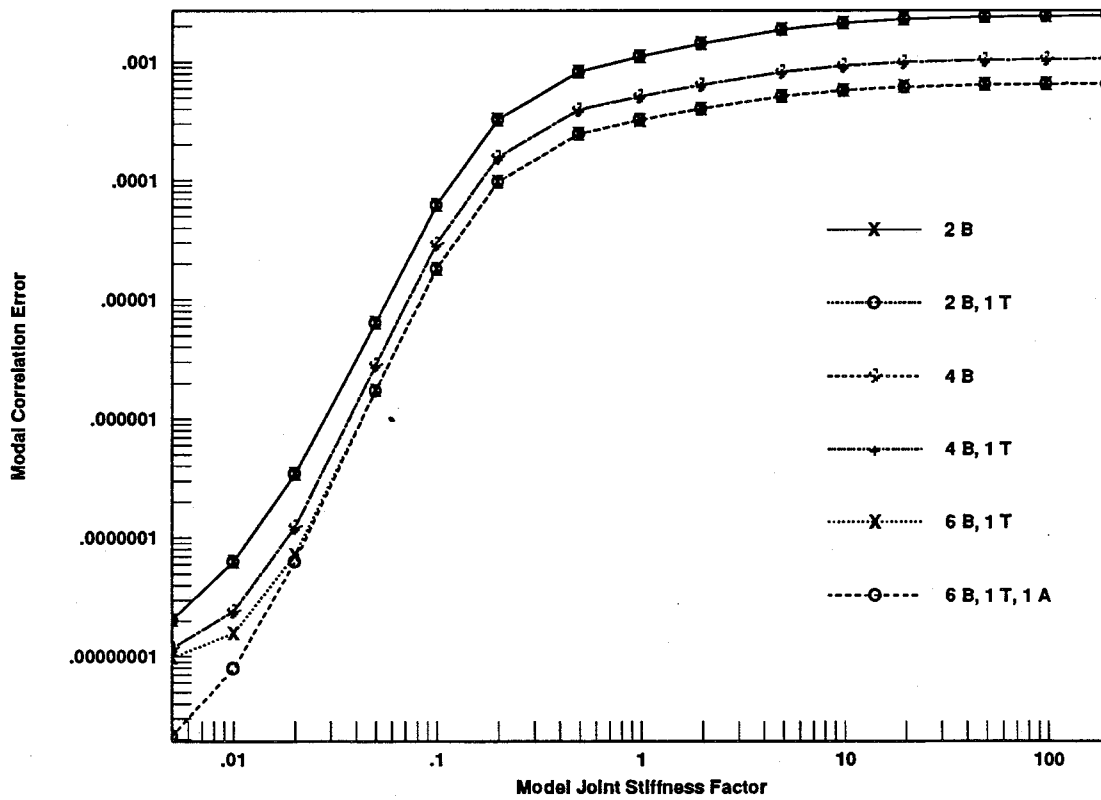
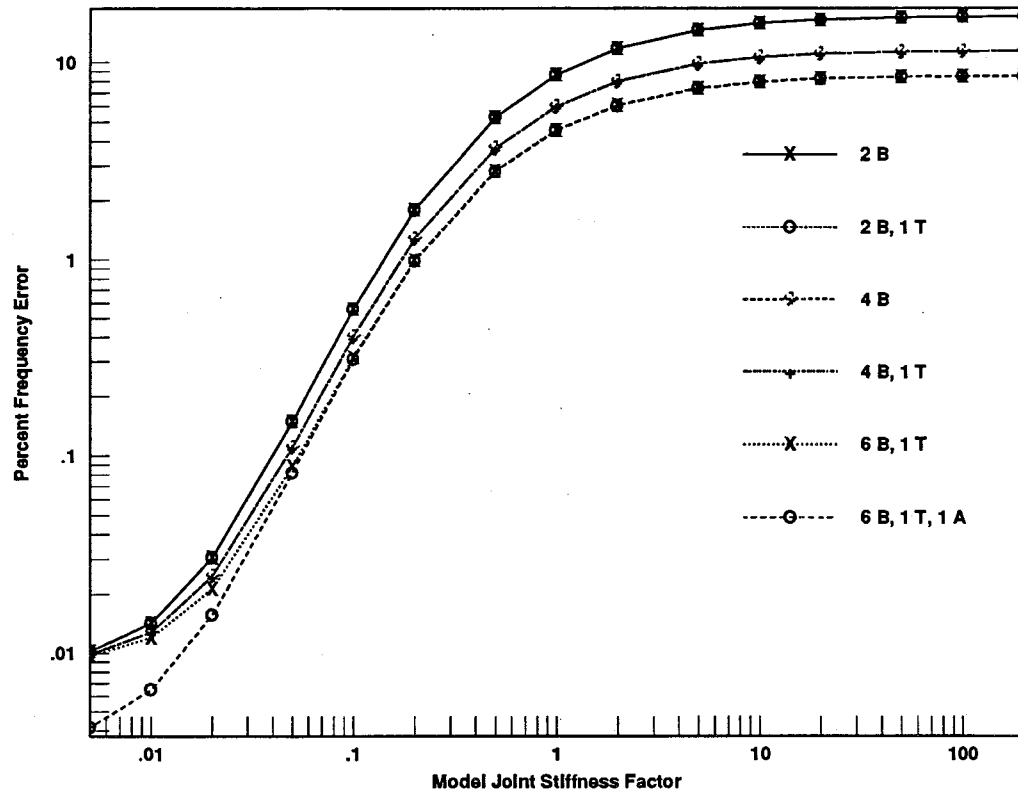


Figure C.5: 2nd System Z-Bending Mode, Free-Interface, $\theta = 90^\circ$

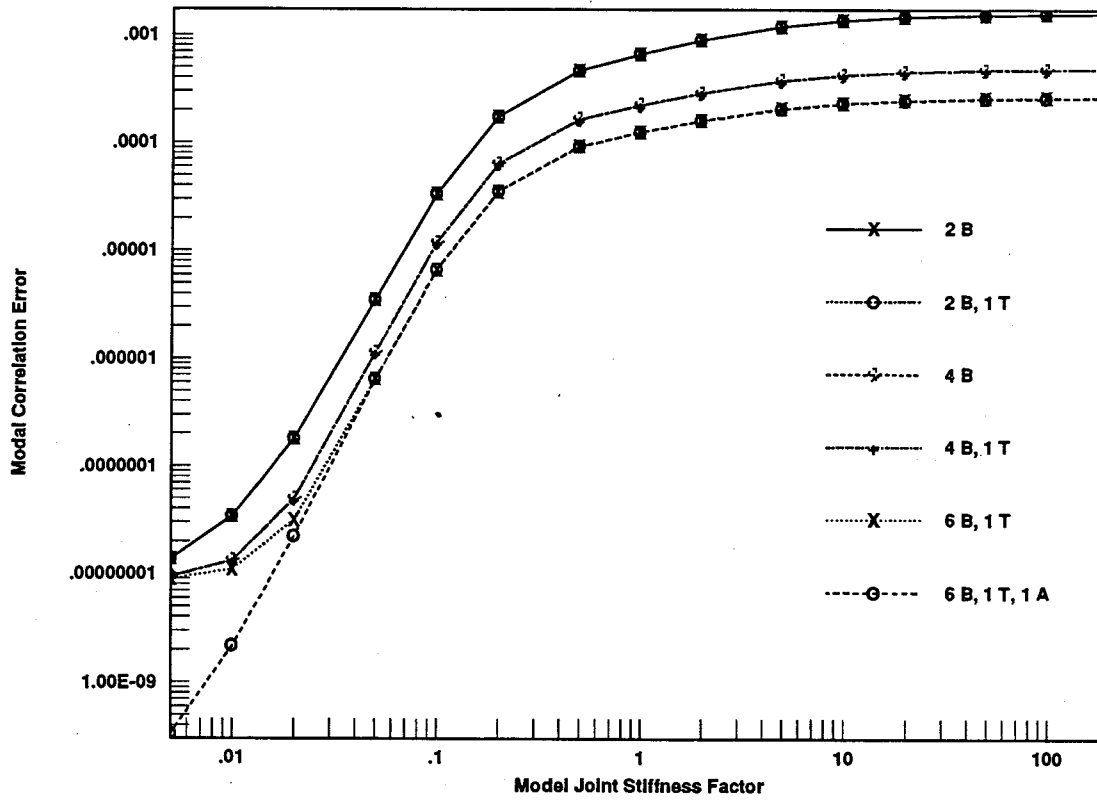
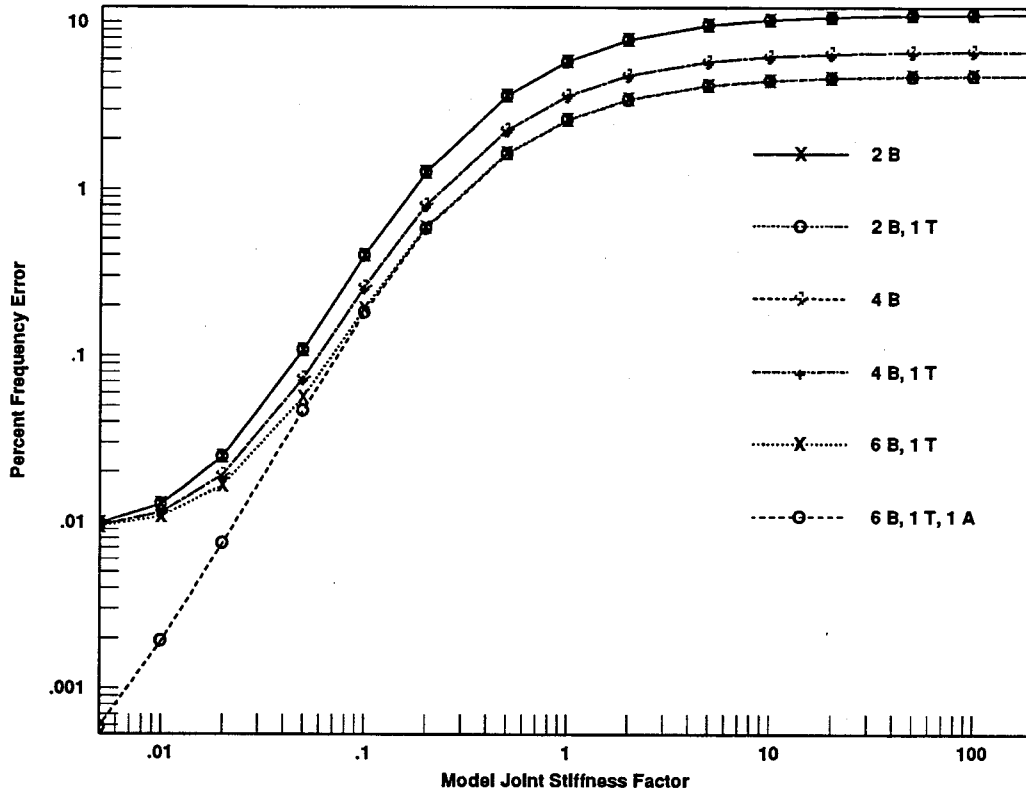


Figure C.6: 2nd System Z-Bending Mode, Mixed-Interface, $\theta = 90^\circ$

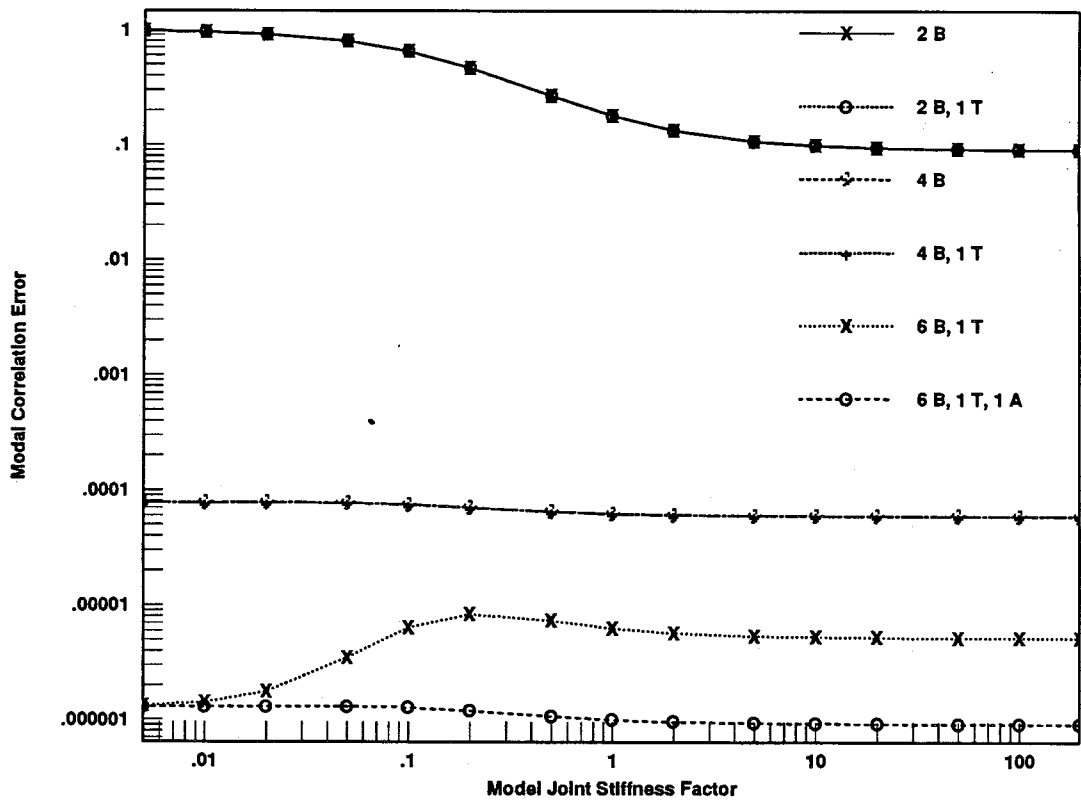
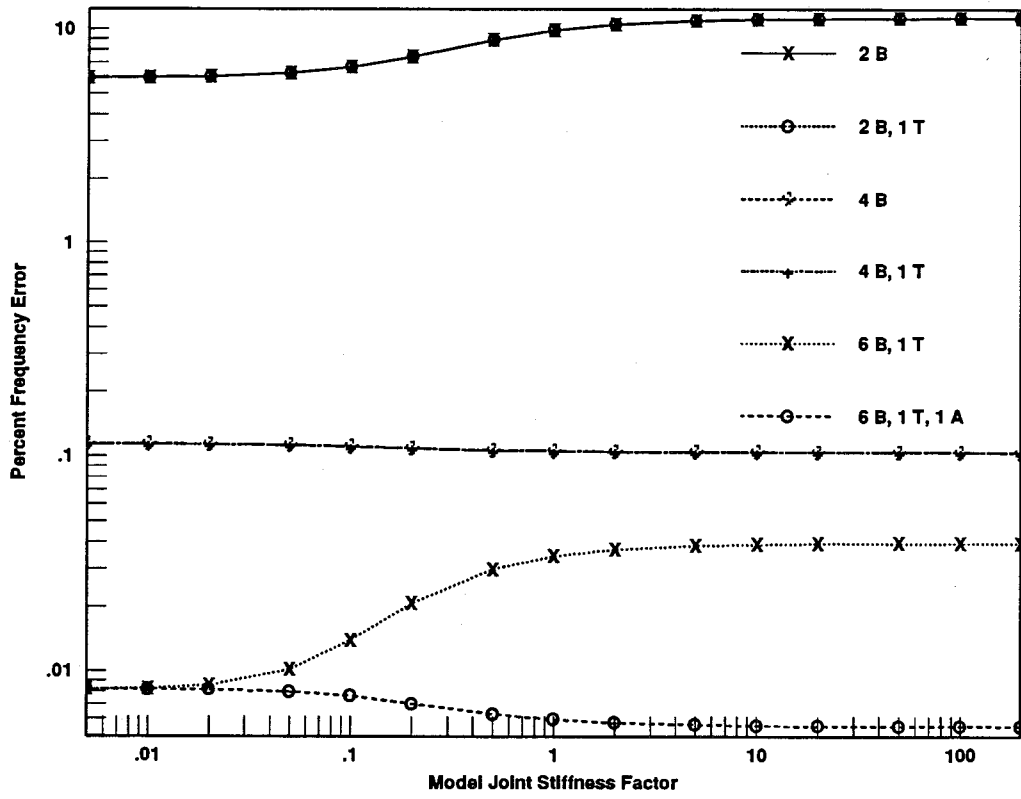


Figure C.7: 3rd System Z-Bending Mode, Fixed-Interface, $\theta = 90^\circ$

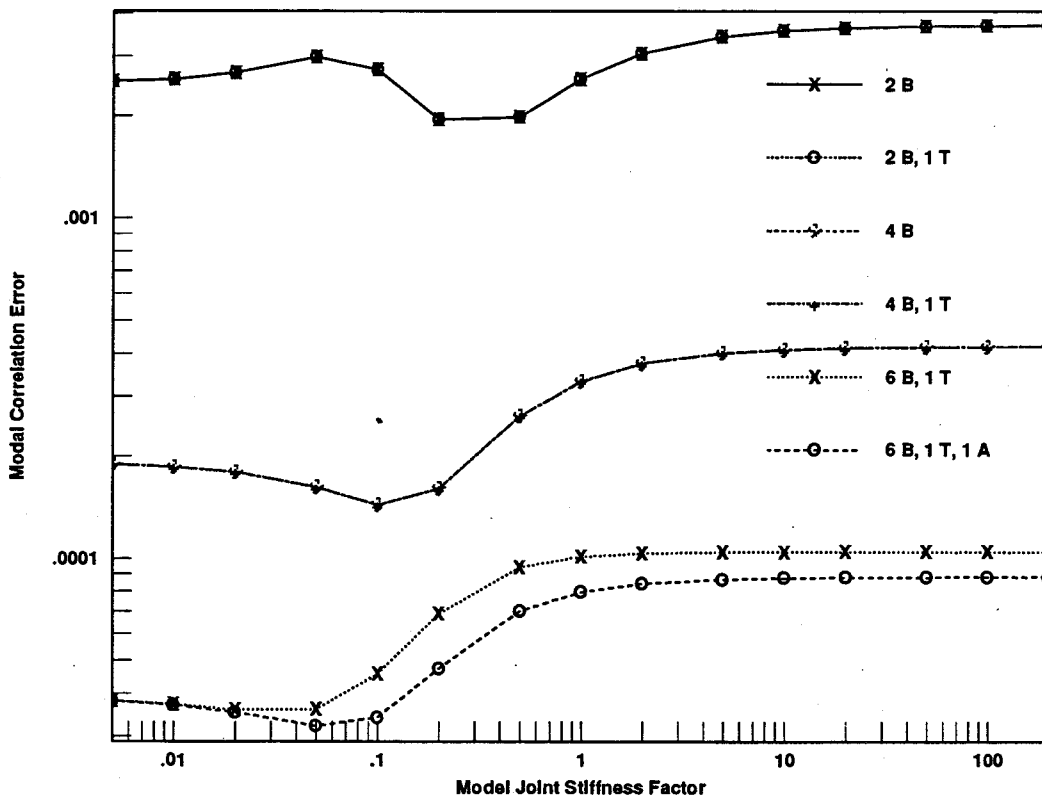
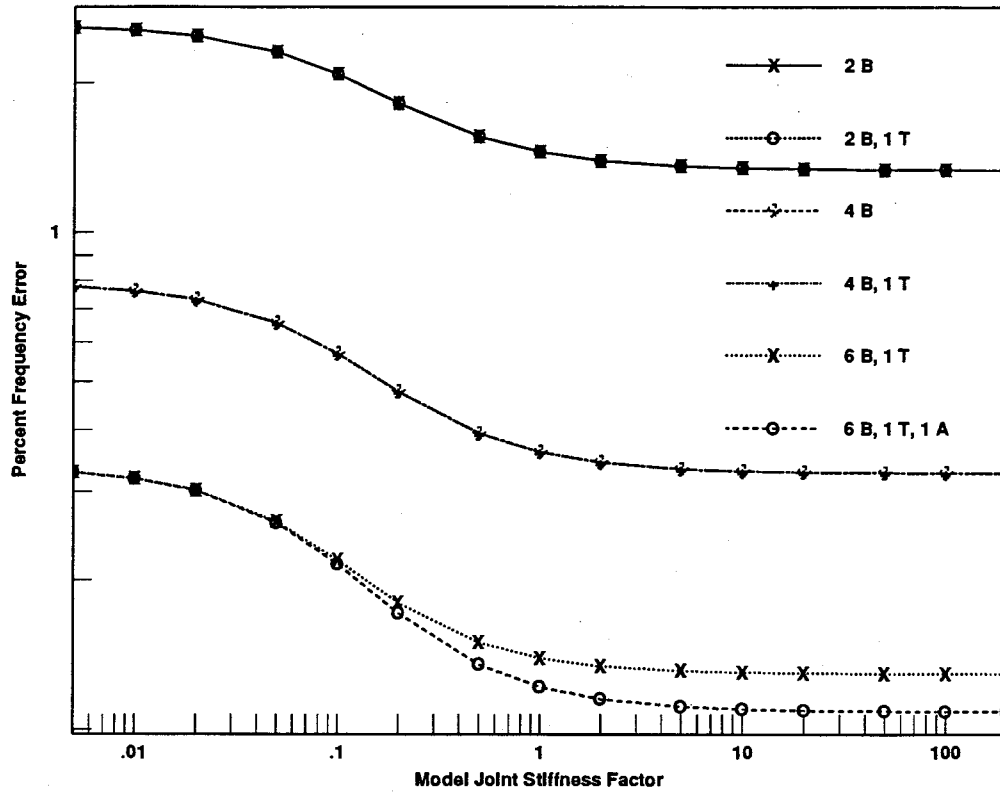


Figure C.8: 3rd System Z-Bending Mode, Free-Interface, $\theta = 90^\circ$

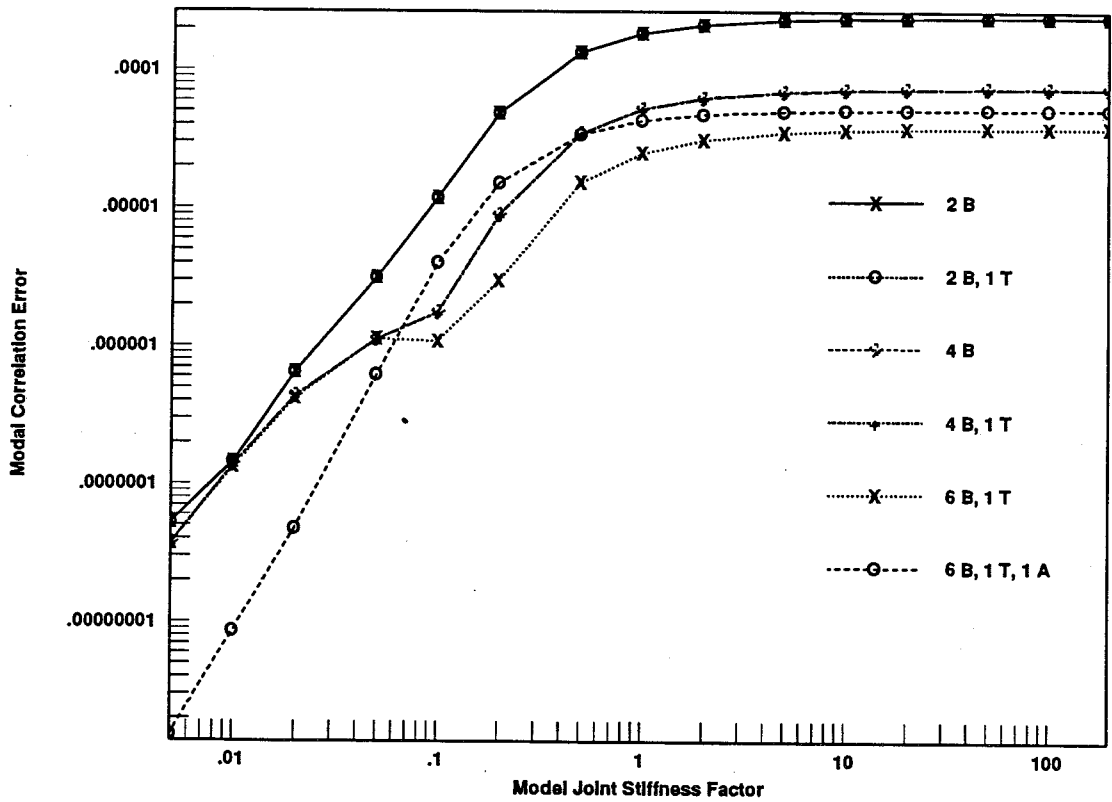
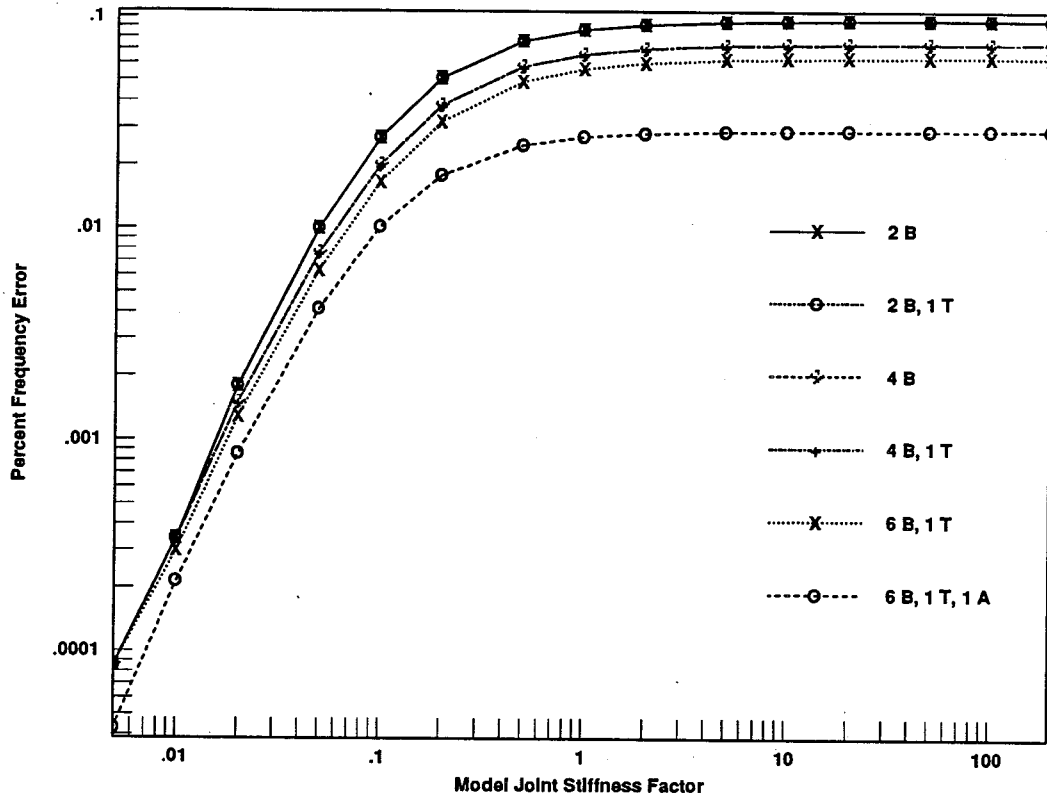


Figure C.9: 3rd System Z-Bending Mode, Mixed-Interface, $\theta = 90^\circ$

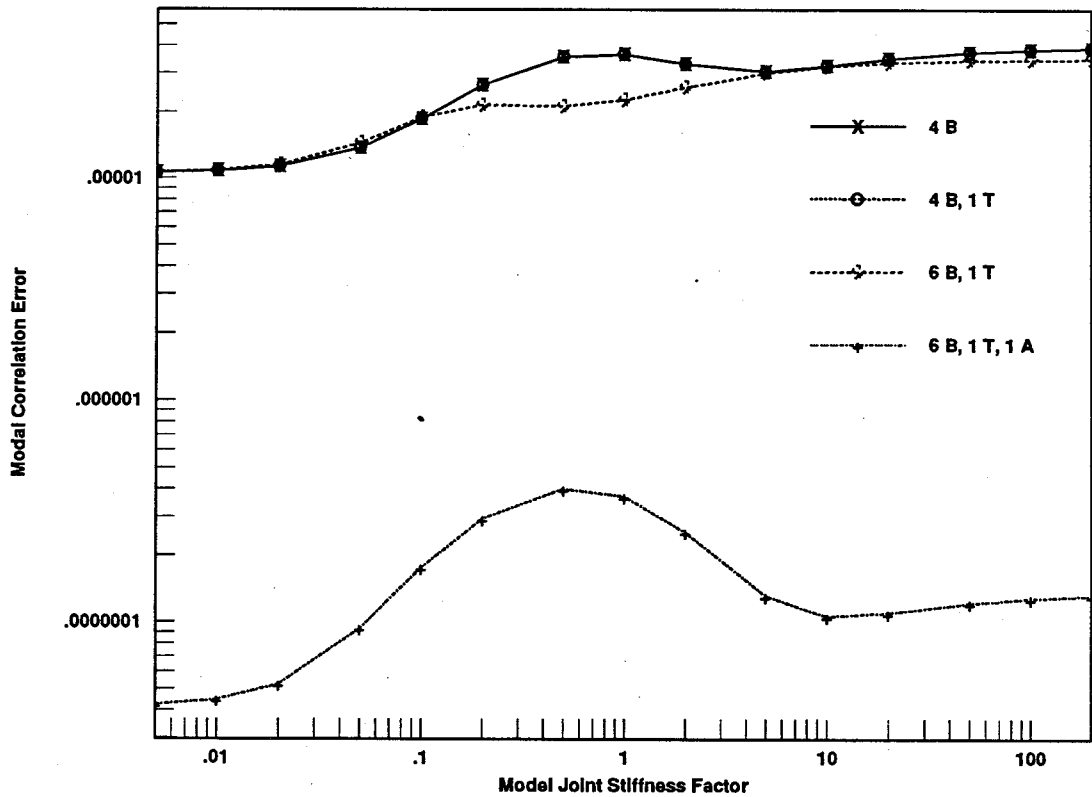
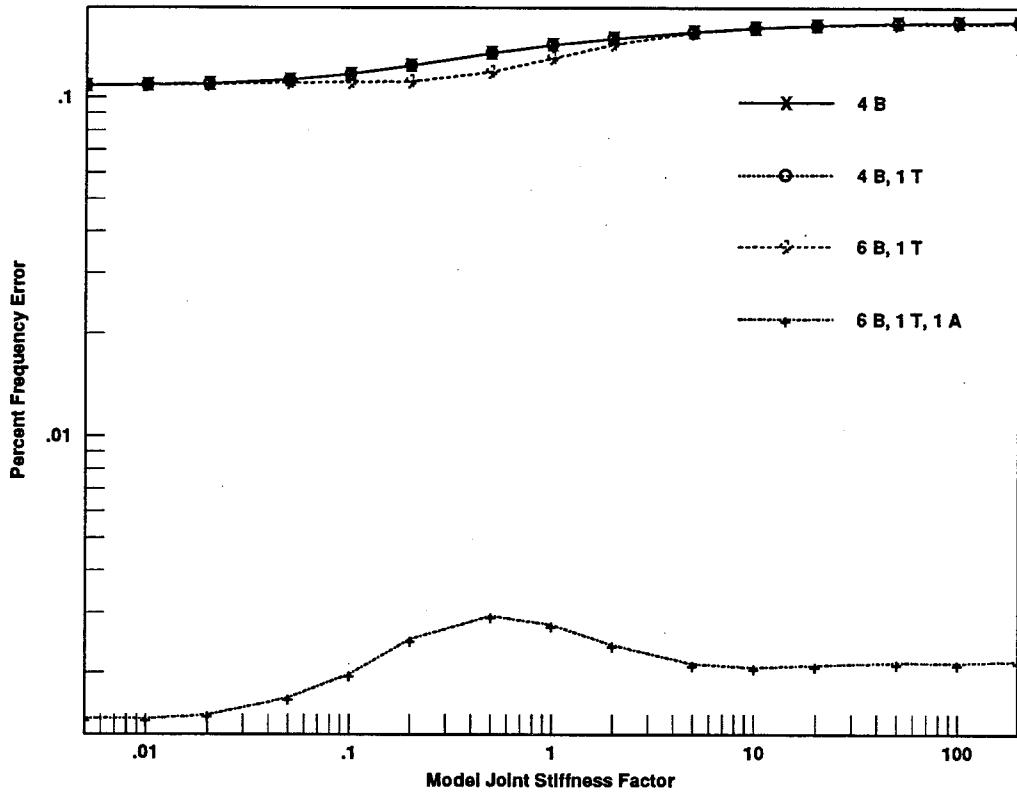


Figure C.10: 4th System Z-Bending Mode, Fixed-Interface, $\theta = 90^\circ$

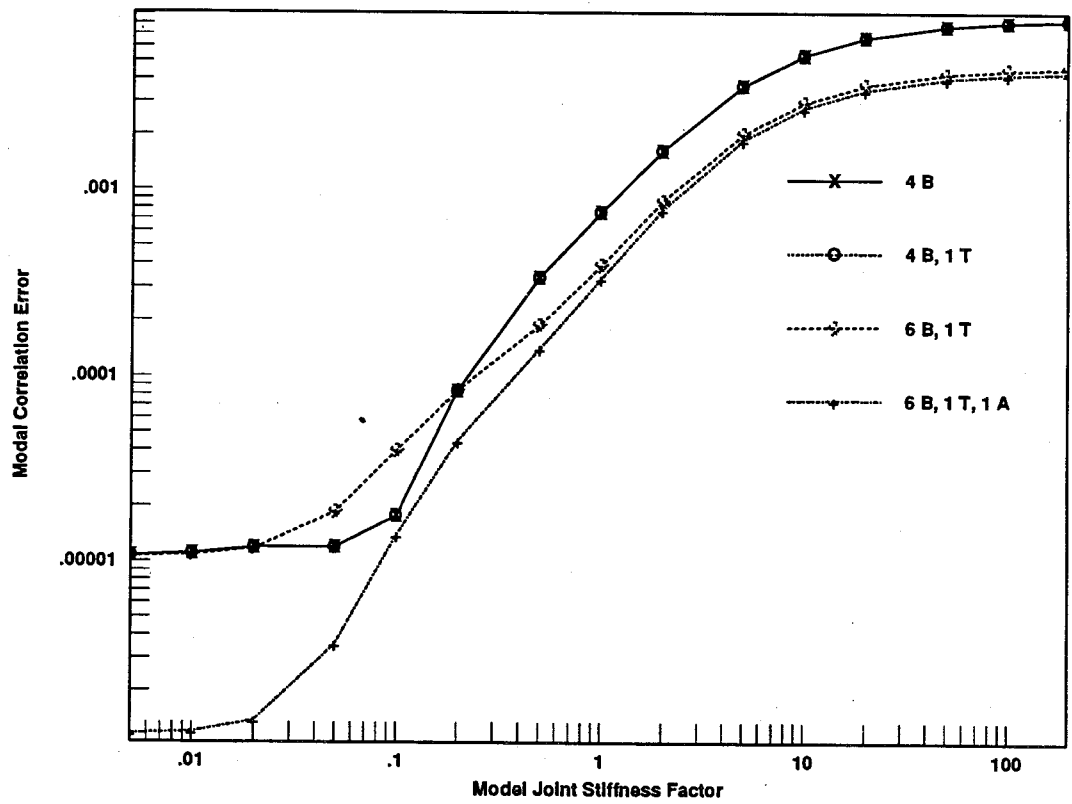
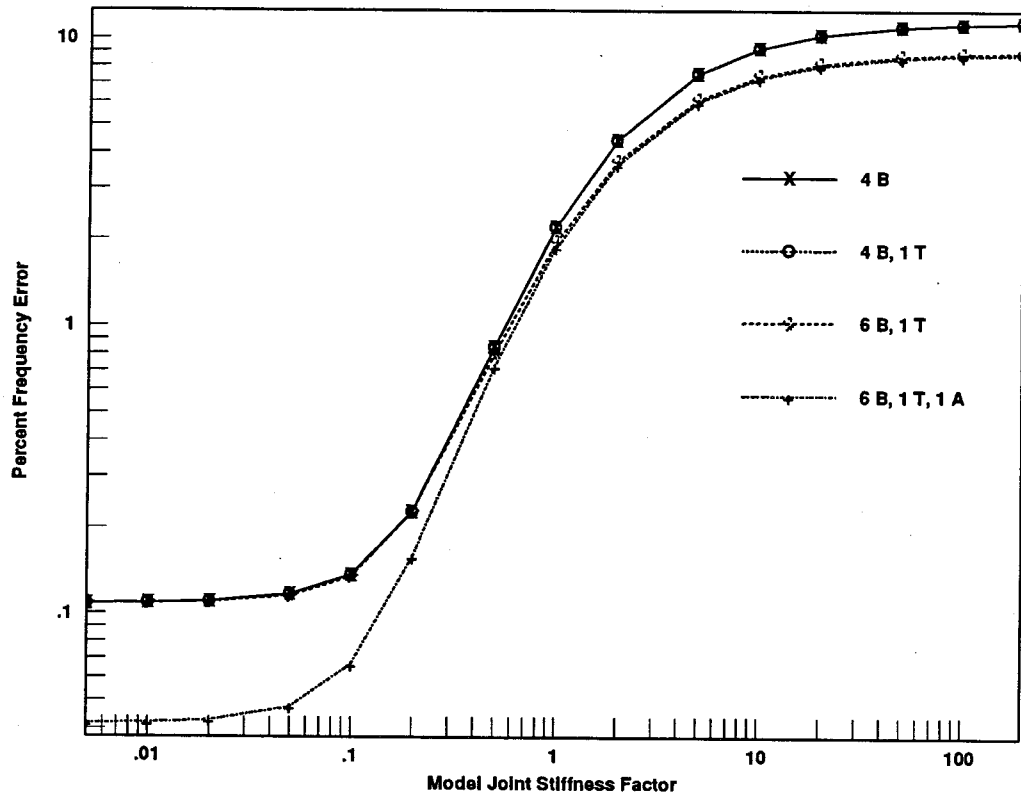


Figure C.11: 4th System Z-Bending Mode, Free-Interface, $\theta = 90^\circ$

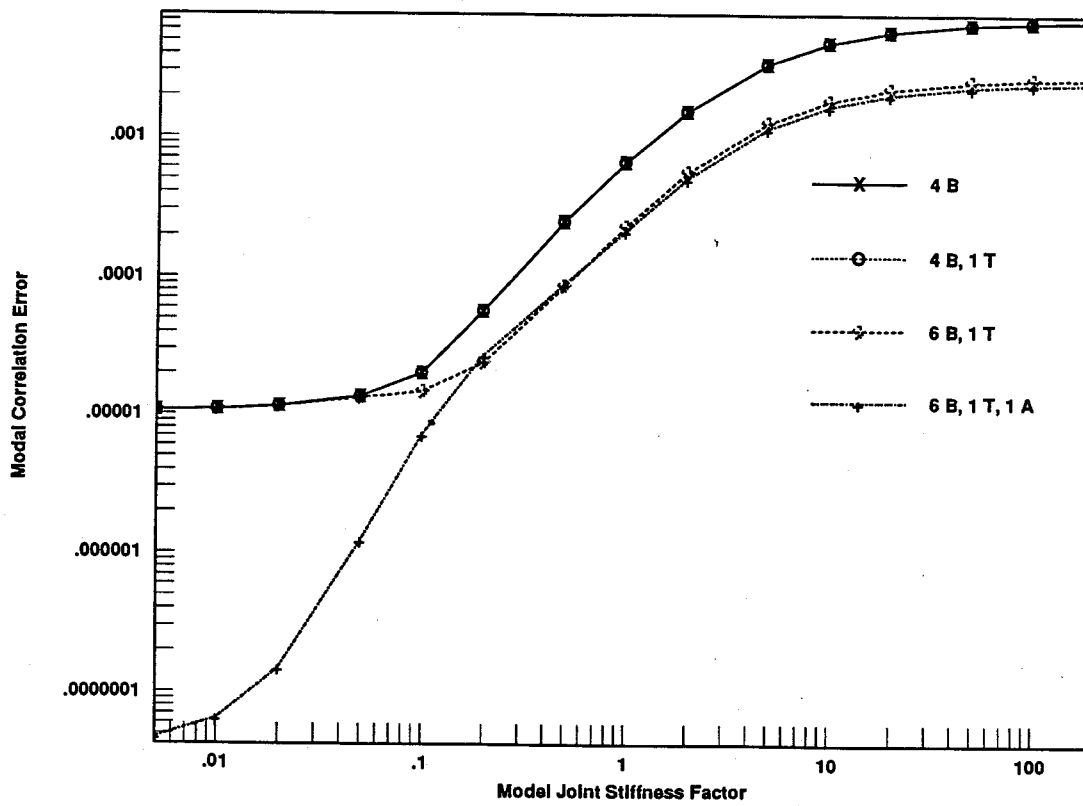
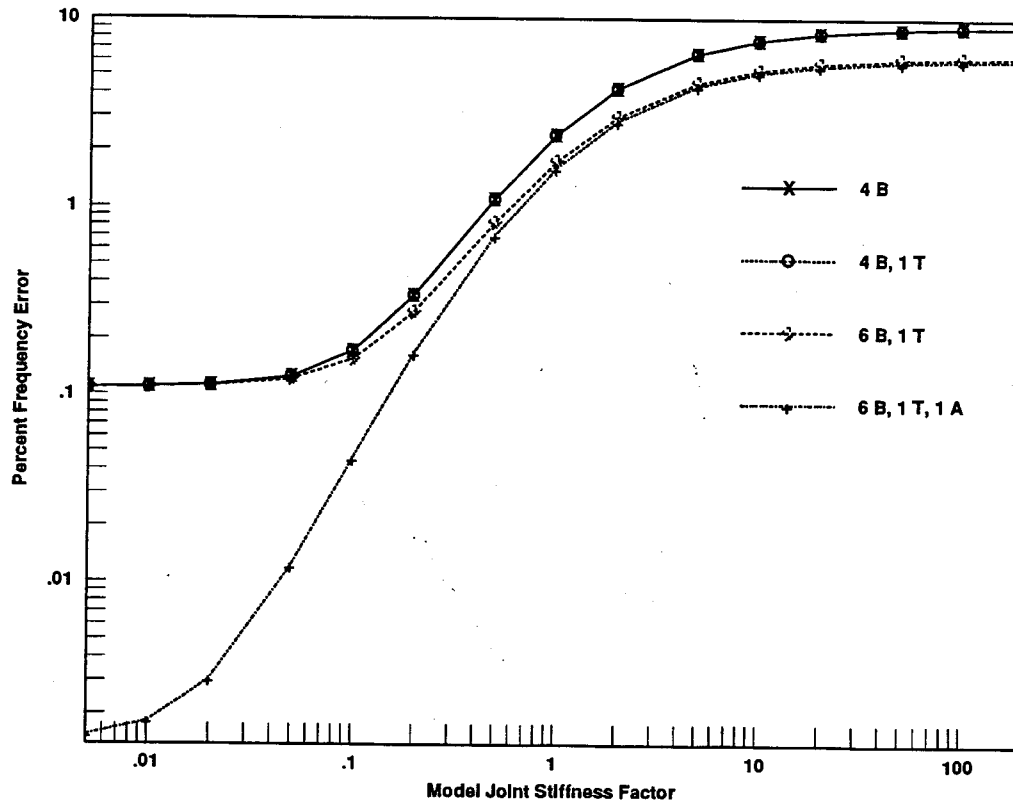


Figure C.12: 4th System Z-Bending Mode, Mixed-Interface, $\theta = 90^\circ$

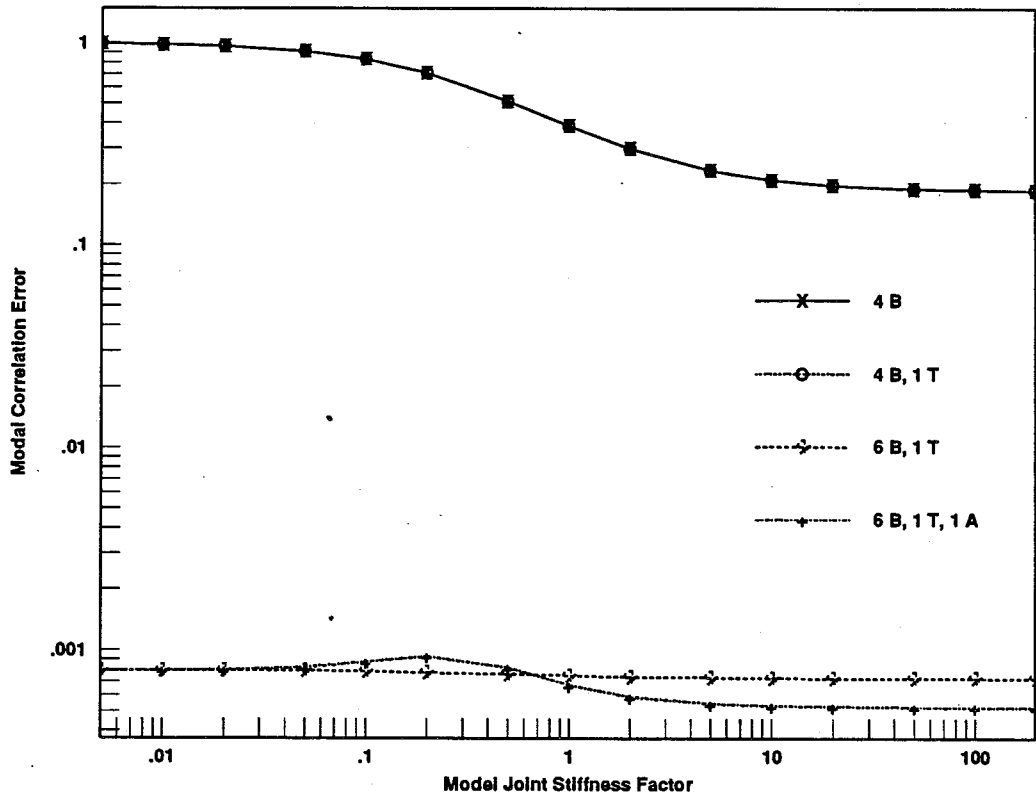
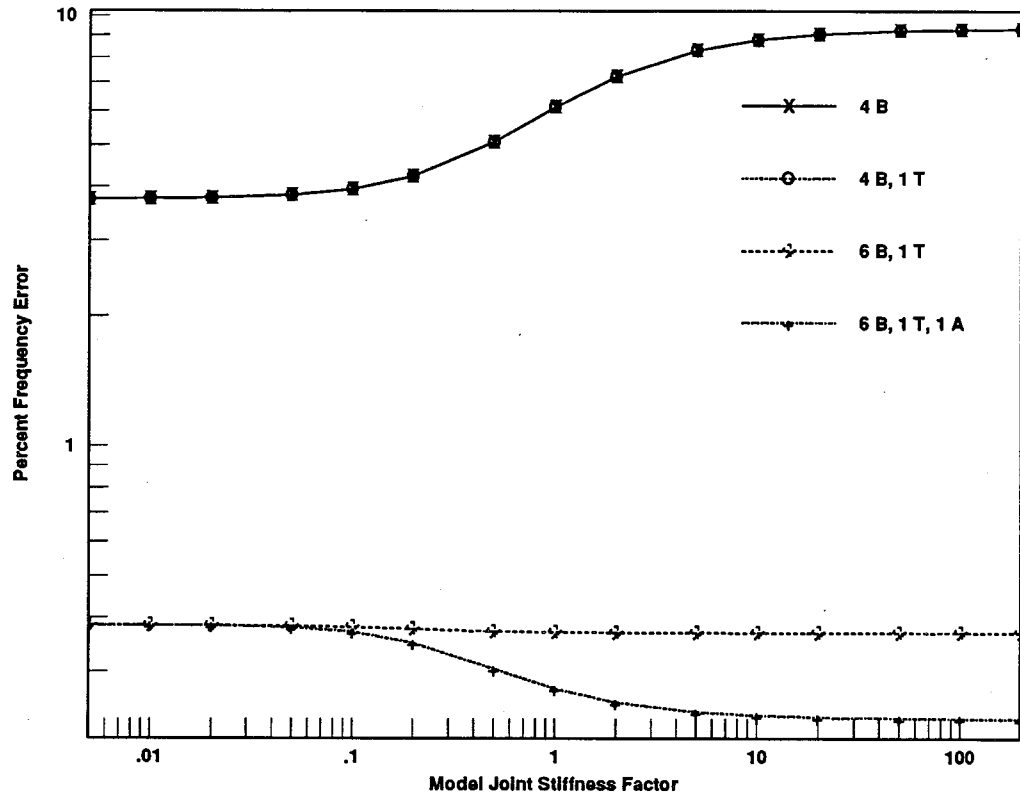


Figure C.13: 5th System Z-Bending Mode, Fixed-Interface, $\theta = 90^\circ$

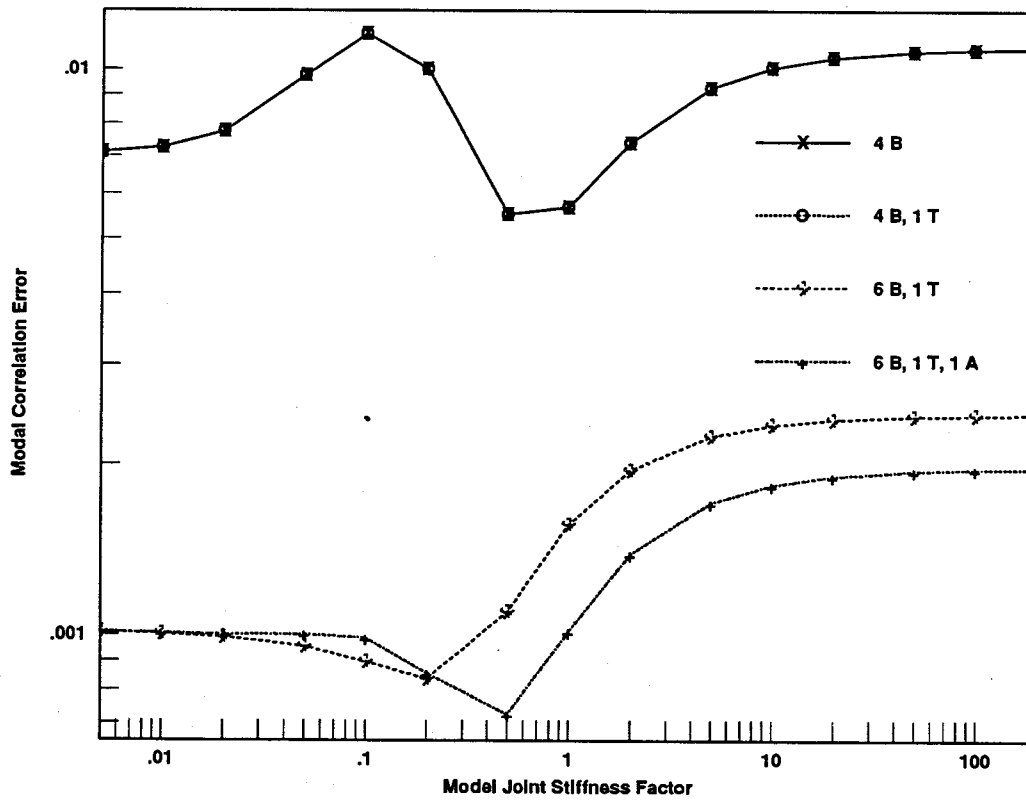
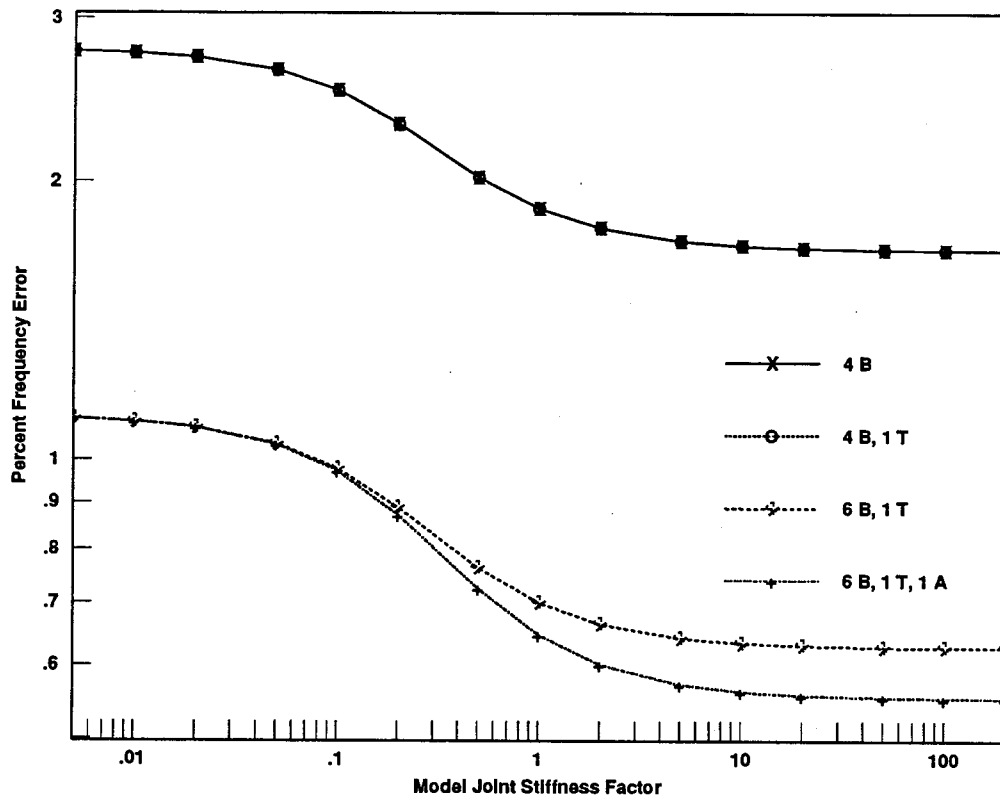


Figure C.14: 5th System Z-Bending Mode, Free-Interface, $\theta = 90^\circ$

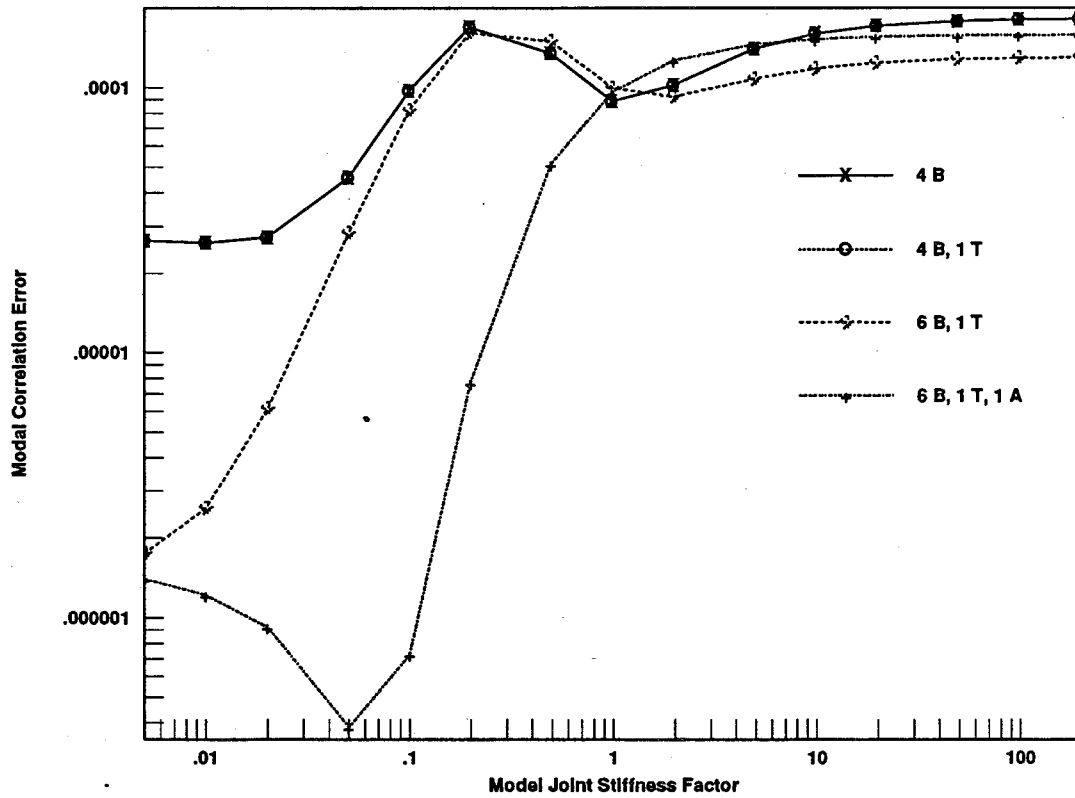
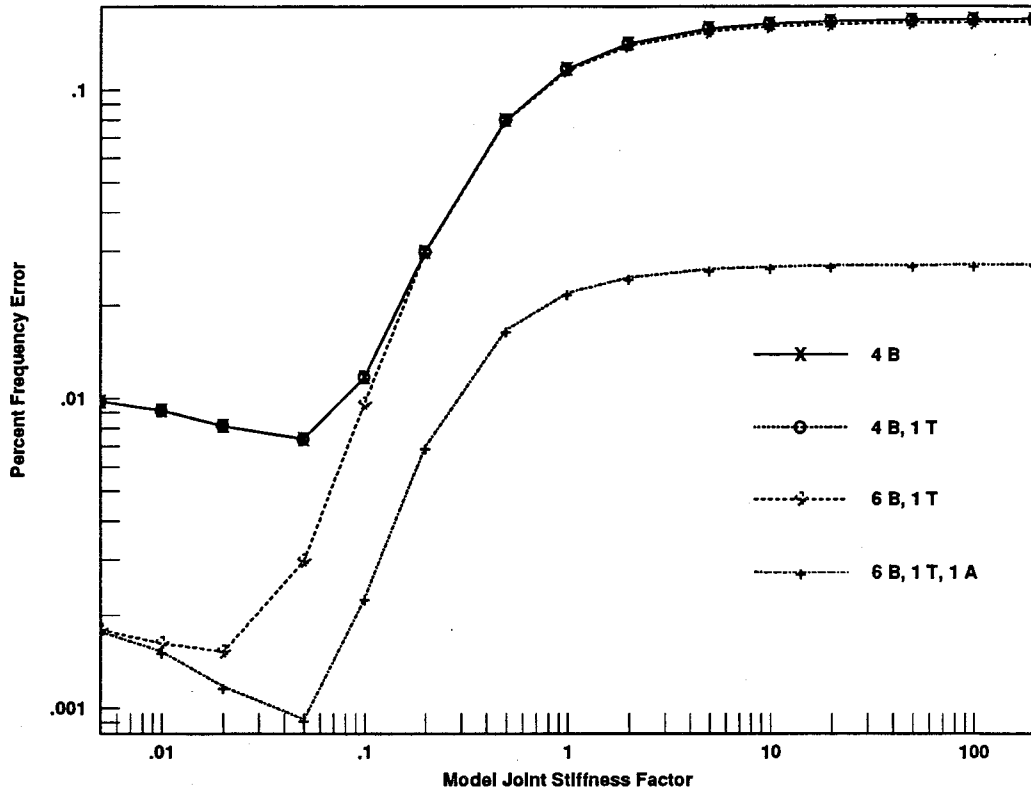


Figure C.15: 5th System Z-Bending Mode, Mixed-Interface, $\theta = 90^\circ$

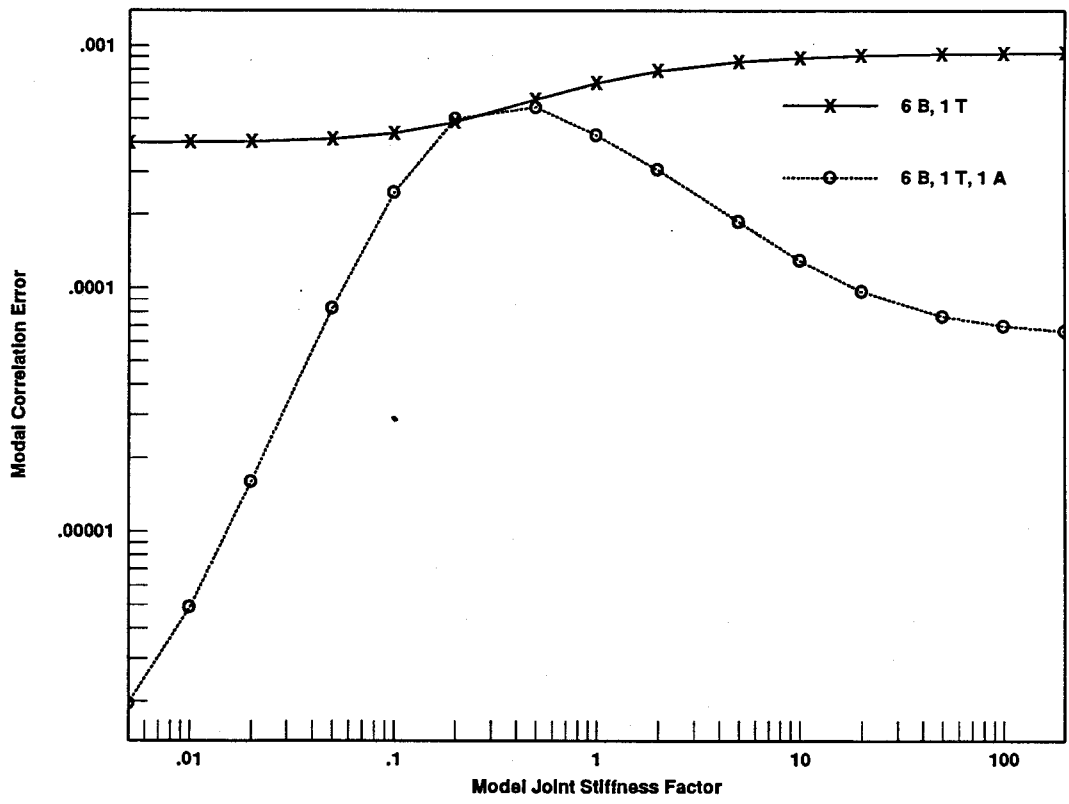
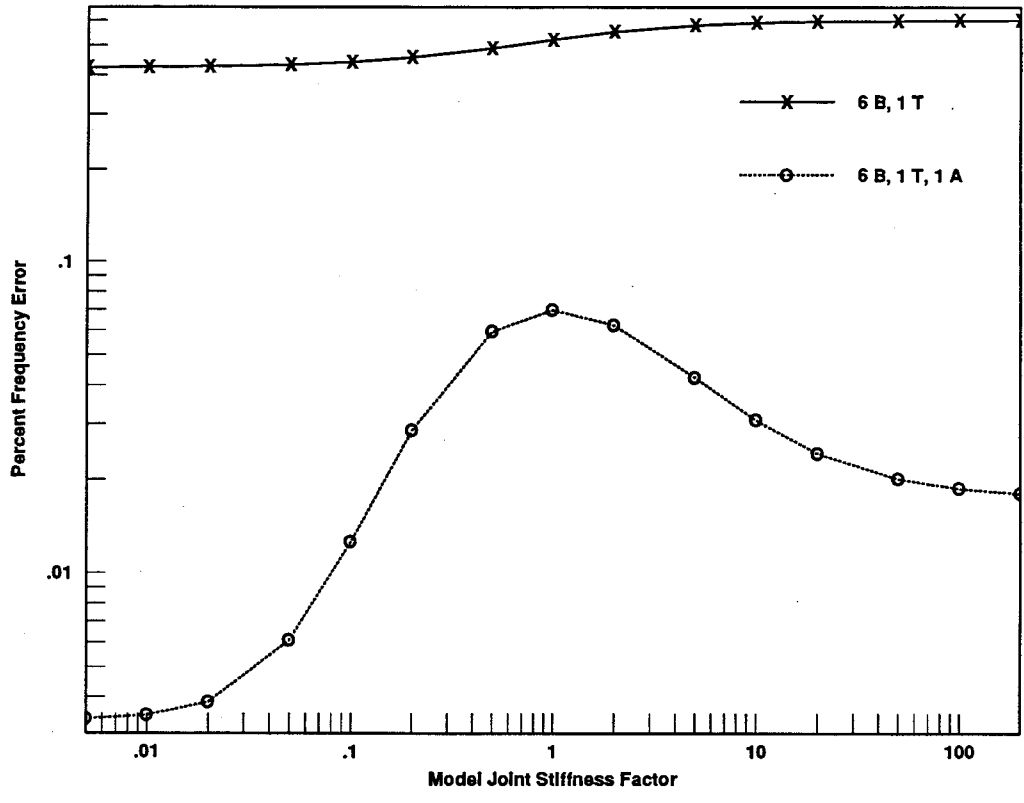


Figure C.16: 6th System Z-Bending Mode, Fixed-Interface, $\theta = 90^\circ$

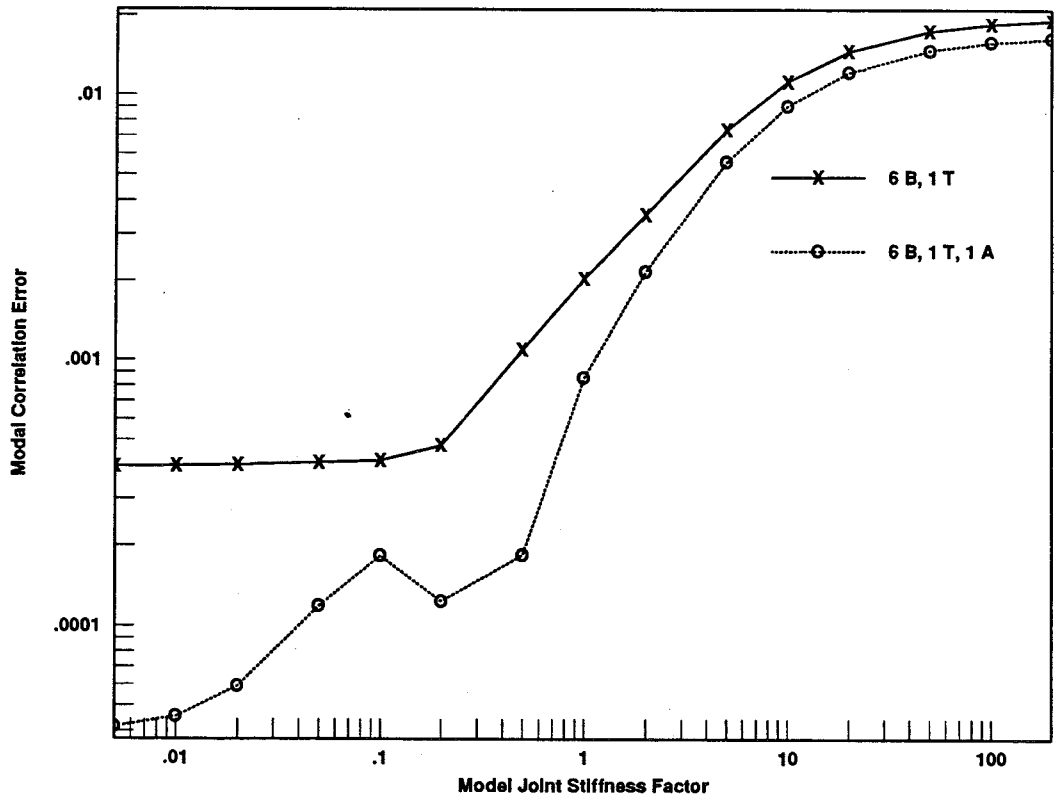
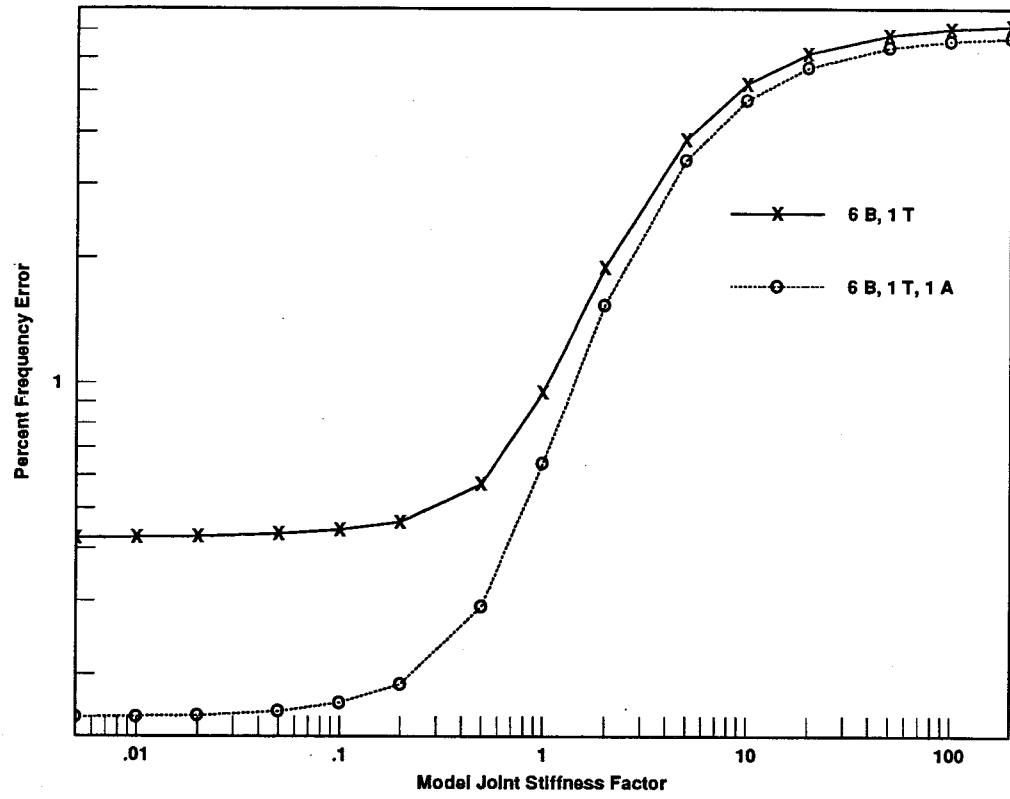


Figure C.17: 6th System Z-Bending Mode, Free-Interface, $\theta = 90^\circ$

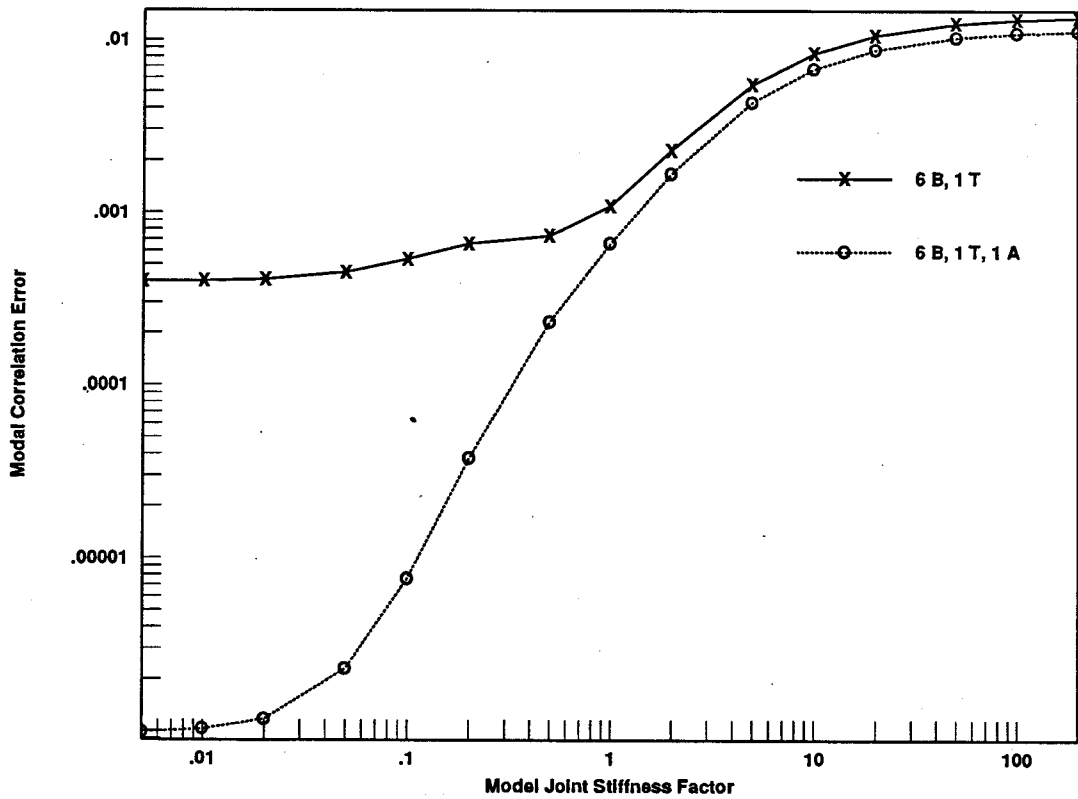
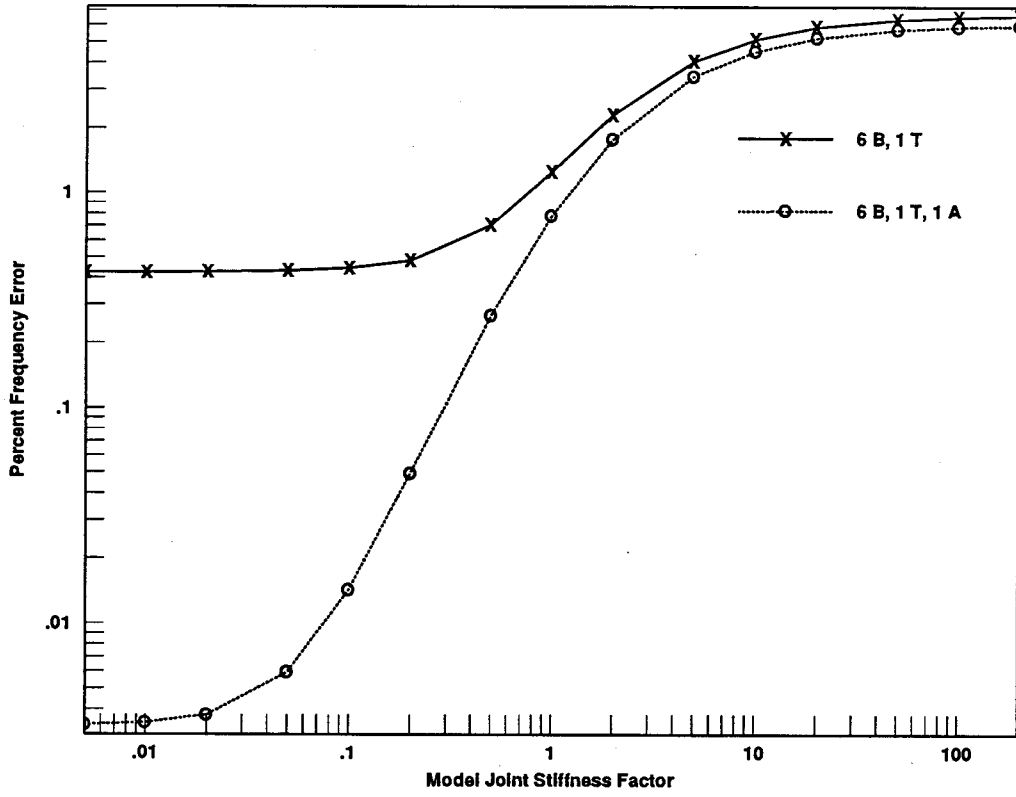


Figure C.18: 6th System Z-Bending Mode, Mixed-Interface, $\theta = 90^\circ$

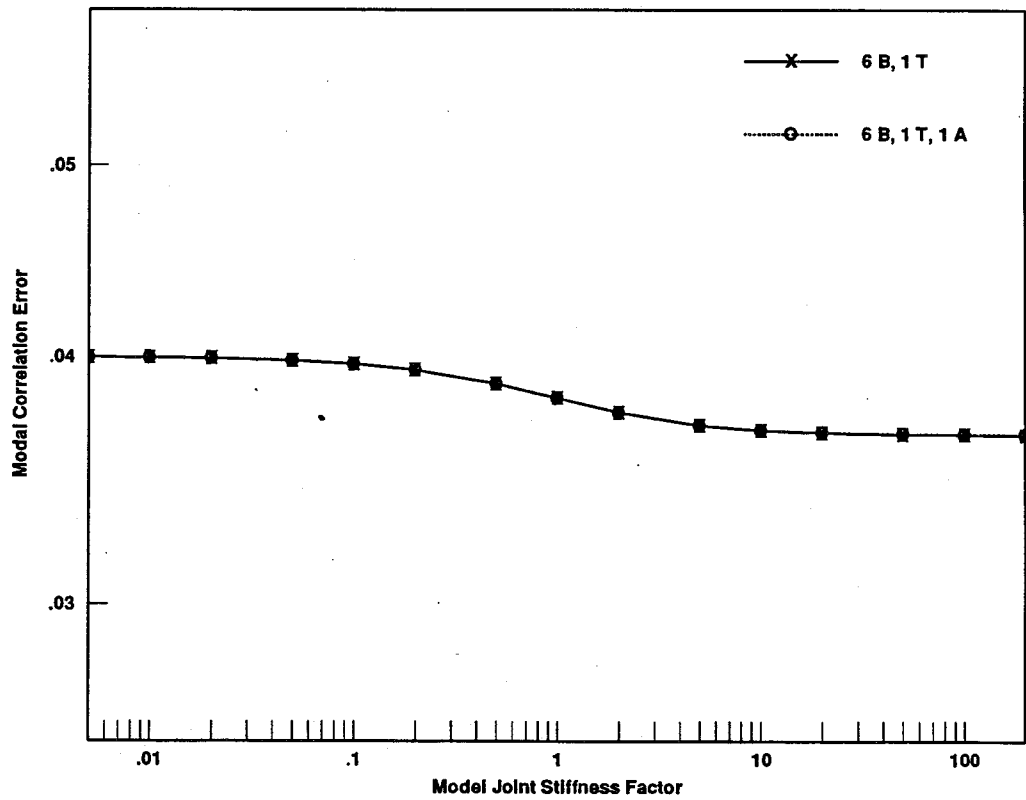
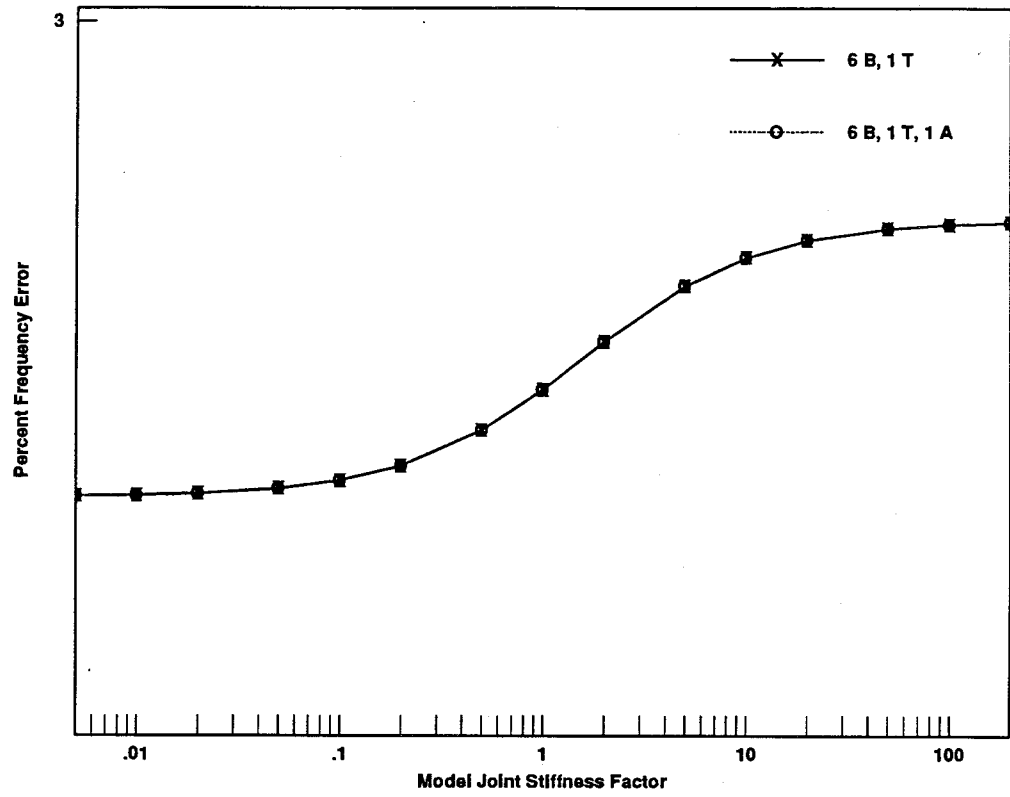


Figure C.19: 7th System Z-Bending Mode, Fixed-Interface, $\theta = 90^\circ$

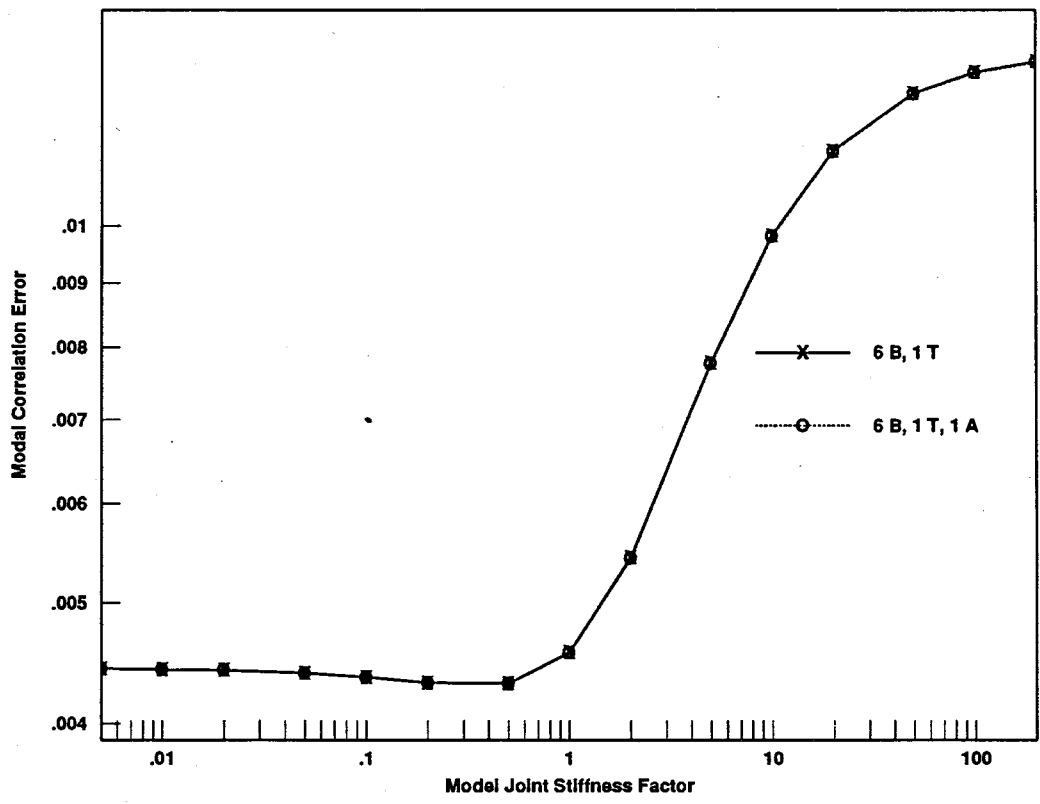
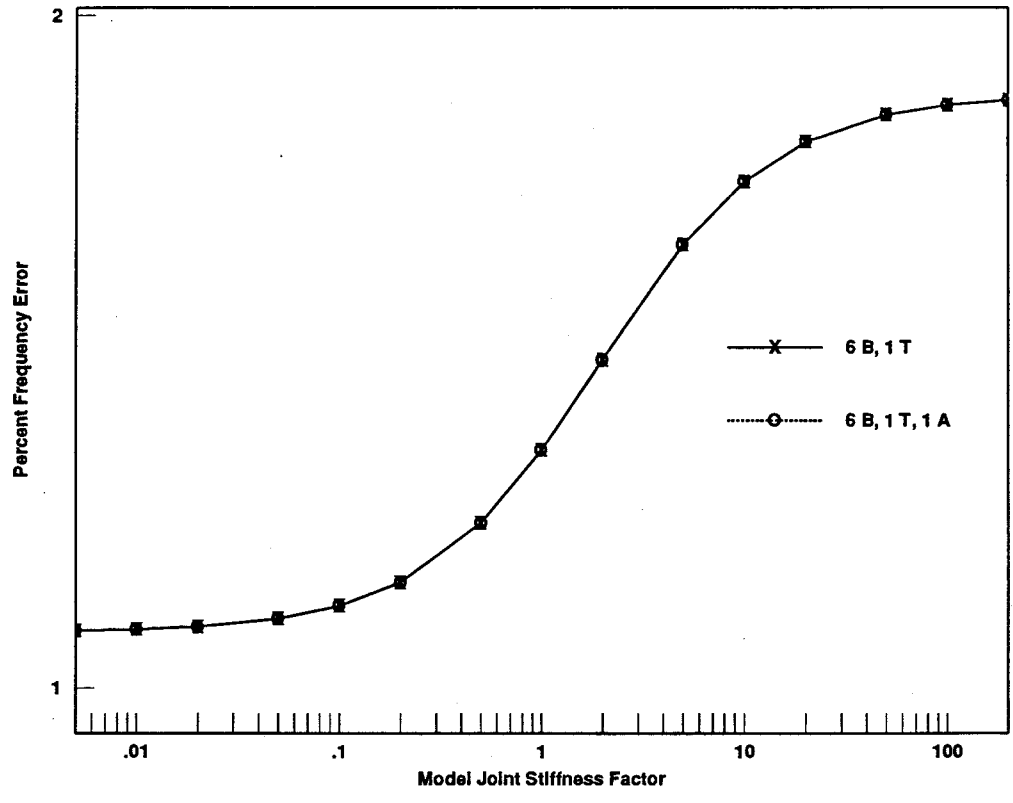


Figure C.20: 7th System Z-Bending Mode, Free-Interface, $\theta = 90^\circ$

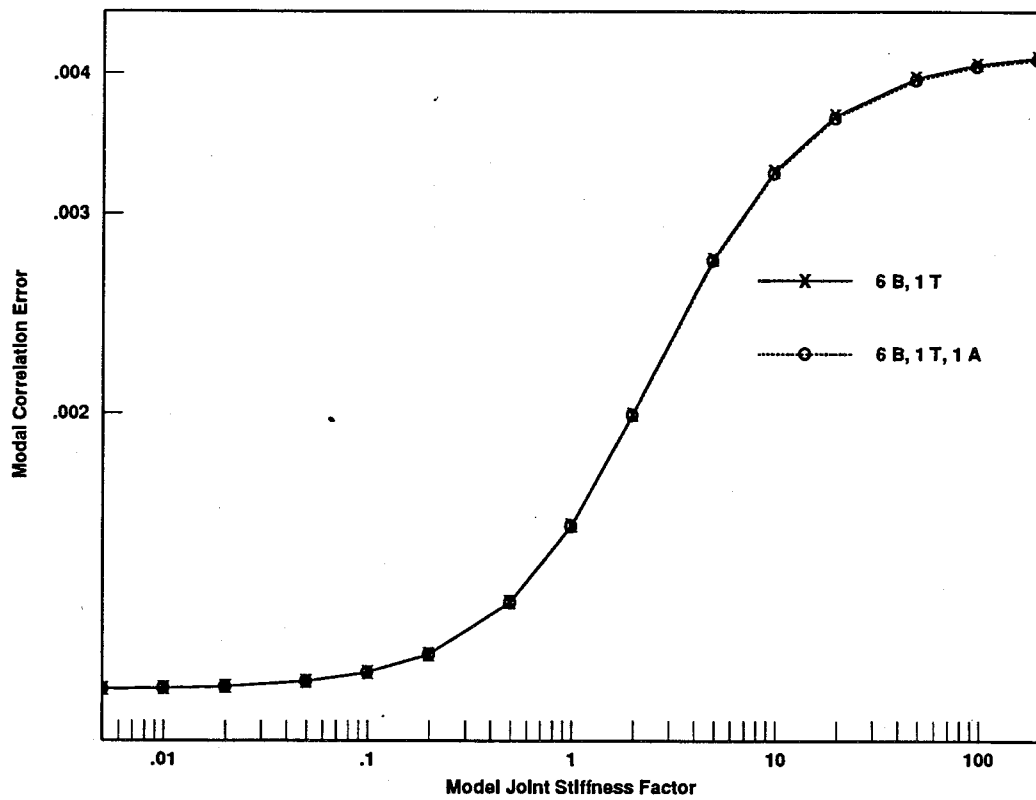
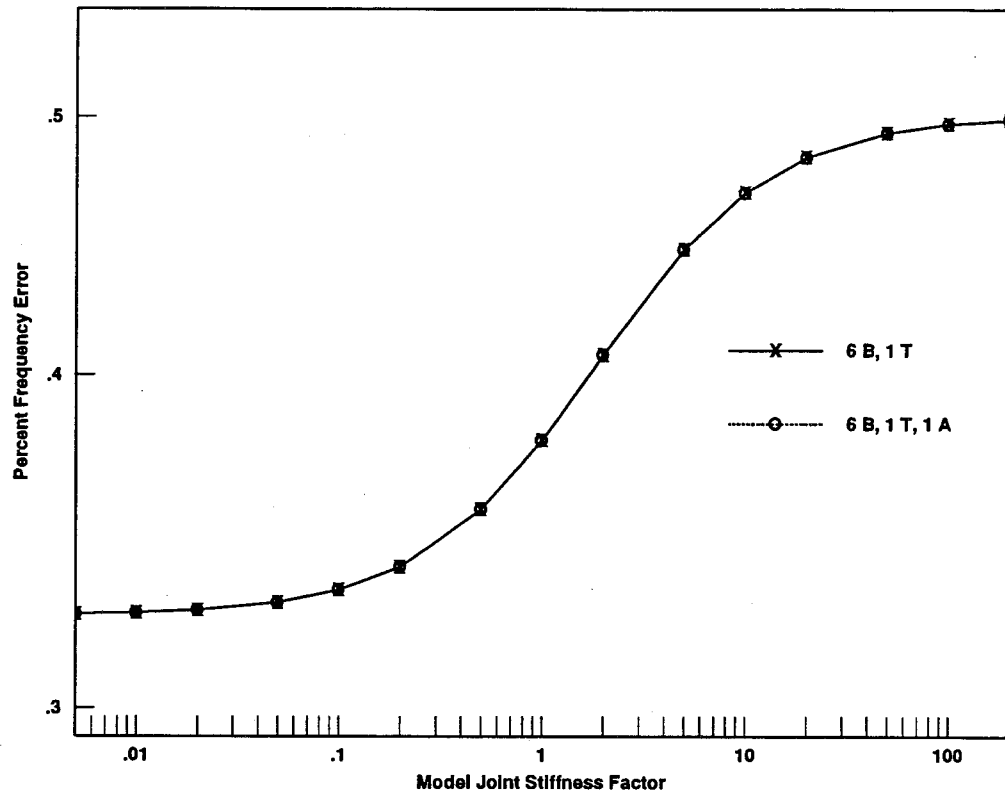


Figure C.21: 7th System Z-Bending Mode, Mixed-Interface, $\theta = 90^\circ$

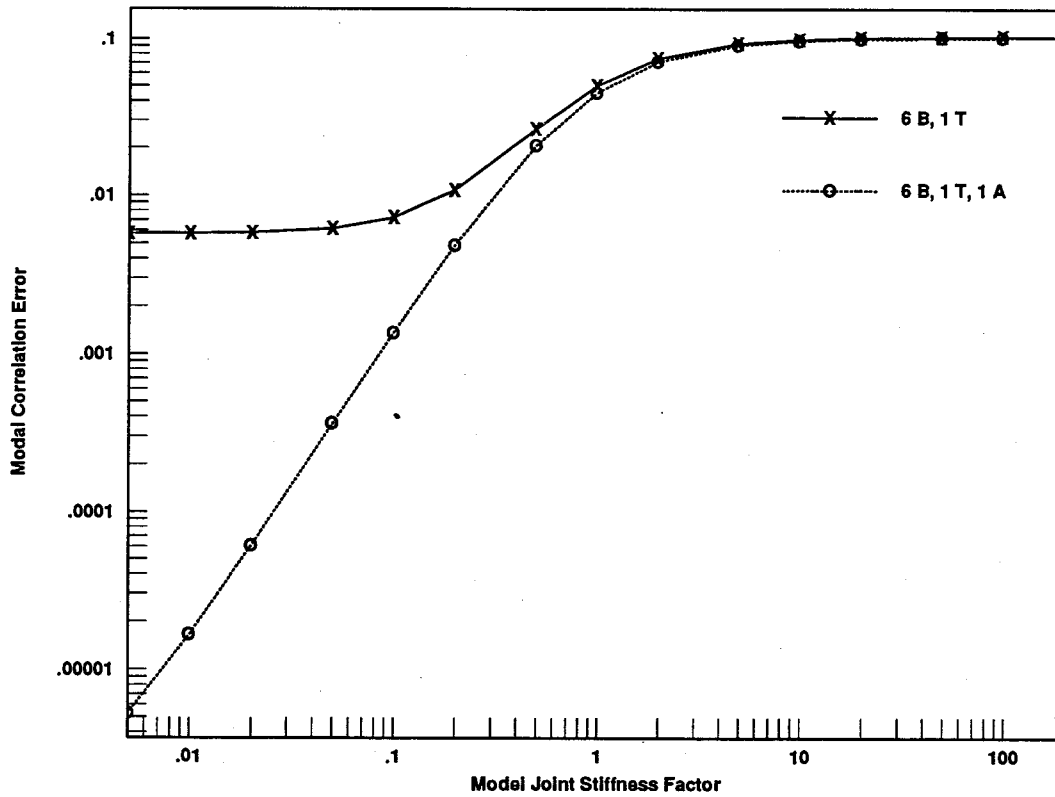
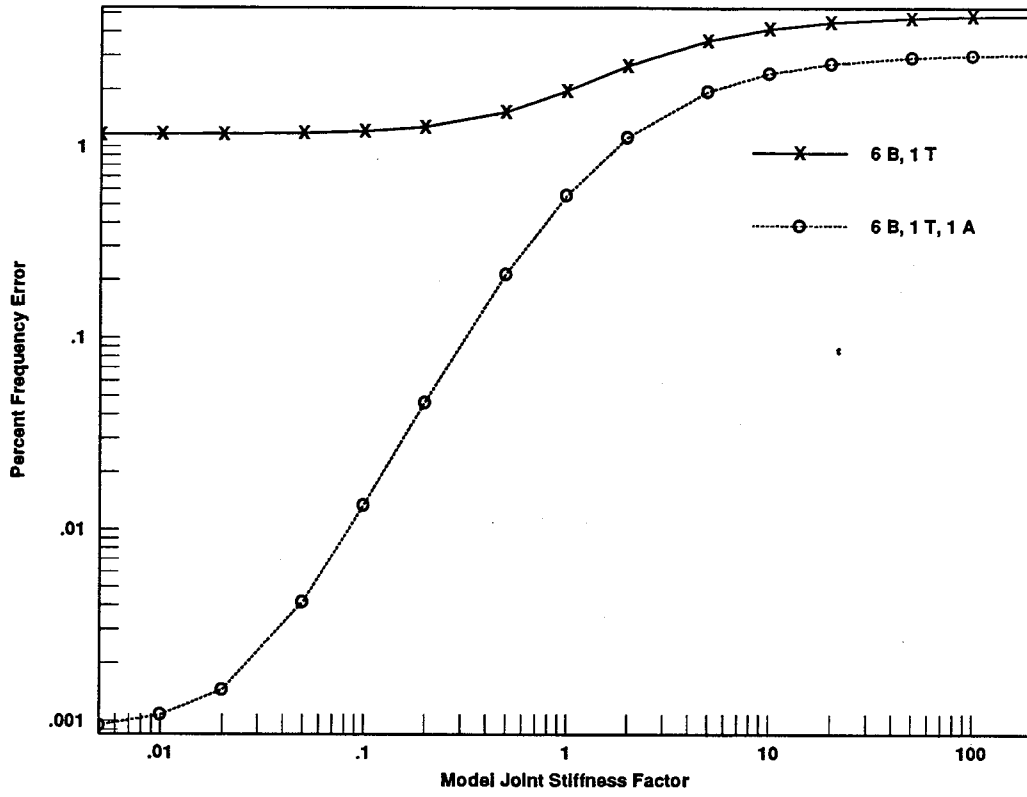


Figure C.22: 8th System Z-Bending Mode, Fixed-Interface, $\theta = 90^\circ$

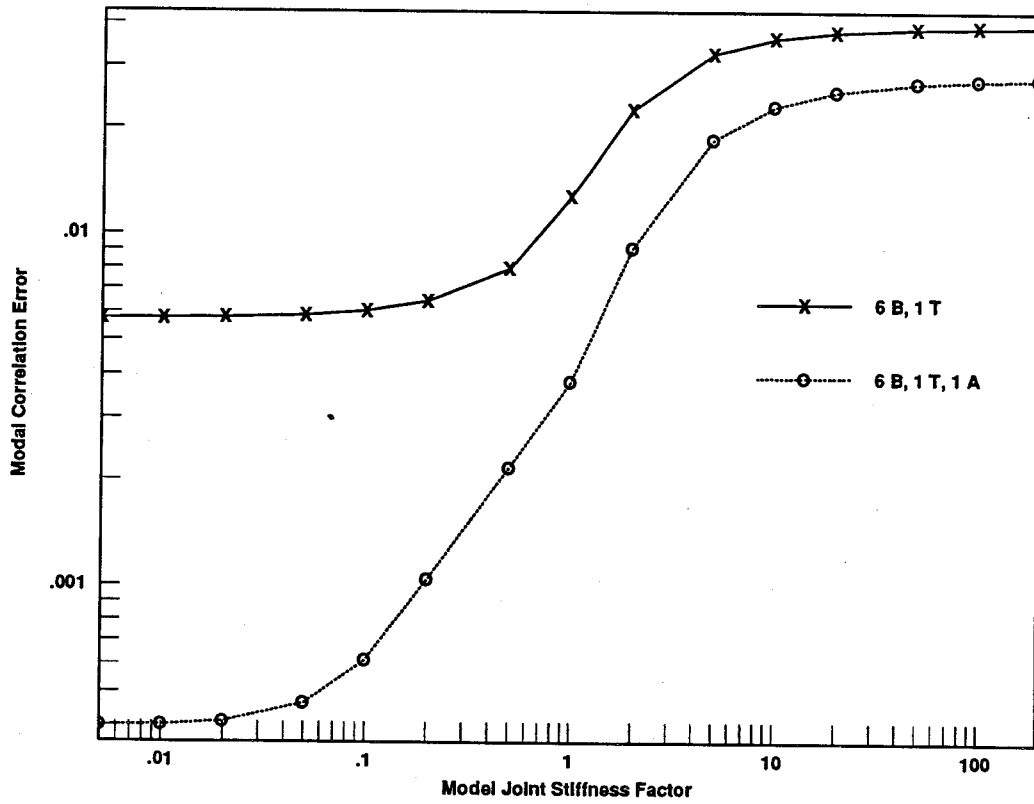
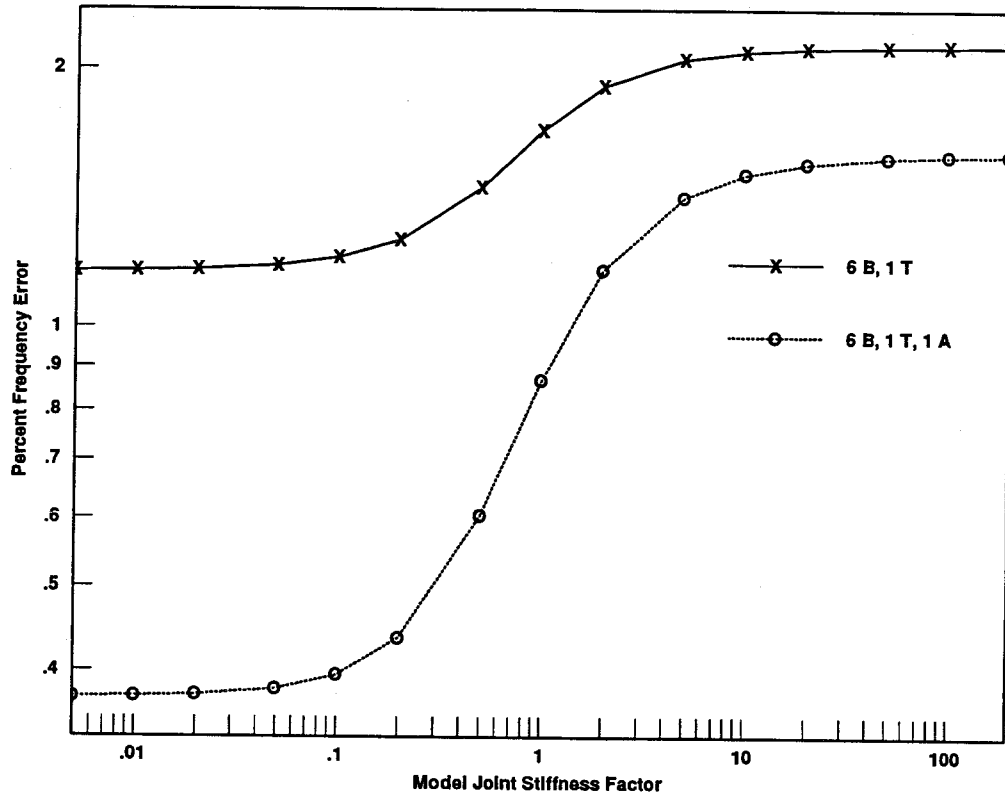


Figure C.23: 8th System Z-Bending Mode, Free-Interface, $\theta = 90^\circ$

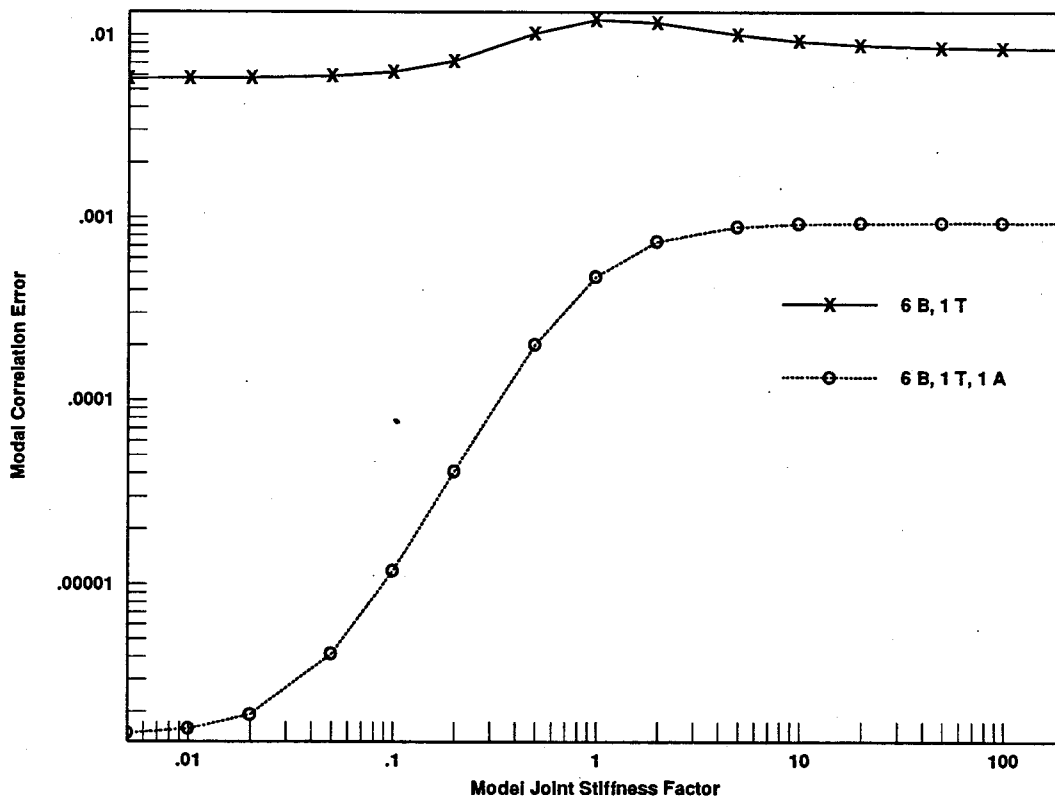
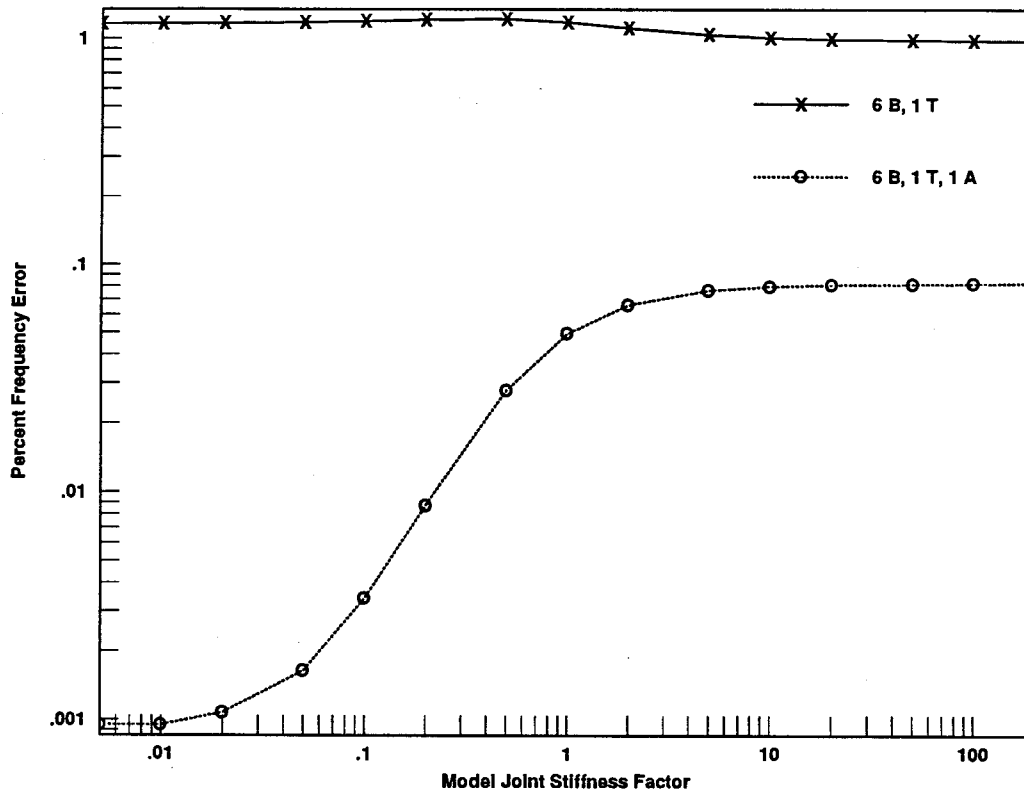


Figure C.24: 8th System Z-Bending Mode, Mixed-Interface, $\theta = 90^\circ$

D. Guide To the Included Floppy Disk

Included with this report is a floppy disk containing computer files that might be helpful should the results of this study be reproduced in any way. On the floppy disk are three NASTRAN input files, and four FORTRAN subprograms. The NASTRAN input files are:

fixed_in.dat
free_in.dat
mixed_in.dat

They are similar to the input files used to obtain data for this study. The three files are input files for component mode synthesis on the model of this study using the methods of fixed-interface, free-interface, and mixed-interface respectively. The mode set size is 8 component modes, and used in the $\theta = 90^\circ$ configuration with Model Joint Stiffness Factor equal to 1. Changing joint stiffness or model configuration can be done by replicating these input files and editing the appropriate Bulk Data Deck "cards".

The 3 FORTRAN subroutines and 1 FORTRAN function included are:

f06_eval.sub
f06_evec.sub
pch_ese.sub
rownum.ifn

The subroutines were used to extract eigenvalue (f06_eval.for) and eigenvector (f06_evec.for) matrix data from the NASTRAN output "f06" files, as well as to get modal strain energy data (pch_ese.for) from the NASTRAN output "pch" files. The integer function (rownum.ifn) is called by f06_evec.sub.



